

Proposal for:

“Large Air Tanker for Wildfire Attack”

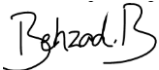


ANAHITA



May 2016

SIGNATURE SHEET

 <p>Sepehr Sharifi Team Leader Undergraduate 687654</p> 	 <p>Behrooz Ashrafi Propulsion, Sys. Eng. Undergraduate 687534</p> 	 <p>Mohammad Sadegh Nasrabadi Aerodynamics Undergraduate 688282</p> 	 <p>Seyed Soheil Yousefi Bonab Performance Undergraduate 687581</p> 
 <p>Mohammad Hosein Hamed Tavasoli Life Cycle Cost Undergraduate 687710</p> 	 <p>Abdolreza Taheri Systems Undergraduate 688365</p> 	 <p>Sepideh Faghihi W & B, Stability Undergraduate 644954</p> 	 <p>Soheil Firooz Structure, Drop System Undergraduate 688362</p> 
 <p>Behzad Baleghi Project Advisor MS. Aerospace Eng.</p> 	 <p>Saleh Khosroabadi Project Advisor MS. Aerospace Eng.</p> 	 <p>Prof. Seyed Mohammad Bagher Malaek Faculty Advisor</p> 	

Executive Summary

“All the calculations show it can't work. There's only one thing to do: make it work.”

Pierre Georges Latécoère,

RFP has called for a purpose-built Large Air Tanker (LAT) pointing to many problems associated with the existing fleet. It is quite clear that current aerial fire-fighting fleet does not live-up to the national expectations and standards, in terms of mission-effectiveness and drop precision as well as accepted level of safety. On the other hand, recent studies clearly indicate that the global change in meteorological patterns have led to a substantial increase in both frequency and sizes of wildfires. We, in ShadX, firmly believe that we have understood the immediate and near future challenges regarding the importance of the environment and the damages wildfires can cause. In this line of thought, we proudly present Anahita as a purpose-built LAT for the challenges described by both RFP and other important challenges discovered by our team-members.

In brief, Anahita is a multi-role LAT, with forward and down-looking capabilities to enhance its operational safety. Such capability allows Anahita to help suppress fires in shortest time possible and with relatively less risk compare to that of its rivals and predecessors. Anahita's capability to perform aerial surveillance missions in the area effectively limit or even eliminate the need for a lead-plane and it helps facilitate the role of incidence commander. In fact, we have been able to show that Anahita is able to perform its mission in both cost-effective and time-efficient manner. Anahita has also been designed to assume the role of a cargo-plane and perform alternative missions during wet-seasons whence no wildfire is expected.

During the design process, comprehensive risk assessments have been conducted to clarify the feasibility of converting Anahita to a Remotely Piloted Aircraft. Unfortunately, our initial studies suggest that despite having the technologies for being remotely piloted, the introduction of such version is limited to the time when remote aircraft in the size range of Anahita are flight proven. It is well noted that Anahita must conduct a ferry mission, during which she needs to fly within national corridors and that is obviously a concern for other conventional passenger aircraft that still have a pilot in their flight-deck. Nonetheless, we expect such remotely-piloted configurations become acceptable to the flying public by employment of communication links between air traffic controllers and operator. The RPA version will experience lower direct operating cost as much as 15% and in

addition to that there is no threat of losing a pilot during the fire-fighting missions. Our plan includes manufacturing the first builds of Anahita with a conventional flight-deck that needs two pilots with an optional observer on board and the future builds with automated and remotely piloted capabilities.

To observe sustainability requirements, systemic approaches have been employed as the basis of problem solving in order to account for every stakeholders' needs and requirements in the design process. Design objectives were also derived and elicited from results of studies and the conclusion was made that not only should the system be reliable, but always responsive when needed. It should also enjoy safe operational cost with lowest possible LCC with respect to considering the best options available on the market.

Requirements and figures of merit were derived with regard to the design objectives on which decisions are quantitatively based on, using the Analytic Hierarchy Process (AHP) method and carpet plots that show the consequences of each decision with regard to cost and time.

Design is a highly iterative process thus, automated design tools were developed to study each individual characteristic imposed by requirements on LCC and the time to establish a fire line (i.e. 4 sorties for Anahita). In order to establish a fire line as quickly as possible, Anahita can perform two sorties without refueling. Anahita is optimized for its primary mission and the mission itself is optimized with respect to total incurred cost of fire and aerial fire suppression combined. This required a detailed calculation in initial sizing that was not employed in aircraft design text books.

All aspects of life-cycle phases were meticulously investigated and possible options for disposal were discussed. Studies conducted so far have shown that any increase in annual aerial firefighting operations decreases the operating cost per flight hour. Therefore, an alternate solution was proposed for Anahita operations during non-firefighting days nation-wide. That is, we do not expect Anahita fleet to remain idle in hangers. In order for the proposed fleet to be an acceptable one different scenarios of acquisition plan were studied and a feasible solution is suggested.

Contents

1	RFP Analysis	11
2	OUR DESIGN PHILOSOPHY	12
2.1	ShadX Design approach	12
2.2	ShadX Design Objectives.....	16
3	CONCEPTUAL DESIGN	17
3.1	Risk Assessment	17
3.2	ShadX Proposed Concept of Operation	23
3.3	Objective & Requirements Hierarchy	28
3.4	Mission Profiles	32
3.5	Overall Configuration Selection	33
4	INITIAL SIZING.....	36
4.1	Weight Sizing.....	36
4.2	Performance Sizing	41
4.3	Performance Parameters Consistency.....	45
4.4	Cost Analysis in Performance	47
4.5	Drop Maneuver Scenarios	49
5	LIFE CYCLE COST ANALYSIS	50
5.1	Aircraft Life Cycle Cost	50
5.2	Wildfire forecast.....	56
5.3	Acquisition Plan	57
5.4	Results	60
5.5	Conclusion	63
6	PARAMETRIC STUDY	65
6.1	Mission Parameters Trade-off Study	67
6.2	Performance Parametric Study	68
6.3	Results of Initial Sizing and Mission Refinement	68
7	Anahita COMPONENT SIZING	70
7.1	Drop System Design	70
7.2	Fuselage	71
7.3	Wing.....	74
7.4	Tail Sizing	81

7.5	Sizes and Dispositions of Longitudinal and Lateral Control Surfaces	85
7.6	Propulsion System Selection and Placement.....	87
7.7	WEIGHT AND BALANCE	90
8	CONCLUSION AND RECCOMENDATION	92
9	References.....	94
10	APPENDIX A.....	96
11	APPENDIX B	99

LIST OF FIGURES

Figure 1: Three general aspects of design	12
Figure 2: Sustainability and its relation to other aspects of design	13
Figure 3: V model of system design	13
Figure 4: Single Step vs. Evolutionary Development Model [2]	14
Figure 5: ShadX Design Process	15
Figure 6: The Schematic of an AHP Decision Making Tree	15
Figure 7: RPV Communication Network	21
Figure 8: Mass domains of manned and unmanned Aircraft [12]	22
Figure 9: Anahita during fire attack (Illustrator: M. Moradi)	24
Figure 10: IDEF0 diagram for the system and its boundary	25
Figure 11: Firefighting mission profile	26
Figure 12: Repositioning Mission Profile	26
Figure 13: ASM mission profile	27
Figure 14: Freight mission profile	27
Figure 15: Requirements Hierarchy	28
Figure 16 AHP Scores Of Design Objectives	29
Figure 17 AHP Scores of Value Branch	30
Figure 18 AHP Scores of Reliability Branch	30
Figure 19 AHP Scoring in the Safety branch	31
Figure 20: 2D Schematic Firefighting Mission Profile	32
Figure 21: Aircraft Distinguishing Characteristics and Allocation of Functions and Physics	34
Figure 22: Continued configurations studied by ShadX	35
Figure 23: Initial Sizing Procedure	37
Figure 24: $\ln(W_E)$ vs. $\ln(MTOW)$	39
Figure 25: Max Allowable Drop Load Factor vs. Drop Altitude	44
Figure 26: DTE Cost Breakdown	51
Figure 27: Acquisition cost breakdown	51
Figure 28: Detailed LCC Contributing Items	52
Figure 29: O&M Cost Breakdown	54
Figure 31: Annual Retardant Drop per Acre	56
Figure 32 Prediction of number of sorties (based on a 5000 gallon airtanker)	56
Figure 33: Aerial fire suppression stakeholders	57
Figure 34: Finance Leasing	58

Figure 35: Non- Recourse Investor Loan.....	58
Figure 36: LCC Breakdown for scenario no.1	61
Figure 37: LCC Breakdown for scenario no.2	62
Figure 38: LCC Breakdown for scenario no.3	63
Figure 39: LCC per Unit of Different Scenarios.....	64
Figure 40: FHR and Daily Availability comparison of scenario 3 and 4.....	64
Figure 41: Anahita’s Lifecycle Plan	66
Figure 42: Export Credit Loan (Ex-Im Bank).....	65
Figure 43: Mission Parameters Carpet Plots.....	67
Figure 44: FHC vs 4 Sortie Time Sensitivity to Cd0 and AR Carpet Plot.....	68
Figure 45: Matching Diagram of Anahita	69
Figure 46: Payload vs. Range Diagram for Anahita	69
Figure 47: 3-view of drop system	71
Figure 48: Limitations and their impact zone	72
Figure 49: Procedure of Class I Tail Sizing	75
Figure 50: Wing Figures of Merit	75
Figure 51: Lift and Drag Coefficients vs. AoA for MS (1)-0317 & MS (1)-0313.....	77
Figure 52: Dimensioned Drawing of the Wing	80
Figure 53: Procedure of Class I Tail Sizing	81
Figure 54: Tail Figures of Merit	82
Figure 55: Static Stability Mode	84
Figure 56: Lift and Drag Curves for NACA 0014	84
Figure 57: Dimensioned Drawing of the Horizontal Tail	85
Figure 58: Planform of the Vertical Tail.....	85
Figure 59: Rudder Planform Parameters.....	86
Figure 60 Engine’s Cutaway (Source: MTU Aero Engines)	90
Figure 61 Side view of Anahita	91

LIST OF TABLES

Table 1: The Success definition of ShadX.....	11
Table 2: Mitigation Priority Index	18
Table 3: Hazards and Mitigation Measures	19
Table 4: Risk Factor as a measure of Safety	20
Table 5: Sensing Instruments	23
Table 6: Aviation Accidents Statistics [17]	31
Table 7: Forest firefighting accidents causes	31
Table 8: Comparison Between Viable Options.....	35
Table 9: Stall Speed Condition in Drop Phase	42
Table 10: Stall Speed Condition in Approach Phase	42
Table 11: Stall Speed Condition in Landing Phase.....	42
Table 12: Max Allowable Drop Gust Velocity scenarios	50
Table 13: Aircraft Loan Parameters.....	59
Table 14: contractor parameters in scenario no. 1	60
Table 15: manufacturer parameters in scenario no. 1	60
Table 16: USFS parameters in scenario no. 1	60
Table 17: contractor parameters in scenario no. 2	61
Table 18: contractor parameters in scenario no. 3	62
Table 19: manufacturer parameters in scenario no. 3	62
Table 20: contractor parameters in scenario no. 4	63
Table 21: USFS parameters in scenario no. 4	63
Table 22: Design Point Characteristics	69
Table 23: Pros and cons of each drop system	70
Table 24: Geometry of the container	70
Table 25: Fuselage cross sections	73
Table 26: Cargo door dimensions	73
Table 27: Fuselage Length Summary	73
Table 28: Sweep Angle, Thickness Ratio and Taper Ratio of the Wing.....	76
Table 29: Performance Requirements	76
Table 30: Geometric Parameters of the Wing	76
Table 31: Re Number and Maximum Lift Coefficient.....	78
Table 32: Incremental Values of Maximum Lift Coefficients	78
Table 33: Calculation of $C_{l_{\alpha}}$	79

Table 34: Results of High Lift Devices Sizing	79
Table 35: Geometric Parameters of the Aileron.....	79
Table 36 Dihedral, Twist and Incidence Angles	80
Table 37: Material of Different Parts	81
Table 38: Moment Arms, Tail Volume Coefficients and Control Surfaces' Fractions.....	83
Table 39: Calculated Tail Areas.....	83
Table 40: Characteristics of the Horizontal Tail Planform Geometry	83
Table 41: Horizontal Tail Geometric Parameters	84
Table 42: Critical Mach Number for Horizontal Tail in Different Missions and Legs – $\alpha = -3.5$ deg.....	84
Table 43: Planform Ratios for Vertical Tail	85
Table 44: Planform Parameters for Vertical Tail.....	85
Table 45: Summary of Rudder Dimensions.....	87
Table 46: Turboprop Vs. Turbofan Pros and Cons	87
Table 47: Position of the Engine Relative to the Wing Pros and Cons	88
Table 48: Engine Required Thrust	89
Table 49: Selected engine performance characteristics	90
Table 50: Weight Components	91
Table 51: Final Location of C.G. & Components	92
Table 52: Tip over and clearance criteria.....	92

Nomenclature

L	Lift Force	lbs
C_L	Lift Coefficient	-
$C_{Lmax_r} - C_{Lmax_t}$	Max. Lift Coefficient at the Root/Tip of the Wing	-
$C_{Lmax_{clean}}$	Max. Lift Coefficient at Clean Conditions	-
$C_{Lmax_{Drop}} - C_{Lmax_{T.O.}}$	Max. Lift Coefficient at Drop/Takeoff	-
$C_{Lmax_{Approach}} - C_{Lmax_{Landing}}$	Max. Lift Coefficient at Approach/Landing	-
C_{l_α}	Lift Slope	$1/rad$
D	Drag Force	lbs
$C_D - C_{D_0}$	Drag/ Zero Lift Drag Coefficient	-
$V_{cruise} - V_{stall}$	Cruise/Stall Velocity	ft/s
V_1	Decision Speed	ft/s
$MTOW$	Maximum Takeoff Weight	lb_f
T	Thrust Force	lb_f
S	Wing Area	ft^2
μ_r	Friction Coefficient	-
$a_{d_{Brakes-on}} - a_{d_{Thrust Reverse}}$	Deceleration due to Brakes/Thrust Reversers	ft/s^2
BFL	Balanced Field Length	ft
$\Delta x_a - \Delta x_d$	Displacement due to Acceleration/ Deceleration	ft
S_g	Ground Roll	ft
n	Load Factor	-
AR	Aspect Ratio	-
$AR_w - AR_h$	Wing / Horizontal Tail Aspect Ratio	-
$l_f - D_f$	Fuselage Length/Diameter	ft
$D_w - D_h$	Maximum Fuselage Width / Height	ft
$\Lambda_{c/4_w} - \Lambda_{c/4_h}$	Wing / Horizontal Tail Quarter-chord Sweep Angle	degree
$(t/c)_{r_w} - (t/c)_{r_h}$	Wing / Horizontal Tail Thickness Ratio at Root	-
$(t/c)_{t_w} - (t/c)_{t_h}$	Wing / Horizontal Tail Thickness Ratio at Tip	-
$\lambda_w - \lambda_h$	Wing / Horizontal Taper Ratio	-
$b_w - b_h$	Wing / Horizontal Span	ft
$\bar{c}_w - \bar{c}_h$	Wing / Horizontal Mean Aerodynamic Chord	ft
$c_{r_w} - c_{r_h}$	Wing / Horizontal Root Chord	ft
$c_{t_w} - c_{t_h}$	Wing / Horizontal Tip Chord	ft
α	Angle of Attack	degree/radian
δ_f	Flap Deflection Angle	degree
$\eta_i - \eta_o$	Flap Starting/ Finishing Span as % of $b_w/2$	-
$\eta_{i_a} - \eta_{i_o}$	Aileron Starting/ Finishing Span as % of $b_w/2$	-
$c_{i_a} - c_{o_a}$	Aileron Starting/ Finishing Point Chord	ft
V_{WF}	Wing / Horizontal Tail Fuel Volume	ft^3
$\Gamma_w - \Gamma_h$	Wing / Horizontal Tail Dihedral Angle	degree
$i_w - i_h$	Wing / Horizontal Tail Incidence Angle	degree
$\varepsilon_{t_w} - \varepsilon_{t_h}$	Wing / Horizontal Tail Twist Angle	degree
$x_h - x_v$	Horizontal/Vertical Tail Moment Arm	ft
$S_h - S_v$	Horizontal Tail/ Vertical Tail Area	ft^2
$S_a - S_e - S_r$	Aileron/Elevator/Rudder Area	ft^2
$\bar{V}_h - \bar{V}_v$	Horizontal/Vertical Tail Volume Coefficient	-
$M - M_{cr}$	Mach/Critical Mach Number	-
d_{e_v}	Vertical Displacement of Elevator	ft

1 RFP Analysis

In the beginning, the RFP is studied thoroughly and decomposed into several criteria which are addressed as success definition as presented in Table 1.

Table 1: The Success definition of ShadX

Success Definition	Sections
To be able to carry water/retardant payload in an operational radius of 200 nm	CONCEPTUAL DESIGN
To be able to dispatch quickly to the entire continental United States	CONCEPTUAL DESIGN
To be a purpose-built large size firefighting aircraft	CONCEPTUAL DESIGN
To be able to function as a water/fire retardant dispersing aircraft while maintaining a quick turn-around time	OUR DESIGN PHILOSOPHY
To minimize the time from initiation of the mission to the drop zone	INITIAL SIZING
To be able to drop on its own along a smoke line	CONCEPTUAL DESIGN
To build an effective fire line or firebreak quickly	INITIAL SIZING
To balance minimizing time to establish a fire line with minimizing ownership cost to justify the acquisition of the greater capability versus refitting and old frame	OUR DESIGN PHILOSOPHY
To address the issue of pilot and justify the corresponding decision	CONCEPTUAL DESIGN
To pass FAA certification Part 25 with special attention to fatigue	Anahita COMPONENT SIZING
To enter into service by year 2022	LIFE CYCLE COST ANALYSIS and Anahita COMPONENT SIZING
To have proper sensing and actuating capabilities for adequate drop precision in order to establish a fire line	Anahita COMPONENT SIZING
To carry equipment in order to perform a forward observer function	Sensing
To meet performance requirements mentioned in RFP including stall speed, etc.	INITIAL SIZING
The proposed design aircraft should be feasible and practical	LIFE CYCLE COST ANALYSIS Anahita COMPONENT SIZING
Include tradeoff studies performed to arrive at the final design	Anahita COMPONENT SIZING and PARAMETRIC STUDY

The aforementioned criteria are comprehended as the measures defined emphasized by the RFP and must certainly be addressed by a winning proposal.

2 OUR DESIGN PHILOSOPHY

This section explains the design approach employed by ShadX. Design objectives are also decided upon **after** rigorously studying RFP as a baseline for decision making.

2.1 ShadX Design approach

Systems engineering and design approach was adopted by the team towards this problem since a systemic approach can obtain a solution in which all external systems and their relations are considered in design. Systems design dictates the need to take every stakeholders' requirement into account so the team aimed to pay attention to people, profit and planet aspects of design all together [1].



Figure 1: Three general aspects of design

Taking all of these three parts into account is translated into measuring the impact of decisions on each aspect. Organizations responsible for fire suppression are governmental which means they have limited budgets from taxpayers' money that should be spend effectively and efficiently. They also represent the people and must reduce the risks to safety of citizens and firefighters. Furthermore, the process of fire suppression should be accelerated especially in early phases of fire during the initial attack. Hence, the design must address the three P's with an emphasis on Planet since the other two essentially depend on it. As it will be explained more thoroughly in sections to come every aspect has been considered in design objectives, bringing together a sustainable design (Figure 2).

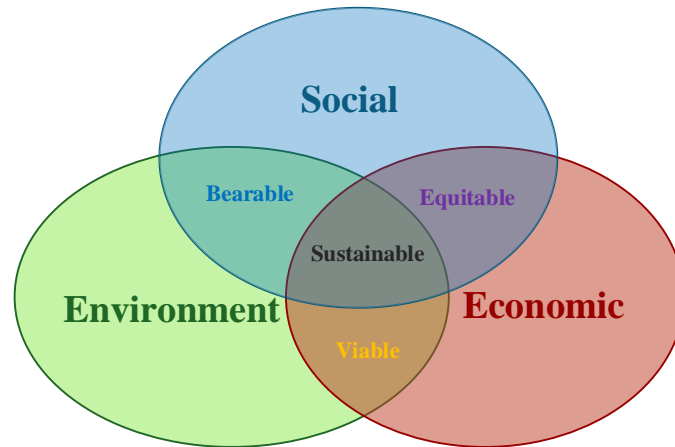


Figure 2: Sustainability and its relation to other aspects of design

V model was adopted in order to breakdown requirements and engage in problem solving (see Figure 3). In the first loop of design after technology risk assessment, the conclusion was reached that an evolutionary development model would be best suited to develop the LAT. Incremental development model was decided to be the evolutionary model for the design process due to the lack of sufficient reliability of current flight systems for the LAT to become an unmanned aircraft by 2022. The LAT will be delivered in builds, each following the V model design process. The first build will be a manned and piloted aircraft and the builds to come will bring it closer to becoming a remotely piloted aircraft (see section 3.1.6).

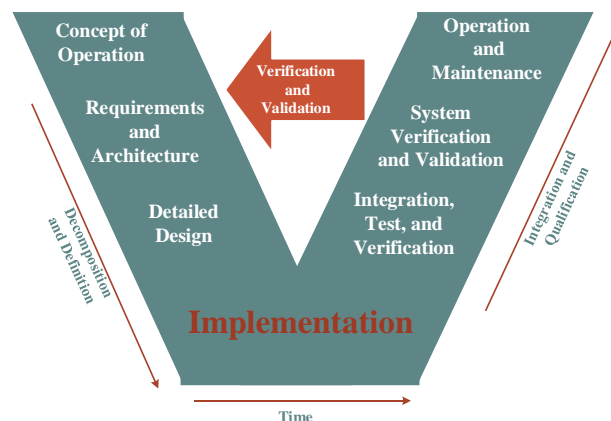


Figure 3: V model of system design

As it is indicated in Figure 4, delivery of system capabilities in individual builds is most suitable when the technology base is improving and the system is most likely to be used beyond its intended service life time as it is observed from existing fleet of airtankers (see section 1). This approach enables quick initiation of operation with acceptable capability and improving it via each build until it reaches its full operation capability [2].

The flowchart in Figure 5 represents the design process of the first build of aircraft until discovery of a feasible solution in a general manner:

Decision making process: to overcome the challenges of determining the best decision in a complex problem domain, one of the methods in decision analytics, namely Analytic Hierarchy Process (AHP) [3] was adopted by the team. This quantitative method is suitable for group decision making and it also has the profit of examining each member’s mental model and activates the second learning loop introduced by Argyris [2]. This method minimizes the effect of common sense. Nevertheless, the harm of group conformity bias was known and monitored by the team. It is also applicable to the posed problem because of its hierarchy of decomposed design objectives which exists in the nature of systems design.

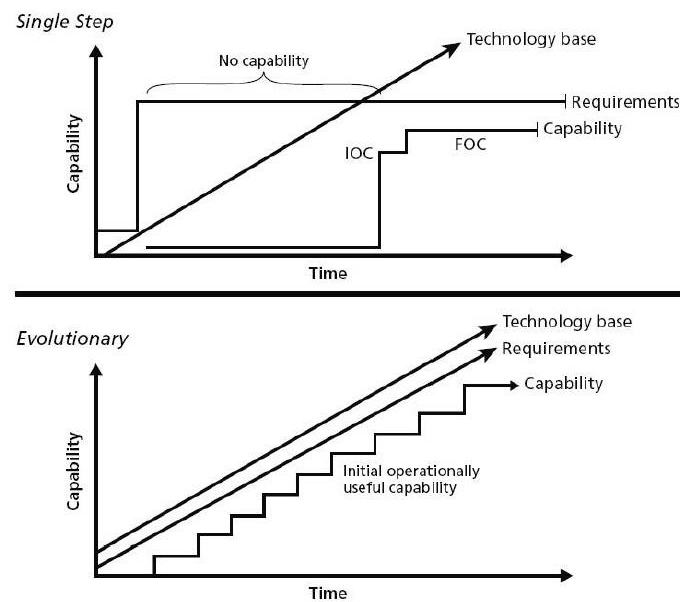


Figure 4: Single Step vs. Evolutionary Development Model [2]

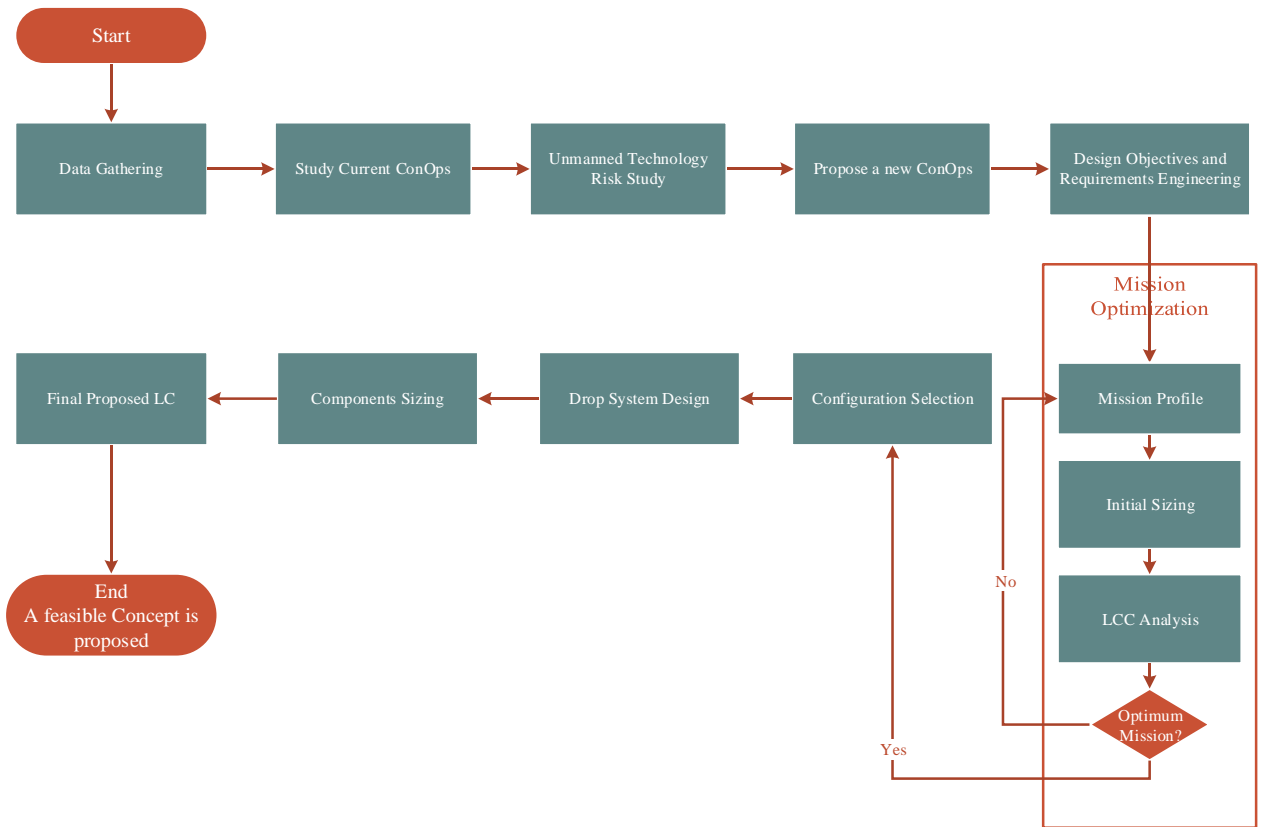


Figure 5: ShadX Design Process

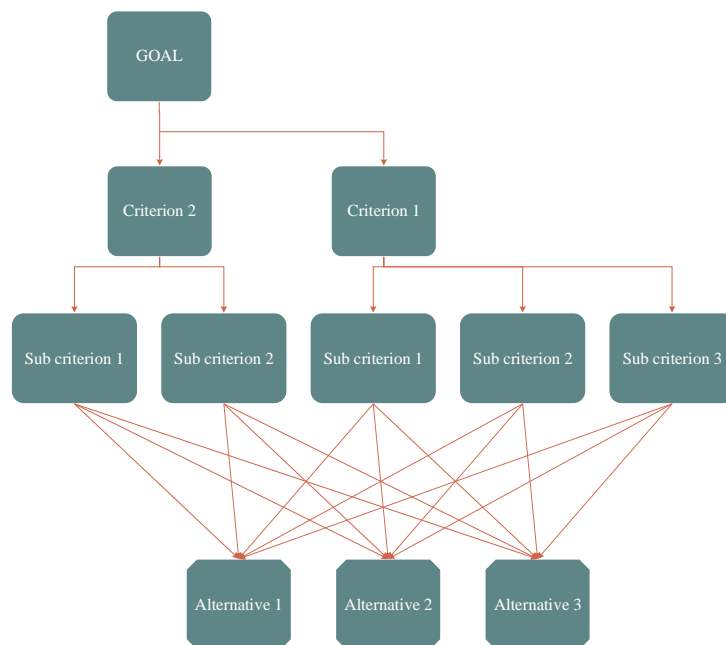


Figure 6: The Schematic of an AHP Decision Making Tree

AHP method alongside carpet plots are the tools that are used to study tradeoffs. The design was conducted mostly in conceptual and upper levels of preliminary design so as to reach a feasible baseline for future works. The conceptual design procedure is through the process of designing Anahita two series of aircraft design text books, written by Dr. Jan Roskam & Dr. Leland M. Nicolai were mainly used as references in each section also indicate.

2.2 ShadX Design Objectives

In this section major design objectives are derived by detailed examination of the RFP. The reader should bear in mind that all of design objectives are different aspects of sustainability.

2.2.1 Design to value

“... The objectives for the design should balance minimizing time to establish a fire line with minimizing total ownership cost.”

“Minimize cost of ownership to justify the acquisition of the greater capability vs. refitting an old airframe.”

Statements above draw attention to Design to Value (DTV) objective which is a strategy adopted by the United States Air Force (USAF) as one of the initiatives proposed by the Reduction in Total Ownership Cost (R-TOC) program. The aforementioned design objective employs an effective tool which concisely expresses the whole idea of DTV, Cost as an Independent Variable (CAIV) [4]. This initiative is usually concerned with budgeted programs. This program implies that between the three types of constraints on design which are Time, Cost and Quality (TCQ), cost is a fixed and limited parameter amongst all and the rest are to be compromised [5] considering they must satisfy their bottom-line which are the defined measures of effectiveness, performance and suitability [2] and are to be presented in sections to come. Though private sector is highly involved in aerial firefighting, their revenue is provided from USFS budget.

2.2.2 Reliability (Effectiveness)

“Minimize time to establish a fire line ...”

“... Achieve drop precision adequate to build a fire line of retardant.”

“This aircraft should have the ability to function as a water and fire retardant dispersing aircraft while maintaining a quick turn-around time.”

It is deduced from RFP that quickly establishing a fireline in four sorties as a measure of mission success, is a key contributor to stakeholder satisfaction [2]. A reliable aircraft makes sure that the taxpayers' money will be spent in an efficient manner. The LAT should be able to overcome operating environment hazards and uncertainties. Drop precision, quick turnaround time (i.e. ground operation) and quick operation is considered to be facets of the LAT reliability.

2.2.3 Safety

“Wildfire fighting has been extremely dangerous over the past decades.”

The impact of uncertainty and risks in wildfire fighting environment are significant. Hence, safety management is of utmost importance. This also can be deduced considering the history of accidents and fatalities; 1.6 accidents and incidents per year and 1.5 fatalities per year. In summary, there have been accidents in 70% of years. [6]. Therefore, the implementation of Safety Management is completely necessary. High risk hazards and primary causes for most frequent mishaps are to be addressed and mitigations should be considered in design.

3 CONCEPTUAL DESIGN

3.1 Risk Assessment

In this section, hazard of airtanker operations are evaluated and the mitigations to reduce the impact of the hazards are selected. Then, technologies are introduced to increase safety and effectiveness of Anahita, indicating how in the future it may be remotely piloted for more safety of the crew and lower operation costs.

3.1.1 Operation Risks

In a recent risk assessment research, Controlled Flight into Terrain (CFIT) was identified as a leading cause of fatal accidents in the BAe 146 all of which occurred during flights conducted under instrument flight rules (IFR). Following the recent safety impact analysis on large airtankers [17], which includes definition of possible hazards and specific measures to mitigate each hazard and evaluation of these measures by assigning values of risk based on analysis of severity and likelihood of the risks, a new index was developed by the team, making it possible to compare the hazards and their corresponding mitigation measures in order to choose the proper mitigations to be implemented in the design of Anahita. That is, if the mitigations pass a pre-defined cost/benefit

index with respect to the risk of their corresponding hazards, they will be implemented in the design. Table 2 summarizes the mitigation priority index.

Table 2: Mitigation Priority Index

		Hazard Risk				
		Very Low	Low	Moderate	High	Extreme
Mitigation Benefit/Cost	Best					
	Better					
	Good					
	Minimal					

Mitigations that are considered most effective appear in the green area of the Risk Matrix and are suited for implementations in the design for Anahita. Mitigations in the yellow region will have lower priority and those in the red region will not be implemented mainly because of cost. Table 3 summarizes the final mitigation measures considered to be implemented into Anahita:

3.1.2 Introducing Automation Technologies

The workload and stress levels of pilots can be significantly reduced by means of automation support in decision making and action implementation. Autonomous technologies are introduced as extra mitigations to operational hazards by the team, to be implemented in Anahita in order to add more safety and effectiveness to operations.

In the initial process of addressing the piloted or unpiloted dilemma posed by the RFP, a matrix was developed to assess the risk of operations in three phases of the mission: the base operations, the flight to mission zone, and in the fire zone, in order to realize how automation can reduce the risk of operations and time between missions that inspires safety and effectiveness of the design. Later, partial automation was also added to the evaluation, further reducing the risk levels, the finalized result of the matrix can be seen in Table 4.

The problem with automation is mainly the reliability discussed in section 3.1.7, Automation helps human in reacting in a timely manner, but can only manage the situations they are designed for. The partially autonomous technology takes less time to develop, is cheaper and is more reliable as the unforeseen situations can be handled by a human [7]. A brief description of the automation technologies are as follows:

Table 3: Hazards and Mitigation Measures

Hazard ID	Hazard	Mitigation ID	Mitigation
AW1	Maintenance and inspection programs that have not been modified to account for structural loads experienced in the fire mission can result in component failure leading to an in-flight structural failure	AW1M1	Implement contractual requirements commensurate with industry standards required by FAR 25.571 and FAR 25.1529 for aircraft employed as large airtankers
EP3	Risk of CFIT due to maneuvering low level with a non-initial attack rated captain	EP3M4	Use ASM or lead plane until flight crew experience increases
HF2	Limited number of tankers has resulted in more frequent travel and change of duty station has negative effect of crew equality of life, which results in increased stress and fatigue	HF2M2	Adhere to duty limits
HF3	Target fixation and tactical maneuvering errors may cause CFIT or midair collision	HF3M2	Aircraft performance planning for successful outcome in a high rate of descent, level off and climb out profile
ME4	Mission operations below 500 feet AGL increase the likelihood of CFIT	ME4M2	Utilize radar altimeter, EGPWS (Enhanced Ground Proximity Warning System), TAWS, and other technology
		ME4M3	Fly using visual flight rules
ME5	Close proximity of multiple aircraft in the fire traffic area pose a threat of midair collision	ME5M1	Utilize personnel and tools such as TCAS II, ATGS, lead plane, ASM, good visibility from flight deck, standard operating procedures, fire traffic area and airspace management
TE3	CFIT accidents can occur as a result of the lack of use of current technology	TE3M3	Implement contract specifications that ensure adequate instrument flight rules (IFR) using GPS technology for cross country navigation systems

A **health monitoring system** adds the ability to identify deterioration of sub-systems. This will focus maintenance efforts hence decreasing the time of ground operations such as turn-around times and reducing costs per flight hour. **Contingency management system** reacts properly in the event of unforeseen system failures, changing or canceling mission plan therefore guaranteeing aircraft survival. **Collision Avoidance system** will allow aircraft to detect other aircraft or obstacles at a sufficient distance and avoid them. **Mission management technologies** reduce the direct human interaction allowing for one operator to monitor several vehicles at a time hence decreasing cost of operations. For a complete description of technologies refer to [8].

The cost of implementing these technologies is minimal compared to the amount of quality they promise, but the cost of research and development of technologies are generally high, it was assumed that the technologies will be developed in the future by other associations so the RDTE cost is zero, for instance, in [8] NASA indicates a schedule to develop the technologies. Cost is discussed further in 5.1.1.

3.1.3 Partial Automation

In this section, using a level of automation taxonomy [9], the optimal automation level of the technologies are determined and proved to provide a safety level of equal or greater than full automation or piloted operations.

The automation levels were determined by evaluating the risk of human action and the risk of full automation in each level, finally, the automation level that generated the lowest risk of operation was selected to be implemented in the risk matrix. Refer to [9] for a full description of automation levels, as an example, the D6 level of automation initiates and executes a sequence of action automatically in the event of a contingency or a collision and can be interrupted or modified by the operator.

3.1.4 Risk Matrix

In order to understand the effect of automation in flight safety, a risk matrix was generated in three steps. In the first step, a value of 1-5 was assigned to a situation that is being handled entirely by human for each of the three phases of mission, decisions were made based on the severity of hazards of human performance [10]. For instance, pilot’s inability to react in time in the event of an unexpected situation poses a high risk as indicated by red in Table 4. Similarly, in the next two steps, the same procedure was done for a situation that is being handled by a fully autonomous technology without any involvement of pilot or operator, and a combination of both. It can be deduced from Table 4 that full automation does not always result in lower risk levels.

Table 4: Risk Factor as a measure of Safety

Automation level		Risk Factor								
		Base operations			from Departure to mission zone			attack zone		
Technology		No Auto.	Full Auto.	Partial Auto.	Pilot ed	Full Auto.	Partial Auto.	Pilot ed	Full Auto.	Partial Auto.
Mission management	C2	1	Not required		2	2	1	4	3	2
system health monitoring	B4	Reduces turnaround times			4	1	1	5	1	1
Contingency management	D6	Not essential			3	2	2	5	3	3
Collision avoidance	D6	Not essential			2	1	1	4	2	1

3.1.5 Conclusion

It is concluded from Table 4 that the human action alone is extremely poor in the fire attack zone, therefore the implementation of automation support is essential. It also shows that fully autonomous systems are risky in low level environment as they cannot manage all possible situations. Furthermore, automation helps reduce the

time of operations. Technologies for automation support will be implemented in the incremental builds of Anahita as soon as they are developed. Furthermore, when these technologies are in place, Anahita can be operated remotely as the pilot will not be required to be on board. Hence Anahita can move to an RPA version when the reliability of remotely piloted systems is proved. That is, remote piloted aircraft in the size range of Anahita are flight proven. This will increase quality of operations and ensure pilot safety and will also save on operating costs as will be discussed in 5.1.3.

3.1.6 Remotely Piloted Aircraft (RPA)

Operating Anahita from a fixed control station assures safety of crew. If the plane is operated remotely, the costs of operation and maintenance will drop as will be explained in 5.1.3., Anahita utilizes cameras that provide sufficient view for remote piloting, and the pilot uses Virtual Reality goggles on board, the same operation could be done in a control station with today's technology of web-based over-the-horizon communication, this way, the flight data along with the video feedback is received allowing control of aircraft from a fixed control station. The communication network also satisfies the requirement to provide a link between the Air Traffic controller and UAV operator. Figure 7 shows an example of this type of communication [11].

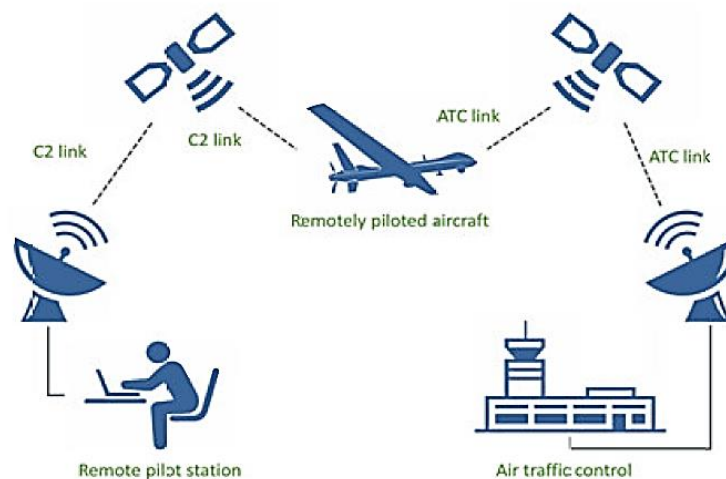


Figure 7: RPA Communication Network

By the time Anahita becomes RPA, it will have sufficient automation level of technologies to ensure aircraft survival to react to contingencies and avoid collisions. The only constraint to the RPA program remains one thing, Reliability.

3.1.7 Reliability of Autonomous Systems

The technical challenge of operating Anahita remotely or autonomously is that no aircraft has yet been built in the size range of Anahita, RPAs will be developed sooner than fully autonomous aircraft, however, it can be realized from Figure 8 that this strictly constraints the RPV build to a time when reliability of autonomous flight systems for heavy aircraft has been proven, since RDTE cost on technologies was required to be zero.

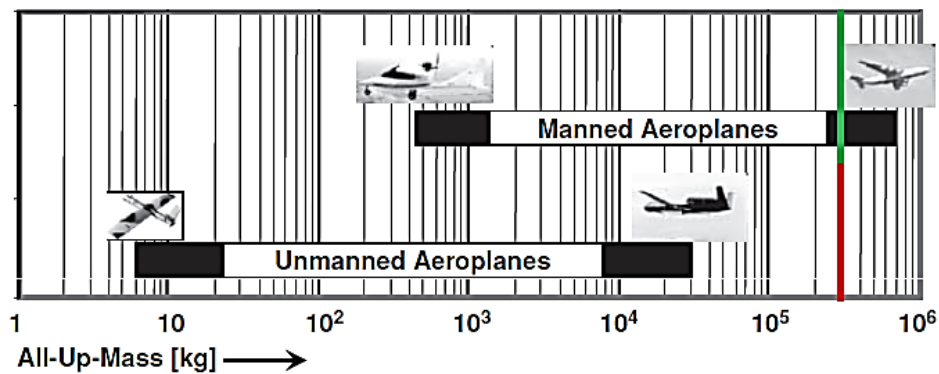


Figure 8: Mass domains of manned and unmanned Aircraft [12]

3.1.8 Sensing

Sensing is the act of gathering information (Visual, Thermal, Communications, etc...) from the environment. This section describes how Anahita benefits from Virtual Reality System and embedded cameras to have a precise sensing so it can drop on its own. Table 5 summarizes the necessary description and placement of the instruments to achieve the sensing requirements:

3.1.8.1 Prediction of fire behavior

In order to determine the location of the drop, two Infrared cameras are implemented in the nose of Anahita to map the fire, hence, with the help of the geological data of the terrain and wind speed and direction, the fire behavior can be predicted by a computer and the optimal location of drop can be realized.

Table 5: Sensing Instruments

Infrared Cameras	Two installed in the nose making it possible to sweep the ground and pass the visibility pattern of cockpit. one in the middle and two in the aft part, for integration with VR System and fire prediction system.
Wind meter	Wind speed and direction is required for of fire rate and direction of spread.
Operational load monitoring system	This system will measure the amount of load experienced by Anahita in each direction, this will be particularly useful during drop while integrated with the system health monitoring and contingency management system.
Heat sensors	Senses the temperature profile of the fire.
Precise altitude meter	Precise altitude meter is essential for drop in low level environment.
Weather radar, Radar, GPS, TCAS, Radio	Standard flight instruments necessary for accurate sensing that provide communication with ground and air crew, detection of danger and mid-air collision avoidance and navigation.

3.1.8.2 Virtual Reality System

Anahita must be able to drop on its own without the need for a lead plane, presence of an observer will be required in the cockpit who can monitor the fire data. Unfortunately, extra windows cannot be installed in the cockpit as this will greatly increase fatigue. So for the observer to have an effective view of the fire area, five cameras are embedded in the skin of Anahita providing visual to a Virtual Reality (VR) helmet that is worn by observer.

The virtual reality helmet system of F-35 has proven to be fully operational. So it is reasonable to assume that the technology can be implemented in Anahita. The VR system implemented in F-35 has additional capabilities such as 360° view, integration with systems and sensors, night vision, precision tracking of friendly aircraft maneuvering in the area which can also assist firefighting missions [13].

The initial version of this system should be simple enough to provide situational awareness for the observer. Minimum instruments needed for conducting these operations have been described in Table 5. This system can be advanced further to provide visual for pilot and night vision for night time operations.

3.2 ShadX Proposed Concept of Operation

Studying current operations of LATs has granted ShadX a relative insight to the problem domain. Hence, different missions were proposed and also a breakdown of the design objectives was created that should be addressed in ShadX solution.

3.2.1 The Whole Picture

Preventing every fire is an ideal situation though it may not be a viable one. Forest fires will occur and data show it is likely that their frequency and size will rise. The vision is that the entities involved in firefighting, let it

be ground or air attack, are unmanned ones that work in harmony and try to keep humans from any harm in addition to reducing costs. An entity that has the operational capability for supervision and suppression simultaneously while having the adequate sensing equipment to operate independently (no need for a lead plane). Figure 9 illustrates the envisaged future in a comprehensive manner.

3.2.2 External Systems

After studying the current situation of firefighting, the system boundary is drawn in Figure 10. It is useful as it determines the inputs and outputs of the system with respect to its surroundings. These inputs and outputs are measures system effectiveness. In other words, these are the validation criteria of Anahita.

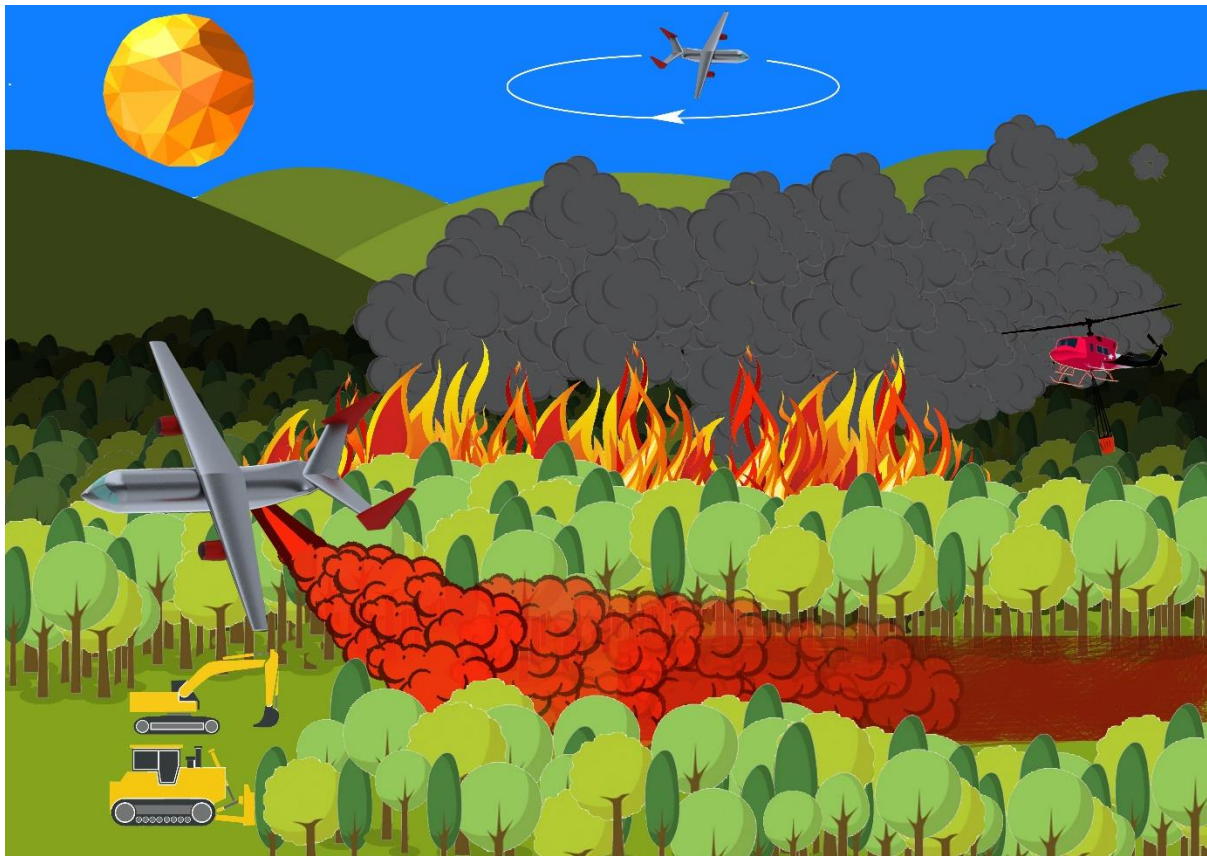


Figure 9: Anahita during fire attack (Illustrator: M. Moradi)

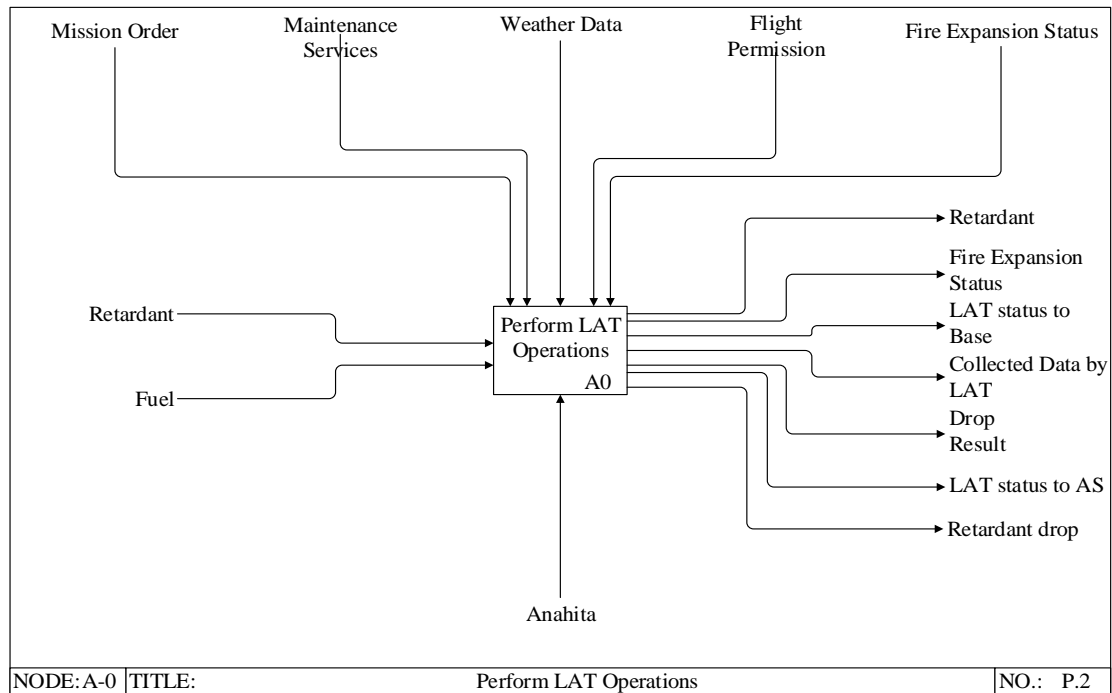


Figure 10: IDEF0 diagram for the system and its boundary

3.2.3 Proposed Missions

After studying the operating environment and the mission requirements, several missions were proposed by ShadX in which the primary missions are fire attack and repositioning plus additional missions namely aerial supervision and freighting. Anahita will be optimized for its principle mission i.e. fire attack and it is only designed so as to be able to perform the others.

3.2.3.1 Fire Attack

The primary mission that Anahita must carry out is fire attack especially initial attack that implores the quickness of aircraft in performing that operation. Having observing capabilities allows Anahita to drop and examine its quality independently. Hence its mission is designed so as to have loiter before and after each drop in order to examine the accuracy of previous and drop, provide fire data to fire personnel and decide on how the next drop is to be done.

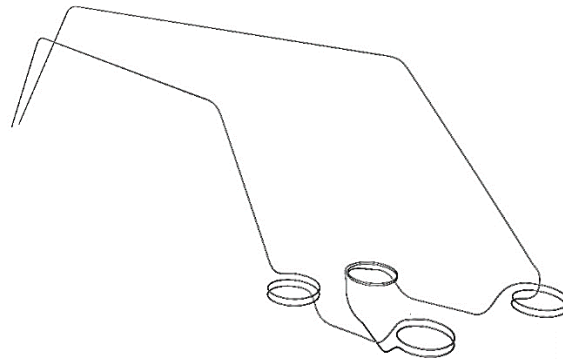


Figure 11: Firefighting mission profile

3.2.3.2 Repositioning

Fires are forecasted at least a day earlier and nearest airbases to areas that are most likely to suppress a wildfire, request an LAT from the bases in possession of available LAT(s). In worst case scenario the only available LAT is in an airbase across the continent. Hence the LAT must be able to fly cross-continental.

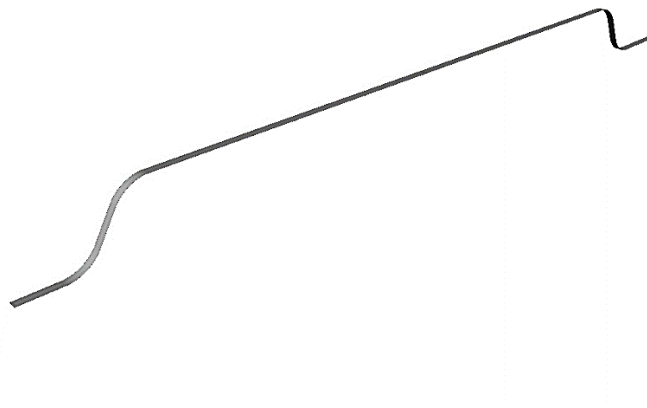


Figure 12: Repositioning Mission Profile

3.2.3.3 Aerial Supervision

Anahita will have effective observation capabilities and designed to be agile in gusty and hostile environments such as wildfires in such a way additional aircraft in area for coordination and leading airtankers are no longer needed and the result is saving on expenditures.

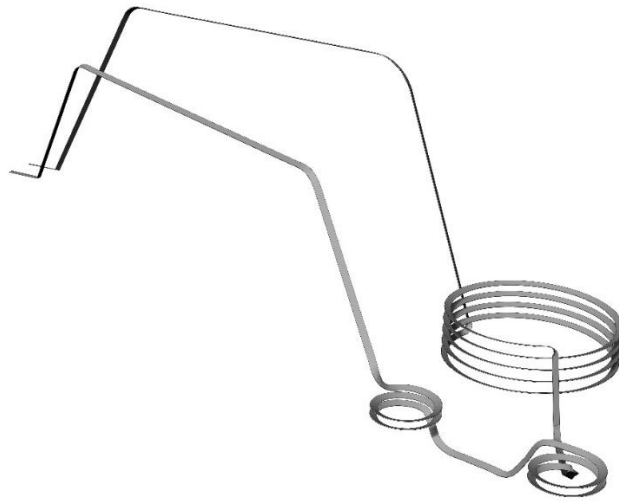


Figure 13: ASM mission profile

Mission can be performed in a relatively arbitrary manner, it can include zero to two drops and high altitude loiter. It is obvious that the number of drops affect the loitering time. Anahita will have provisions for a crew member who will act as the fire observer and coordinator of aerial operations.

3.2.3.4 Freighting

The summary of FAA forecasts concerning domestic and international cargo transportation are presented in [14] that show an annual growth of 2.3% in the delivered goods as a result of increase in number of freighters.

It can be observed from [15] that most transported cargo (both in tonnage and value) are delivered to destinations within 250-500 miles.

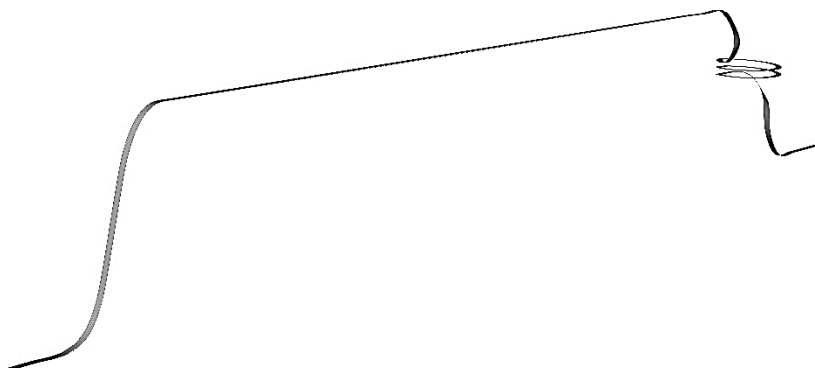


Figure 14: Freighting mission profile

This increase in the amount of total delivered cargo implies that transition to a freighter during non-fire season is a viable option. Nevertheless, Anahita has the capability to fly 700 nm with full payload. As will be discussed in more detail in section 0, adding this extra mission for Anahita will reduce the hourly flight cost, therefore it is considered suitable.

3.3 Objective & Requirements Hierarchy

Objectives and requirements hierarchy is the cornerstone of ShadX decision making process. The three core design objectives and their related lower level requirements are described in this section and the importance of each one compared to another (to be used in AHP) has been described. All decisions in the project were made quantitatively based on the figures of merit and requirements that will be explained in more detail in the sections to come.

3.3.1 General approach

In the process of requirements and figures of merit elicitation, several definitions from [16] and [2] are employed in which are concisely summarized in Figure 15.

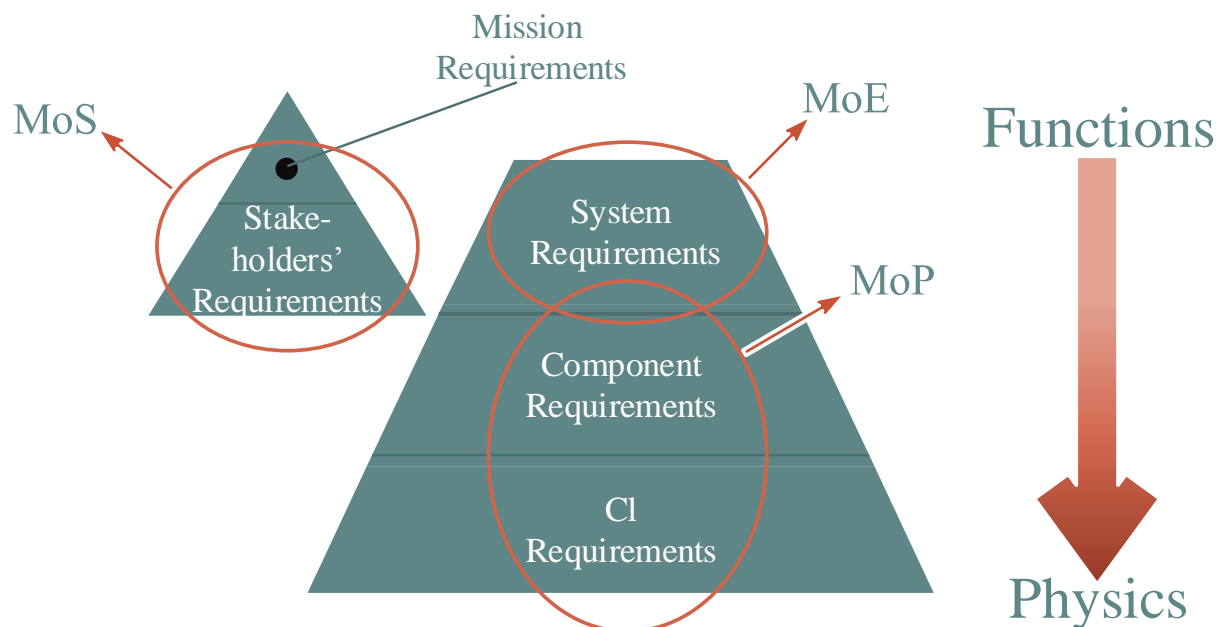


Figure 15: Requirements Hierarchy

ShadX requirements hierarchy starts with design objectives described in 2.2 at the top and ends with component level requirements. In the process of requirement derivation, some design objectives either become a requirement, that have thresholds for a parameter(s), or convert into a figure of merit (FoM) that guides the decision making process.

3.3.2 Design Objective Priorities

Comparing cost of fire against operational cost and dependence of stakeholder satisfaction on mission effectiveness has resulted in the chart below:

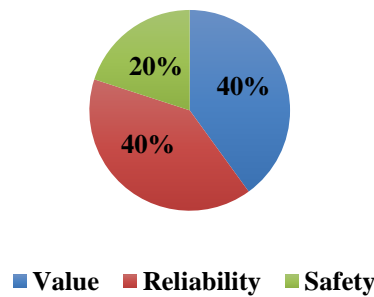


Figure 16 AHP Scores Of Design Objectives

3.3.3 Design to Value

As explained in 2.2.1 having DTV as a design objective means to minimize LCC which is includes RDTE, Acquisition, O&M and Disposal but that does not necessarily means reducing each comprising part. Each of them in turn has been broken into different issues that the LCC is affected by them. A detailed view of the breakdown is presented in APPENDIX A. Relative importance and weight of these criteria were decided and the result is shown in Figure 17. These criteria are divided further in each level (from the most inner circle to the most outer).

3.3.4 Design for Reliability

Reliability and effectiveness have two aspects that are effective fire attack and quick establishment of fireline. The latter can also be broken into quick fire attack i.e. quick dispatch and quick turnaround. Figure 18 presents a detailed view of the criteria and their corresponding weights.

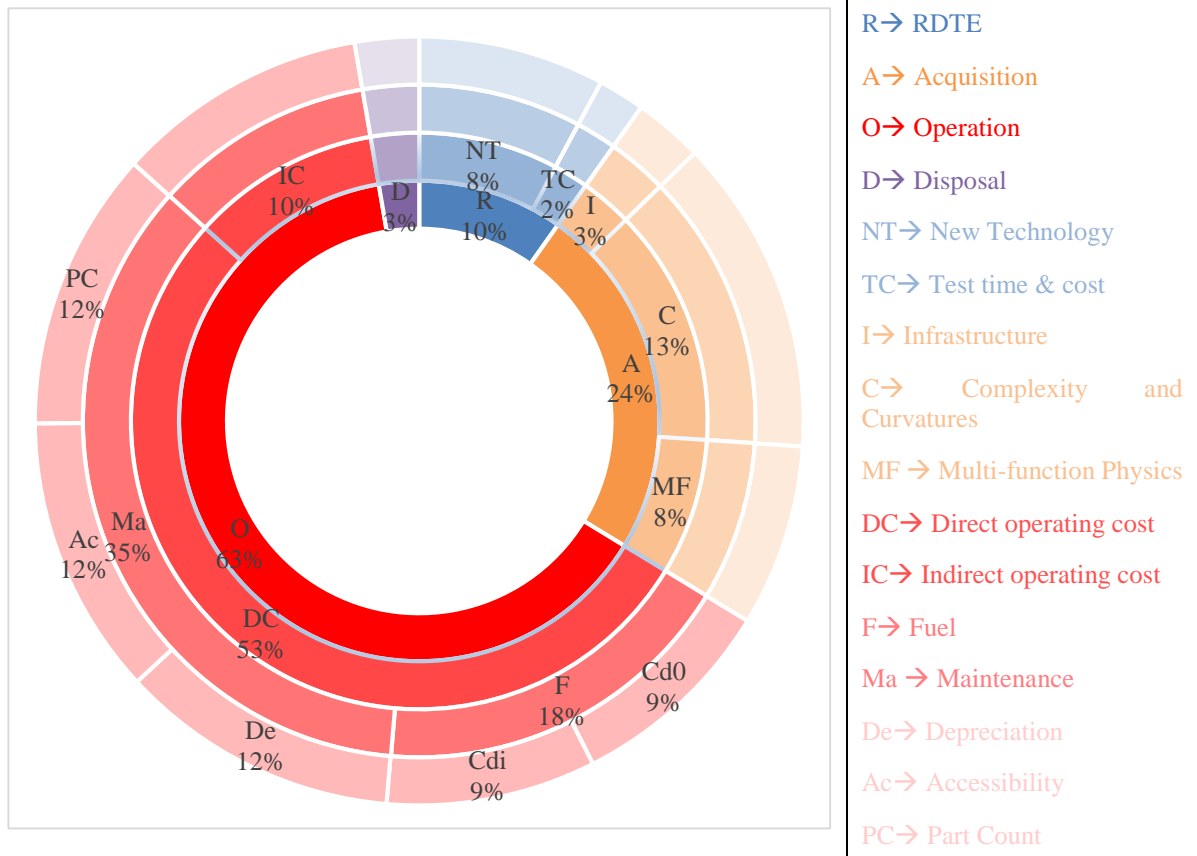


Figure 17 AHP Scores of Value Branch

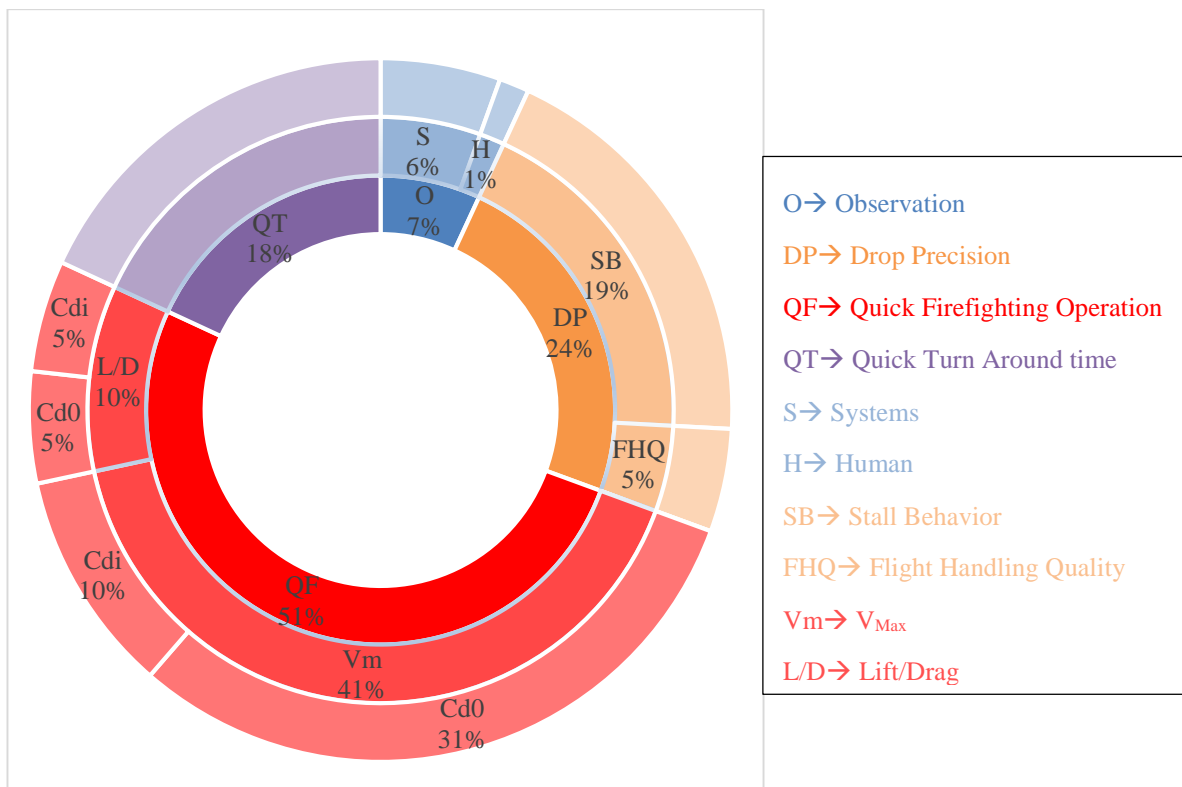


Figure 18 AHP Scores of Reliability Branch

3.3.5 Design for Safety

LATs experience hazardous operating environment as it can be observed from accident records in Table 6.

Table 6: Aviation Accidents Statistics [17]

Fatal Aviation Event	2000-2006	2007-2013
No. of events involving a fatality	28	13
Rate	4.6	2.1
Average per year	4	2
No. of Fatalities	49	29
Rate	8.0	4.7
Average per year	7	4

Therefore, safety was selected as the third most important design objective to be addressed in design. In order to derive requirements correctly, accidents history was studied. Engine failure, fatigue, stall and stability were decided to be addressed based on Table 7. The statistics of Table 7 are for all firefighting related causes. Clearly, those related to aerial firefighting were chosen to be considered.

Table 7: Forest firefighting accidents causes

Cause	Events	(%)	Deaths	(%)
Failure of engine, Structure, or component	10	(24)	18	(23)
Loss of control (Including failure to maintain airspeed)	10	(24)	15	(19)
Failure to maintain clearance from terrain, water, or obstacles	8	(20)	15	(19)
Weather	6	(15)	13	(17)
Midair Collisions	2	(5)	3	(4)
Failure of parachute or rappel equipment	3	(2)	2	(3)
Weight and balance	1	(2)	9	(12)
Cause not reported	1	(2)	2	(3)
Total	41	-	78	-

Figure 19 maps FoMs in decision making to be exploited by AHP method.

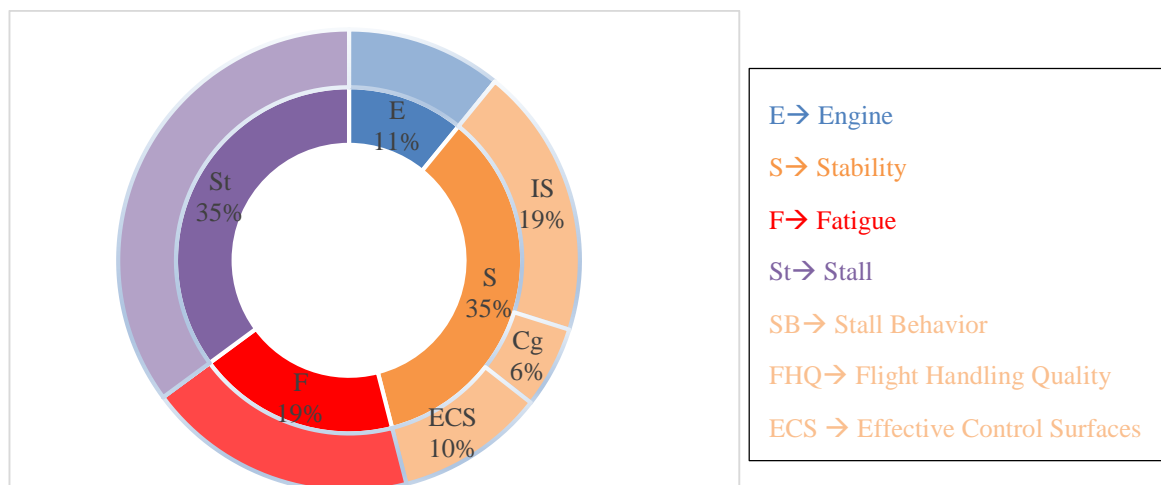


Figure 19 AHP Scoring in the Safety branch

3.4 Mission Profiles

This section summarizes the mission profile, assumptions and finalized parameters. The procedure of determining the parameters are explained in detail in section 4.

Anahita must be able to achieve a primary mission: Fire Attack which includes initial attack and extended fire support, and a secondary mission: a Repositioning Flight.

3.4.1 Fire Attack

The Fire Attack mission is a retardant/water payload delivery to a 200nm, all the operations in the mission zone including the drop maneuver was simplified to an overall of 20 minutes of endurance for reconnaissance, loiter and drop. The Fire Attack mission corresponds to both the initial attack and extended fire support. A sensitivity analysis was done later in section 6.1 in order to realize how the changes in parameters affect the mission profile. Figure 20 presents the mission profile for Fire Attack.

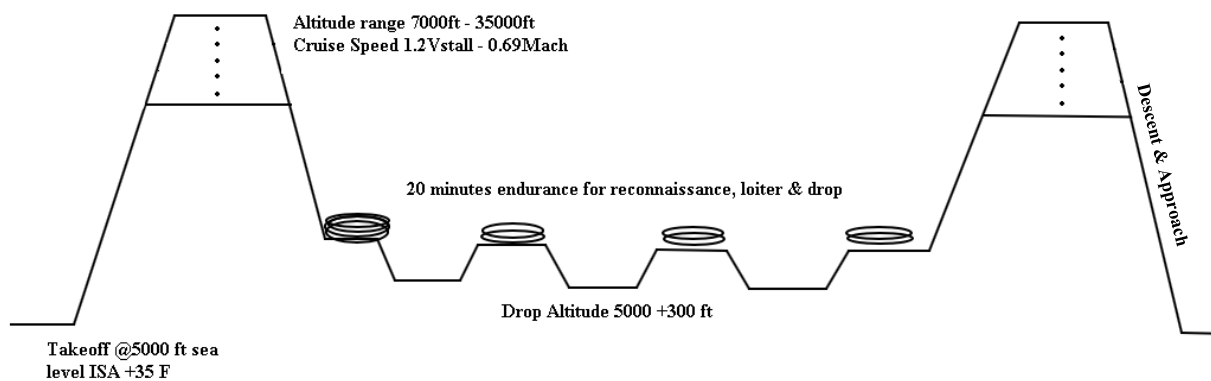


Figure 20: 2D Schematic Firefighting Mission Profile

At this point the in and out cruise speeds and climb altitudes were undetermined, a tradeoff was studied between the total incurred cost and time to establish a fire line between all the combinations of speed and altitudes in order to define the optimal mission profile (see section 4.2). Speed in altitudes lower than 10000 ft. was limited to 250kts as a constraint imposed by FAA in the analysis of all the possible combinations above. Fire Fire Attack mission parameters are as follows:

- ✈ T.O. @5000 ft. above sea level, ISA+27°F
- ✈ Balanced field length of 5000 ft.
- ✈ Climb Rate of 3200 ft. /min.

- Cruise out and cruise in speed of 390 kts
- Cruise out altitude of 27000 ft.
- Overall endurance of 20 minutes for reconnaissance, loiter & drop
- Cruise in Altitude of 38000 ft.

The incurred cost of fire could be minimized by reducing the total time to establish a fire line. This could be accomplished by increasing the fuel capacity of Anahita up to the fuel required for two missions so twice the refueling time is saved in 4 sorties. The possibility of a fuel tank capacity for 4 sorties was also considered to greatly reduce the time but the results concluded that the increased weight was not worth the reduction in time.

3.4.2 Repositioning

The Repositioning mission is a 2500nm point to point flight without payload. Anahita must be able to perform this mission without requiring any modification, the feasibility of this mission was studied in 4.2, the time of operation was assumed to be unimportant .so the parameters of Repositioning flight were determined for an operation with minimized cost. All of the parameters in this mission are the same as Fire Attack mission with the exception of cruise altitude which is 40000 ft.

3.5 Overall Configuration Selection

An airplane has four distinguishing characteristics shown in the most inner circle of Figure 21: fly-ability, controllability, navigability and economic feasibility. Each of them can be translated into the functions shown in Figure 21. The outer circle displays the physics that can be allocated to one or two of the functions they cover. As proposed in ref. [18] the configuration (physics) of the aircraft is a function of its aerodynamics, propulsion and structure that are represented by entities shown in the outer stripe. Different configurations vary in the allocation of functions and physics.

3.5.1 Configuration Figures of Merit

Based on RFP and accident investigations reports, our team decided to use the following items as their primary figures of merit to examine configurations.

- Stall Speed
- Cost

✈ Fatigue Life ✈ Flight Handling Quality

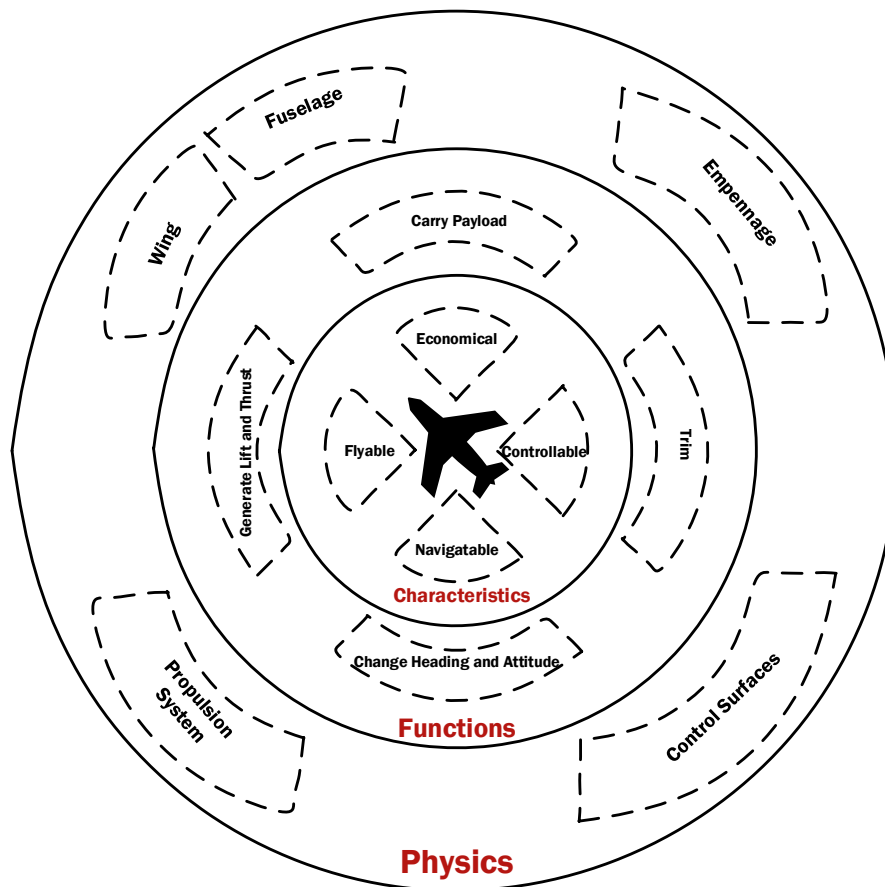


Figure 21: Aircraft Distinguishing Characteristics and Allocation of Functions and Physics

3.5.2 Viable Options

Conventional: Conventional configurations can be employed for different purposes with more ease rather than other concepts. The reason is the one-to-one allocation of functions to physics that allows modification in each entity without having direct effect on the other. Hence, the design can enjoy modularity and reduction in development cost. Furthermore, independent control inputs in the conventional configurations reduces the workload of the pilots. It can also be inferred from existing LATs and military transport aircrafts that the infrastructure for manufacturing is currently available for this type of configuration.

3-Surface: this concept can be trimmed over a wide C.G. range that provides good controllability in drop phase where there is a considerable unloading of retardant in a gusty environment and also the presence of two

sources of lift can assist in decreasing structural weight. But no aircraft in this size has yet been built, which adds uncertainty to the feasibility of design that needs to be addressed in development and test, increasing the cost.

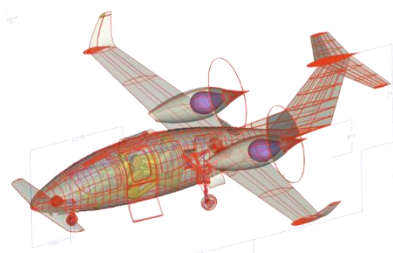
Tilt Rotor: the hovering capability of this configuration makes it the best option for retardant application, highest drop precision is achieved comparable to that of helitankers that makes the tilt rotor worth considering. For fixed wing aircraft Special provisions such as flaps, slats and other high lift devices are required to reduce speed to acceptable levels during critical stages of flight and their flight characteristics are far from optimum during low speed. The manufacturing of this configuration is expensive in comparison to other alternatives. In order to reduce the structural weight to compensate for weight of propulsion system weight, it is constructed mainly out of composite material which creates difficulty for disposal of the aircraft.

Table 8: Comparison Between Viable Options

	Conventional	3-Surface	Tilt Rotor
Divers purposes	✓	-	-
Modularity	✓	-	-
Reduced workload of pilots	✓	-	-
Available manufacturing infrastructure	✓	✗	✗
Good controllability in drop	-	✓	✓
Decreased structural weight	-	✓	-
Feasibility of design	✓	✗	-
Drop precision	-	✓	✓✓✓
Manufacturing cost	✓	✗	✗✗
Disposal difficulty	-	-	✗
STOL	-	✓	✓✓



Conventional



3-Surface



Tilt Rotor

Figure 22: Continued configurations studied by ShadX

3.5.3 Final Configuration Selection

Comparing the pros and cons of each concept against figures of merit of the design, decisions were made quantitatively and a definitive result was reached. While the conventional configuration has limitations amongst the three of them in low speed drop and C.G. control, its benefits from cost and safety point of view compensates for the shortcomings. Therefore, the conventional configuration is chosen to be the baseline for preliminary design.

4 INITIAL SIZING

Figure 23 summarizes the relationships in the iterative process of weight sizing employed by the team. Every procedure is explained in detail in the following subsections. [The project advisor B.Baleghi was of great assistance in developing tools for sizing processes.]

4.1 Weight Sizing

After mission profile was set in section 3.4, weight ratios are estimated based on methods suggested by ref. [19]. And the performance parameters of the mission are initially estimated. These estimates of the parameters will be corrected after each iteration shown in Figure 23 until the takeoff weight of Anahita is defined with 0.5% error margin [19].

Additionally in the climb phase, the possibility of separate sections each having a different rate of climb (RoC) was studied, since the calculation methods for climb weight fraction in a single flight path as suggested by [20] and [21] result in constant RoC and are not accurate enough in the case of climb to high cruise altitudes, the climb phase was broken into three separate sections and parameters were calculated independently in each section. The design is aided by this accuracy in determination of the optimal cruise (out/in) altitudes. As the design objective of increasing effectiveness dictates, the mission parameters must be optimized. The tradeoff here is the fact that Anahita can reach higher cruise speeds in higher altitudes which may lead to reduction in time to establish a fire line, but more fuel is consumed as it climbs to higher altitudes, losing its effective range of operation as a result.

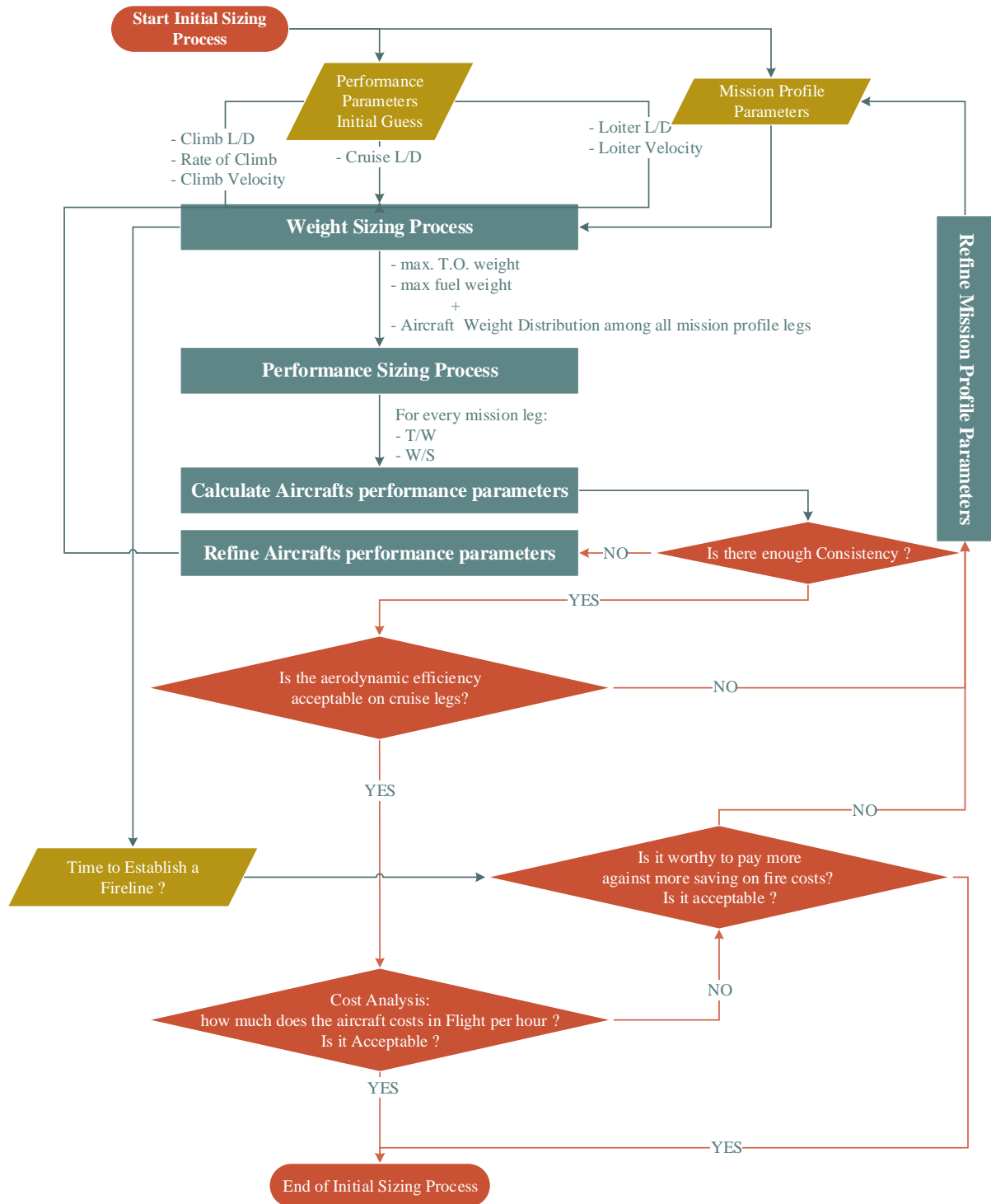


Figure 23: Initial Sizing Procedure

4.1.1 Drag Polar Estimation

For this class of design, a second order drag polar estimation model is employed. Based on the class in which Anahita is categorized, the value of zero lift drag coefficient is assumed to be 0.0175 from Tables 4.12 and 5.2 of Reference [22]. For the induced drag portion of drag polar, some geometric parameters should be defined first.

Table 7.1 of Ref. [22] provides various effects of increasing aspect ratio on airfoil and planform. The only undesirable effects of increasing aspect ratio are on wing weight and wing fuel capacity; initial studies of the team showed that the maximum fuel volume required for Anahita is far less than fuel volume capacity of the wing. Typical values of aspect ratio for “low-subsonic transports” and “high-subsonic transport” are 6-9 and 8-12, respectively [23]. An aspect ratio of 10 is was decided for Anahita at this level of design. The estimated aspect ratio and C_{D0} were evaluated in a parametric study in section 6.1. An Oswald efficiency factor of 0.85 was assumed.

4.1.2 Maximum (L/D)

To determinate performance of Anahita in mission phases, an estimate of $\left(\frac{L}{D}\right)_{max}$ is needed. Using equation (3.10a) of Ref. [22] and 2nd order drag polar model a value of 19.5 for $\left(\frac{L}{D}\right)_{max}$. This value is reasonable based on typical values of jet transport category (12 to 20 according to Table 4.5 of Ref. [23]) and also based on Figure 5.3 of Ref. [22] for a wing aspect ratio of 10.

4.1.3 Engine Specific Fuel Consumption

According to the engine databases, new turbofan engines SFC are ranged between 0.30 to 0.4 [lb./h/lb.]. A value of 0.4 was assumed as the worst case scenario in this design level. After engine selection in section 7.6 the SFC was corrected to 0.31 in accordance with the new engine.

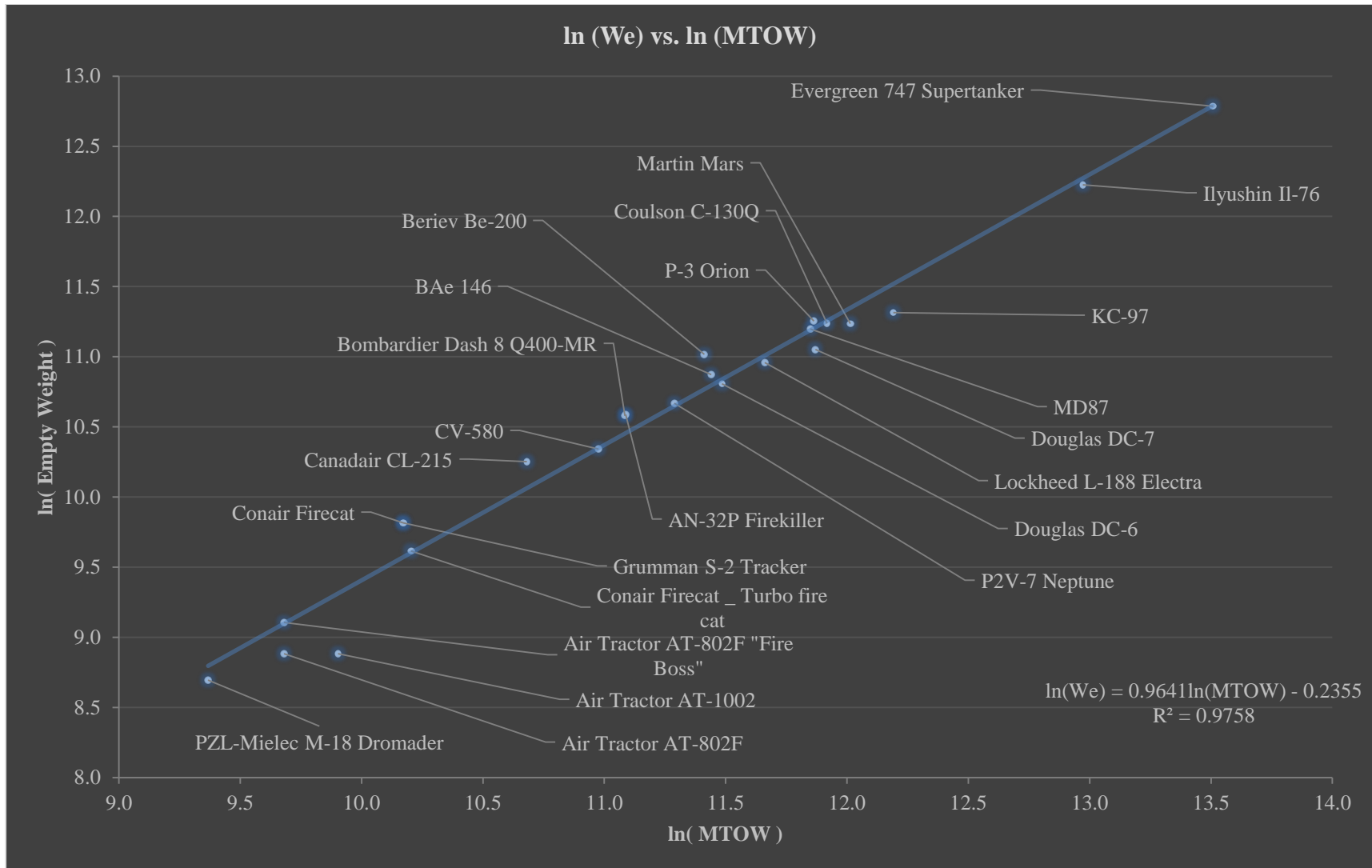


Figure 24: ln (We) vs. ln (MTOW)

4.1.4 Performance Parameters Initial Guess

Performance parameters needed to be initially guessed are in three phases: climb, cruise, and loiter.

4.1.4.1 Climb Parameters and Strategies

Based on Figure 23, three parameters that should be guessed for climb phase are: Climb L/D, Climb Speed, and Rate of Climb. Climb phase can be carried out by three strategies: Maximizing RoC, Minimizing Time to Climb, and maximizing Climb Flight Path Angle Strategy.

First two strategies are from same base, which is climb as fast as possible, but the third one is about minimizing horizontal range flown by LAT. According to “Objective Hierarchy” effective LAT firefighting is achieved if time to establish fire line and operation cost both minimized. From the strategies above, the third one is selected as ShadX team climb strategy. Based on chapter 9 of ref. [24], lift coefficient during climb phase is equal to the lift coefficient in maximum L/D, in this climb strategy.

RoC initial guess for climb after takeoff is 1000 feet per minute and for climb after drop is 1200 feet per minute. Climb speed initial guess for both climb phases is 180 kts.

4.1.4.2 Cruise Parameters and Strategies

Based on Figure 23, only Cruise L/D should be estimated to start weight sizing procedure. Firefighting mission includes two cruise phases, one dash-out and the other dash-in.

There are several strategies for cruise phases. ref. [19] and [23] benefit from altitude varying cruise strategy (constant velocity and AoA) for preliminary design calculations. ref. [24] states that for minimizing fuel consumption while range is constant, the jet-driven plane should fly in $\left(\frac{C_L^{1/2}}{C_D}\right)_{max}$ condition. Since altitude and speed of cruise are predefined, only L/D is to be estimated via using Table 3.2 of ref. [22].

4.1.4.3 Loiter Parameters and Strategies

Based on firefighting mission profile, there will be a 5-min loiter phase after each drop. As Figure 23 shows, two parameters should be guessed for loiter phase; L/D and speed.

Loiter phase can be carried out based on several strategies. Ref. [19] and [23] use velocity varying loiter strategy (constant altitude and AoA) for preliminary design calculations. ref. [24] states that for minimizing fuel consumption while loiter time is fixed; the jet-driven plane should fly in $\left(\frac{L}{D}\right)_{max}$ condition. Since altitude and duration of loiter are predefined, L/D and speed of loiter are to be estimated with the help of Table 3.2 of ref [22]

Initial guess for average airplane speed during loiter phase is 200 kts. Consider that, this parameter will change during iterations.

4.2 Performance Sizing

After determination of weight breakdown, performance analysis should be carried out for critical conditions so the design point on the matching diagram could be defined. Based on system level requirement presented in section 3.3, mission of the LAT will be analyzed.

4.2.1 Stall Speed

Due to system level requirements mentioned in section 3.3, Anahita shall have a stall speed of 90 kts or below.

4.2.1.1 Critical scenarios

All critical points of the mission should be defined considering the stall speed constraint. Stall speed is more important during drop maneuvers or cruise at low speeds, so three candidates for the most critical points, namely drop maneuver, approach and landing are further examined.

The speed of Anahita during takeoff phase is low as well, but acceleration plays a crucial role in preventing it from stalling. On the other hand, calculations in section 0 show that with a stall speed of 90 kts or higher during takeoff, balanced field length requirement is satisfied.

There are three C_{Lmax} correlated to three flap positions: Takeoff, Approach and Landing.

$C_{LmaxDrop}$ should be defined with respect to stall requirement. The values for C_{Lmax} for all critical mission legs, due to different flap positions, are assumed as listed below:

$$C_{LmaxDrop} = 3.1 \quad C_{LmaxT.O.} = 3.3 \quad C_{LmaxApproach} = 3.3 \quad C_{Lmax@Landing} = 3.7$$

Feasibility of parameters above should be checked in the high lift devices sizing section.

- **Drop Maneuver:** The first drop of Anahita is the most critical of all due to higher weight. A scenario in correspondence with the critical stall speed during drop operation was developed, in which Anahita starts to pitch up in the mid part of the drop maneuver. Table 9 shows stall speed in these critical conditions in accordance with the requirement.

Table 9: Stall Speed Condition in Drop Phase

Stall Speed Requirement @ Drop				
Airtanker Weight [lb.]	Flap Position	Altitude (S/L) [ft.]	Atmosphere Condition [°F]	Maneuver Load Factor
Start point of drop – 1/6 max. Payload Weight	Drop Position	300	ISA+75	1
$(W/S)_{T.O.}$ [lb./ft ²]		82.6		

- **Approach:** Based on the definition of approach phase mentioned in the 3.4.1, Table 10 presents the stall critical conditions in the approach phase.

Table 10: Stall Speed Condition in Approach Phase

Stall Speed Requirement @ Approach				
Airtanker Weight [lb.]	Flap Position	Altitude (S/L) [ft.]	Atmosphere Condition [°F]	Maneuver Load Factor
Start point of Approach	Approach Position	Avg. Altitude (Cruise-in & Landing)	ISA+35	1
$(W/S)_{T.O.}$ [lb./ft ²]		88.7		

- **Landing :** Stall speed requirement for landing should be considered at the maximum landing weight. The maximum landing weight can be calculated in a normal procedure or a critical procedure. As the worst case scenario, in the latter the landing weight is equal to takeoff weight Table 11 shows the stall critical conditions in the landing phase in accordance with stall speed requirement.

Table 11: Stall Speed Condition in Landing Phase

Stall Speed Requirement @ Landing				
Airtanker Weight [lb.]	Flap Position	Altitude (S/L) [ft.]	Atmosphere Condition [°F]	Maneuver Load Factor
Max. Landing Weight	Landing Position	5000	ISA+35	1
$(W/S)_{T.O.}$ [lb./ft ²]		82.7		

Furthermore, in the next calculation loops regarding the importance of “T.O. W/S”, the zero-thrust stall relation is enhanced by considering Thrust Installation Angles; this was assumed to be around 3 degrees in this design level.

4.2.2 Climb Gradient

Requirements for Climb Gradient are mandated by FAR 25. The equations to satisfy the gradients and the requirements are presented together in section 3.4 of ref. [19].

4.2.3 Maximum Cruise Speed

In general, each mission has different profiles hence different speed and altitudes. Calculations in this section are based on the equations presented on section 4.3.3 [23], the max cruise speed of the plane was calculated separately for each of the cruise phases; the maximum cruise speed is assumed to be 1.05 times the design cruise speed for all cruise phases.

4.2.4 Balanced Field Length

The RFP requires Anahita to have a BFL of no more than 5000 ft. The initial studies of performance team suggest that, in proposed conditions, the worst case scenario for balanced field length occurs when the speed reaches $1.2V_s$ and deceleration to complete stop is preferred. Equation 6.90 of ref. [25] suggests an equation for takeoff field length. Manipulating this equation will lead to a relation that gives the thrust loading. In this equation, the coefficients of friction for brakes on and off are needed. Table 6.1 of Ref. [25] and Table 10.3 of Ref. [22] provide such data. Moreover, the deceleration is also dependent on thrust-reversers.

$$\Rightarrow \left(\frac{T}{W}\right)_{\max@sea\ level} = \frac{\frac{K_A V_1^2}{e^{Sg \times 2g \times K_A} - 1} + \mu_r}{\frac{\rho}{\rho_0}} \quad \& \quad a_d = a_{dBrakes-on} + a_{dThrust\ Reverse} \quad \& \quad \mu_r = (\sim 0.04)$$

$$a_{dThrust\ Reverse} = -\frac{(Thrust\ Reverse\ Ratio \times Thrust\ @T.O.)}{\frac{W_{\max T.O.}}{g}}$$

$$0^2 - V_1^2 = 2a_d \cdot \Delta x_d \Rightarrow \Delta x_d = -\frac{V_1^2}{2a_d} = -\frac{1.2^2 \times V_{StallT.O}^2}{2a_d} \Rightarrow \Delta x_d = BFL - \Delta x_d = S_g$$

4.2.5 Drop Maneuver

According to Ref. [26] load factors experienced by P3As during drop maneuvers reach 2.5. However, in about 90% of all drop maneuvers, the experienced load factor is lower than 1.7. Operational scenarios will be discussed for determining maximum acceptable load factor for Anahita in various drop altitudes.

4.2.5.1 Drop max. Allowable Load Factor Scenarios

According to ref. [27], Anahita should have a stall speed of 90 kts in altitudes below 300 ft., here 300 ft., will be considered above sea level. For a load factor of 1 the V_{stall} requirement is passed and the scenarios with the allowable load factor will be explained.

Maximum drop speed is 150 kts, which is 1.67 times V_{stall} (90 kts). V_{stall} in drop leg @300ft. above mean sea level is 90kts. For higher altitudes like 5300 ft., (According to RFP T.O. will take place from 5000 ft. above sea level, so it is safe to assume that a majority of firefighting operations will take place in 5300 ft.), stall speed will increase to 105kts. Anahita should carry out drop operation at altitudes in which speed and stall speed are in safe distant from each other. The safe distant is assumed to be 10% of stall speed, which means Anahita should have speed more than $1.1 V_{stall}$.

Stall speed is proportional to square root of load factor. According to Figure 25, @300ft. above mean sea level maximum allowable load factor is 2.3. Note that increment in load factor is due to maneuver pattern, derived gusts, weight loss, and other factors.

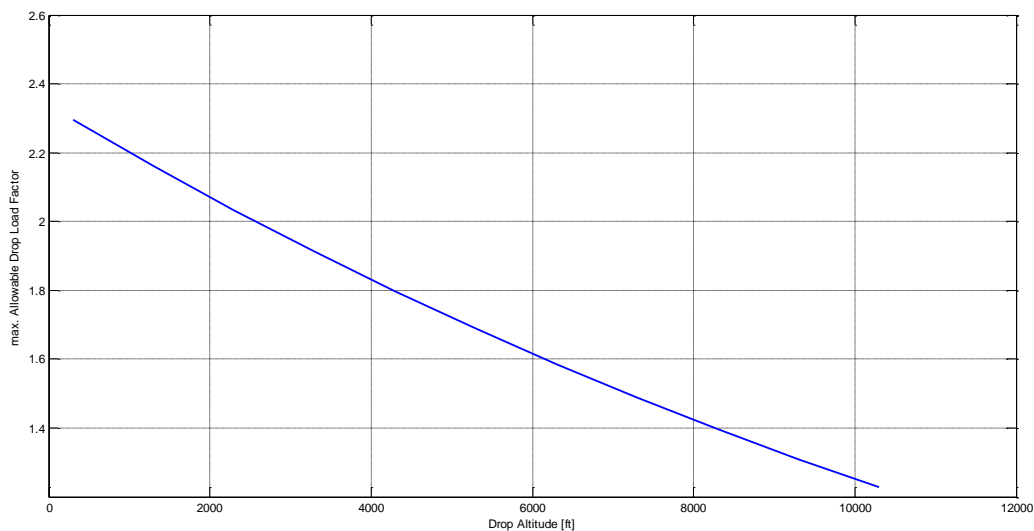


Figure 25: Max Allowable Drop Load Factor vs. Drop Altitude

According to ref. [26] P3As are operated below 1.7 load factor in 90% of operations. Based on the Figure 25, it is deduced that if Anahita carries out drop operation @5300 ft. above mean sea level its maximum allowable load factor will be 1.7.

4.2.5.2 Max. T.O. Thrust Loading due to drop phase

Equation 4-1 for calculation of drop thrust loading has been derived, considering constant value of drop load factor; derivation is left in APPENDIX B Drop altitude is assumed to be 5300 ft. above mean sea level and load factor is assumed to be 1.7.

$$\left(\frac{T}{W}\right)_{drop} = \frac{\frac{1}{2}\rho V^2 C_{D_0}}{\left(\frac{W}{S}\right)_{drop}} + \frac{Kn^2 \left(\frac{W}{S}\right)_{drop}}{\frac{1}{2}\rho V^2}$$

Equation 4-1

The parameters $\left(\frac{T}{W}\right)_{drop}$ and $\left(\frac{W}{S}\right)_{drop}$, should be corrected to $\left(\frac{T}{W}\right)_{max. T.O.}$ and $\left(\frac{W}{S}\right)_{T.O.}$, using appropriate correction factors.

4.2.6 Ceiling

Two missions result in three sets of cruise parameters. According to ceiling definition derived from ref. [23], calculations in this section are based on climb rate of 300 feet per minute at cruise ceiling. The relations used are derived from chapter 4.3.6 of ref. [23].

4.2.7 Typical Trends

Wing Loading and Thrust Loading for similar aircraft will be analyzed in this section in order to compare Anahita with other aircraft.

The power plant system for Anahita is turbojet and it is categorized into military transport and bomber category. Based on the table 6.1 of ref. [22], the desired takeoff wing loading for this category is 50~100 (pound per feet square). Also the table 18.1 of ref. [22] states that expected maximum takeoff thrust loading for this category is 0.3~0.45.

According to the sizing procedure shown in the Figure 23, other factors influencing decision on selecting appropriate mission is discussed; for instance, effects of mission parameters on flight hour cost and the time needed to establish a fire line which defines mission effectiveness of LAT.

4.3 Performance Parameters Consistency

The assumptions made in the section 0, should be validated in this section, so the estimated parameters are calculated here again, and then these parameters are fed back to the previous section. This iteration goes on unless the parameters converge, over convergence criterion of 500 lbs. on max. T.O. Weight.

4.3.1 Calculate Aircrafts Performance Parameters on Mission Profile

Three groups of parameters should be guessed so that weight estimation could start. These groups are: Climb Parameters, Cruise Parameters, and Loiter Parameters.

4.3.1.1 Climb legs

Weight sizing will be done for two missions of firefighting and repositioning, which are described before in section 3.4.

Climb phase is divided to three parts to get more accurate results. Horizontal displacement in climb phase is calculated more accurately using three sets of climb parameters. This accuracy will result in more accurate determination of cruise leg range; used to find the best cruise (out/in) altitude. Weight at the start and end of each phase will leads to estimation of avg. climb speed of each part, by using appropriate C_L values based on climb strategy, section 4.1.4.1. L/D of climb is estimated using drag polar model of section 4.1.1. Rate of climb will be calculated by using calculated LATs max. Thrust loading value, which leads to calculation of climb flight path angle.

4.3.1.2 Cruise legs

Efficient cruise speed and altitude may be different between dash in and dash out because of different weight of aircraft in these phases. Avg. cruise L/D at each phase will be calculated based on LATs weight and velocity at the start and end point of each cruise phase; the value will be feedback to next sizing calculation loop.

4.3.1.3 Loiter legs

Considering the definition of loiter, the repositioning mission cannot have any loiter phase. However, there will be 5-min loiter before and after each drop in firefighting mission. Loiter phase before each drop is essential, because the LAT crew should examine the environmental and fire parameters (such as wind speed, fire speed, etc.) so that they could decide how to approach drop zone and how to perform drop maneuver. Loiter after each drop also helps crew to get feedback from the previous drop, so that they can aim better this time. Loiter phases will help to improve effectiveness of LAT firefighting, due to the ASM's lead of the plane.

Understanding of weight at start and end point of each loiter will lead to calculation of its avg. L/D and velocity value; by using appropriate C_L values based on loiter strategy, section 4.1.4.3

Hence, the procedure of mission refinement are as follows:

parameters calculated here → correct weight sizing input values

→ corrected MTOW & weight breakdown → affect performance sizing output

4.4 Cost Analysis in Performance

As explained in the section 3.3, two primary design objectives for Anahita are the cost and the effectiveness; the first one means reducing LAT life cycle cost and the second one is about minimizing time to establish a fire line.

As discussed in the section 3.4, some of the parameters pertaining to cruise altitude and speed are remained undefined. Changing cruise speed and altitude will affect time to establish a fire line and fuel consumption, which leads to a change in the operation cost. In this section economic performance analysis has taken place so that the most effective firefighting mission will be determined. The LAT sizing and mission refinement algorithm is shown in the Figure 23.

4.4.1 Flight Hour Cost

The parameter for cost of LAT operation is FHC (Flight hour cost). The breakdown of the LAT life cycle cost is presented in section 5. Based on system level requirement mentioned in section 3.3, the proposed LAT should have FHC less than 6000 \$/hr. To adhere to this limitation, the fuel consumption should be reduced. To increase operational efficiency, LAT should fly as high as possible while it is minimizing time to reach the fire zone. Efficiency of cruise phase depends on lift coefficient range at which airplane is cruising.

4.4.1.1 Analyze Aircrafts Aerodynamic Efficiency On Cruise Legs

One of the critical points of an airplane design which is losing great amount of its weight during operation is maintaining operational efficiency while cruising in or cruising out. The cost of operation will increase greatly if cruise operational efficiency decreases since cruise phase is a large portion of the mission. For maintaining the cruise operational efficiency drag coefficient deviation should be too small while lift coefficient is changing due to weight loss.

4.4.1.1.1 How to refine Mission Profile?

Due to major changes in the weight of aircraft in dash in and dash out phases, for preserving the operational performance of the plane in both of these phases, special considerations to the mission is needed. Due to the loss of weight in the dash in vs. dash out, the speed and altitude in the dash in against the dash out should be varied

in a manner that the lift coefficient employed by the plane in both phases be in the appropriate range. Thus, increasing the flight altitude in dash in against the dash out, in addition to reducing the speed in dash out vs. dash in, is one of the choices that can be used to increasing the operational performance of the plane. But on one hand reducing the flight speed will increase the time to establish a fire line; on the other hand, increasing the cruise altitude will increase the time for climb and descent, which can be lead to lowering the operational performance and increasing the operation cost.

4.4.2 Fire costs

The effectiveness of the mission depends on the time for a fire line establishment; because the fire is spreading with a considerably high rate & this means more cost for the system. Lowering the flight time of 4 sorties will lead to less burned forests which leads to less expenses. In the section 4.4.2.1, a mathematical model for evaluation of the hourly forest fire cost will be presented. This model helps to define how much reducing a minute of a fire line establishment time will affect the fire costs paid by the government. The fire cost is imposed in a long-term period; however, the operation cost is imposed in a short-term interval.

4.4.2.1 Fire Cost Model

First, fire spread model should be defined according to ref. [28]. This model depends on the tree type, wind speed, temperature and etc., which here a simple model will be developed for fire spread estimation. The cost of each acre burned will be estimated (according to Ref. [29]) & with combining these 2 parameters the cost of fire will be evaluated.

Fire spread will be considered elliptical. Fire speed in each direction is related to wind speed (Figure 8 in Ref. [28]) and in this manner, fire growth can be modeled. In Ref. [29] cost estimation of 100 burned acres has been provided, so there is a criterion to convert burned acres to cost. Note that in ref. [29] a range of values has been reported and here the best guess value is used.

4.4.2.2 What is the time needed to establish a fire line?

According to ref. [27], there should be 4 sorties with the range of 200 nm from base to fire zone to establish a fire line. The time needed for completing these 4 sorties are time of 4 flight operations plus time of 3 ground operation.

Each sortie will be based on a mission profile that has been described in section 3.4. This mission will consist of T.O, climb, dash out, descent, loiter and drop, climb, dash in, descent, approach, and landing. The flight time of each sortie is equal to the sum of these periods and the whole missions time will be equal to 4 of these mission profiles. The increase in cruise speed and lowering the altitude, are the factors that will reduce the total time; Even though flying with high speed in low altitude, will increase the operational cost.

Beside flight time, ground operation time is also important in determining total time to establish a fire line. The ground operation includes moving LAT from landing location to reloading station, reloading operation, moving to refueling location, refueling operation, preflight checks, and moving to takeoff runway. According to the ref. [30] simultaneously reloading and refueling is not permitted, then these operations should be carried out in series.

Number of refueling operations per fire line establishment is a significant parameter since it affects the maximum takeoff weight, operation time, and consequently FHC. It is obvious that number of refueling operation depends on fuel capacity.

4.5 Drop Maneuver Scenarios

The firefighting mission dictates 4 sorties each including 3 drops is needed to establish a fire line. According to 6.1 it has been decided that the LAT fuel tank should have capacity for 2 sorties. Two sorties each including 3 drops means 6 drop operations per refueling. The main difference between these drop phases is the weight of LAT during drop. In this section max allowable gust velocity of 6 drop phases will be compared with each other based on the max permissible load factor, described in section 4.2.5.1.

4.5.1 Drop Gust Velocity Scenarios

In the drop operation, Anahita gets so close to the fire and near fire there is an up wash flow which affect Anahita as a gust disturbance. As said in the section 4.2.5, for any altitude there is a maximum allowable load factor. In this section max allowable gust velocity for each drop altitude is presented in Table 12.

Gust is modeled as induced angle of attack which cause an increment in lift force and consequently an increment in load factor. Note that for sake of feasibility study in the preliminary phase of design $C_{L\alpha}$ is assumed to be $2\pi \left[\frac{1}{rad} \right]$.

Table 12: Max Allowable Drop Gust Velocity scenarios

Max. Allowable Drop Gust Velocity [ft/s]	Drop Altitude (above Sea Level) [ft]				
	300	3300	5300	7300	9300
1 st drop – 1 st sortie	52	36	27	19	12
2 nd drop – 1 st sortie	45	31	24	17	11
3 rd drop – 1 st sortie	37	26	20	14	9
1 st drop – 2 nd sortie	50	35	26	18	12
2 nd drop – 2 nd sortie	42	30	22	16	10
3 rd drop – 2 nd sortie	35	24	18	13	8

5 LIFE CYCLE COST ANALYSIS

In the following section a detailed breakdown of the so called "Anahita" Life Cycle Cost and a suitable model to assign values to main parameters affecting "Total Cost" is presented. This is followed by a forecast related to the number and size of wildfires which is used for the succeeding sub-sections. Finally, we propose a proper acquisition plan for the Anahita fleet where all three main stakeholders that is manufacturer, operators and the government agency clearly observe their benefits during service life of the Anahita fleet. (The project advisor S.Khosroabadi was of great assistance in developing cost models.)

5.1 Aircraft Life Cycle Cost

An appropriate estimation of the total ownership cost is desired in order to minimize it as indicated in RFP. The proposed estimation methods have the same principles but they differ in values of coefficients. Anahita plays a role comparable to a military aircraft rather than a commercial one. Hence, a military O&M estimation which was proposed by ref. [31] is used. For RDTE and acquisition estimation, the method recommended by ref. [22] was employed by the team in order to achieve a model with desired accuracy. All values are in 2016 dollars ref. [32]. Figure 28 shows a detailed view of LCC structure.

5.1.1 Basic Decisions Related to the Research, Development, Test and Evaluation (RDTE)

- ➔ **Research:** research is concerned with developing and integrating new technologies used in design. In order to minimize LCC and meet the desired entry into service date, ShadX decided to use available technologies and off the shelf equipment. Therefore, the research cost is estimated to be zero.
- ➔ **Development, Test and Evaluation:** the required cost to engineer, fabricate and test. The minimum number of test aircrafts is 2 as indicated in [22]. However, ShadX decided that 3 test aircrafts are required since the history of LAT accidents calls for more accurate work in the test phase. Another important contributor to the DTE cost is test facilities. Anahita would benefit from existing test facilities therefore; the cost of test facilities is assumed to be zero. As the process of manufacturing is slow in the beginning, the test aircrafts comprise most of the DTE cost as depicted in Figure 26.

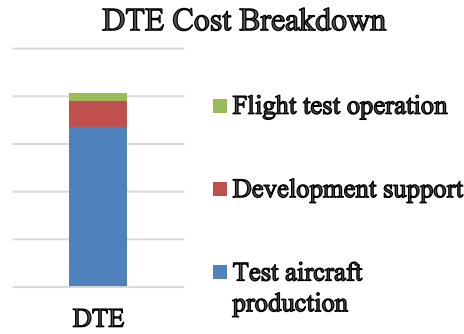


Figure 26: DTE Cost Breakdown

5.1.2 Basic Decisions Related to the Acquisition Cost

Acquisition is the cumulative cost for production of a desired number of aircrafts and associated ground equipment. It is also worth mentioning that airframe engineering, tooling, manufacture labor, quality control, manufacturing material & equipment and engine cost are involved in both DTE and acquisition cost. The required man-hours are multiplied by their hourly rate so as to give an estimation of the aforementioned contributors to cost. Also the cost of manufacturing facilities is presumed to be zero due to the exploitation of the existing ones.

These estimations are based on number of aircraft, aircraft empty weight and maximum speed except for engine cost estimation which is based on maximum thrust, maximum Mach number, turbine inlet temperature and number of aircrafts. Figure 27 exhibits the detailed breakdown of acquisition cost.

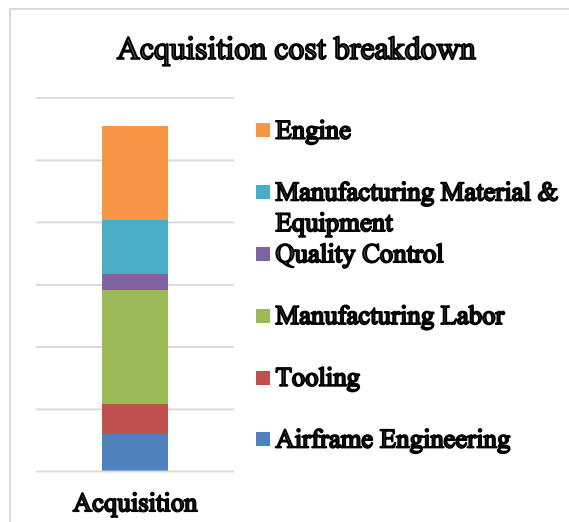


Figure 27: Acquisition cost breakdown

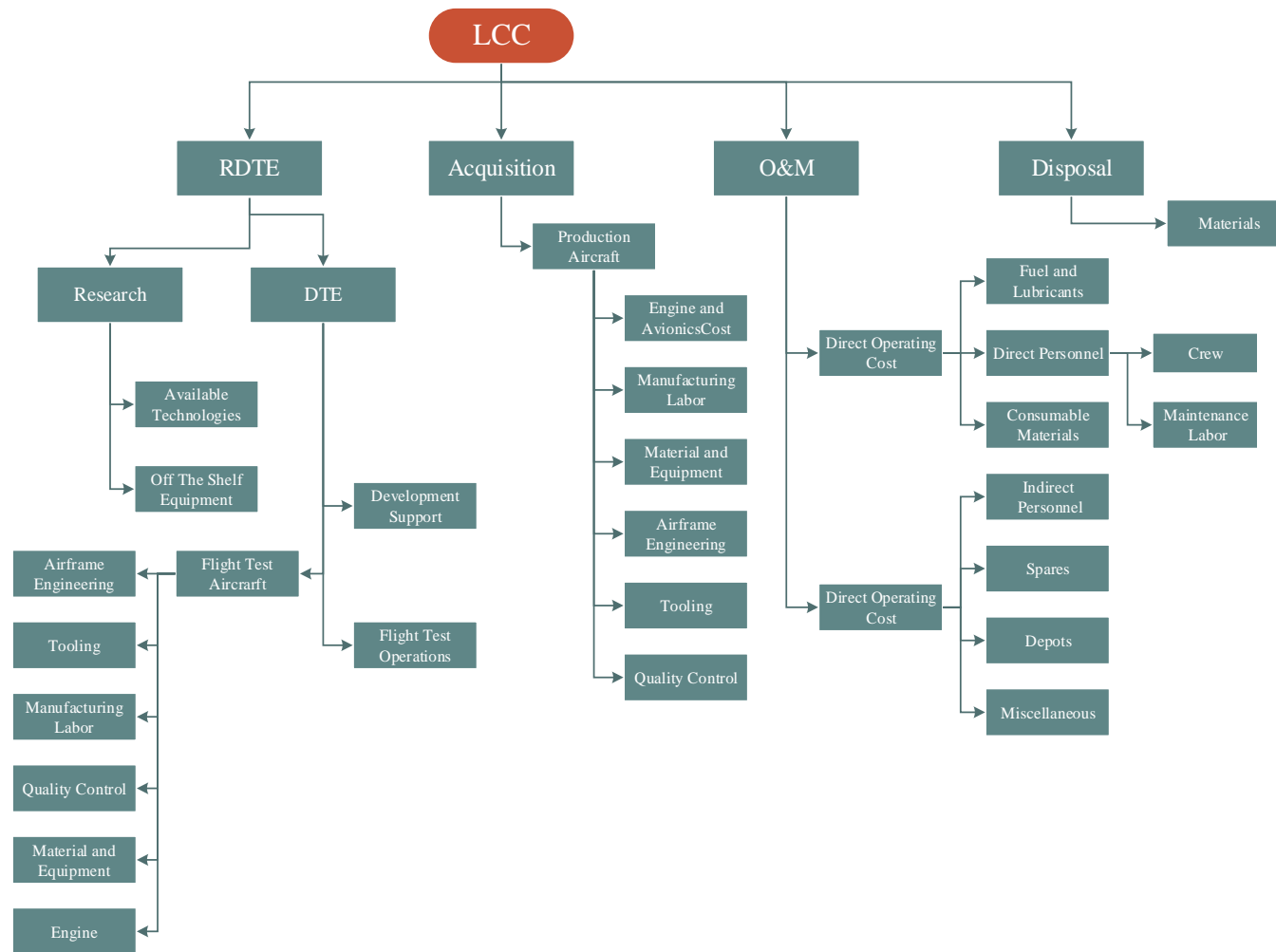


Figure 28: Detailed LCC Contributing Items

5.1.3 Operation and Maintenance (O&M)

Main contributors to O&M cost are presented briefly in below:

- ➔ **Fuel and lubricants cost:** cost of lubricants is considered a constant fraction of 0.5% of fuel cost. Jet A1 is the fuel that is consumed by the engine and fuel price is based on [33] by April 2016.
- ➔ **Direct personnel cost:** consists of aircrews and direct maintenance personnel cost.
 - **Aircrew cost:** Mean USFS pilot salary is based on [34] is 90000\$ per year. The number of crew personnel is 2 and flight hours of each pilot is similar to transport and bomber pilots which is under 1200 flight hours per based on [22] so the crew ratio is considered to be 1.5 for an LAT. An overhead ratio of 3 is considered in calculations regarding aircrew cost.
 - **Maintenance personnel cost:** in order to find maintenance personnel cost, maintenance man-hours needed per flight hour (MMH/FH) is multiplied by maintenance labor rate. MMH/FH is estimated with respect to empty weight and engine characteristic.
- ➔ **Consumable material cost:** some materials and parts are used during each maintenance and to account for their cost, average cost of materials used per maintenance hour is multiplied by MMH/FH.

5.1.3.1 Constant fractions of total O&M cost

The following parts of O&M cost, a constant fraction was utilized as instructed by [31]:

- Spares: 0.18 of O&M cost.
- Indirect personnel: 0.2 of O&M cost.
- Depot: Maintenance actions are done in depots and its cost is considered to be 0.2 of O&M cost.
- Miscellaneous: 0.05 of O&M cost
 - Technical data support for maintenance functions
 - Training, training data and training equipment
 - Support equipment

Relative values of key contributors to O&M cost are presented in 5.1.3.

5.1.3.2 RPV O&M cost

Manned and Unmanned aircraft differ significantly in RDTE and O&M costs. Based on the strategies of cost adopted by the team, transition to a RPV version occurs when the required technologies are fully developed and flight proven for an aircraft the size of Anahita. By that time, infrastructure needed to operate an unmanned LAT will be available. The O&M cost remains the main difference between the two options as a result.

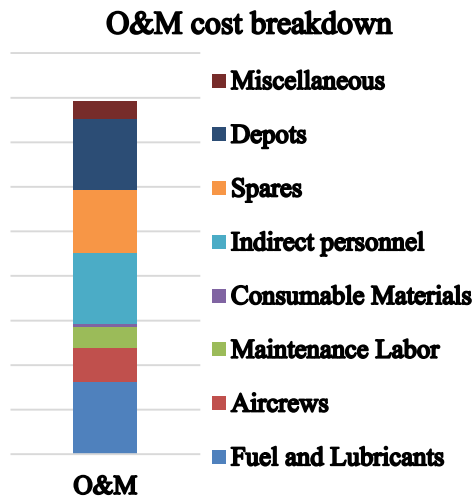


Figure 29: O&M Cost Breakdown

Despite the fact that the RPV version of Anahita can ideally be lighter than its manned counterpart, taking into account the cockpit equipment and environmental control systems can be removed [35], RPV cost was estimated for the aircraft of equal weight. Therefore, the only difference is considered to be the aircrew cost. Workloads are greatly reduced for remote pilots, in such a way, one pilot can handle an entire aircraft while maintaining the same workload as before. The salary remains the same as a result, although the insurance fees are reduced because the pilot's working environment has rendered less hostile. An overall overhead ratio of 2 was determined.

5.1.4 Disposal

Disposal of an aircraft will become an option when the following takes place:

- Increase in O&M and repair costs.
- Difficulty to meet new/changed legislative and environmental requirements.
- Difficulty to meet upgrading requirements and expensive tech upgrades.
- Difficulties with the production and procurement of spare parts.
- Increasing content of time or service expired parts.
- Decision to replace the obsolete aircraft to replace aircraft fleet from other reasons [36].

5.1.4.1 Disposal Process and Procedures

There are 2 international programs for end-of-life aircraft, PAMELA, initiated by Airbus, and AFRA by Boeing. Since, the main customer of this aircraft is USFS, AFRA will be used as a base in this report [37].

After the decision has been made to retire an aircraft the following measures should be taken to complete the disposal sequence [38].

- ➔ **Storage:** The aircraft is stored at special parking areas or at the boneyard waiting to get decommissioned.
- ➔ **Decommissioning:** When the order is given that aircraft has been officially retired. (the criteria that was mentioned in the previous section)
- ➔ **Disassembling and Dismantling:** The aircraft is sent to one of the AFRA member companies for disassembling and dismantling.
- ➔ **Valorization:** In this stage the productive use of resources that has been found during the last 4 phases is desired.
- ➔ **Recycling or disposal:** The aircraft is sent to one of 4 AFRA members companies for recycling or disposal [39].

5.1.4.1.1 Engine Recycling

There are several applications with engine recycling:

1. Re-use and repair the parts in the engine overhaul process and feed these parts into their engines repair network. Which will result in less cost for engine repairing process.
2. Parts that cannot be repaired will be recycled for their material
3. There are materials that classed as aerospace standard material (e.g. platinum bond coat underneath the thermal barrier coating on the turbine blades) these will processed back into the manufacturing.
4. 75% of the metals used in the engine will be recycled.

5.1.4.1.2 Composite Recycling Techniques

According to T. Suzuki and J. Takahashi's findings the Energy to recover carbon fiber is 1/10th that to make new fiber so we will mention 3 recycling techniques for recycling carbon fiber: A nitric acid treatment to dissolve/remove the thermostat resin, thermal pyrolysis, and an incineration process [36].

5.1.4.1.3 Disposal Cost

The cost of disposing of airplanes depends on the type of materials used in construction and/or in operation. Disposal consists of: **Temporary storage, draining of liquids and disposal thereof, disassembly of engines and certain systems, and cutting up of the airframe and disposal of the resulting materials.**

Disposal cost is partially offset by resale value of materials. Care should be taken on materials which pose a danger to environment, they have to be disposed with care. Only in detailed level of design is that the cost of disposal can be estimated with credibility.

5.2 Wildfire forecast

Wildfire behavior changes as time passes, the growing number of wildfires in a year affects the duration of firefighting missions for LATs and the increased size of wildfires demands more firefighting operation hours. For a LAT with a minimum service life time of 20 years, the size and frequency of wildfires must be predicted. Ref. [29] shows an ascending trend in number of fires and acres burned from 1985 to 2013.

Additionally, from 2002 to 2012 almost 20 million gallons of retardant is dropped by airtankers every year [40]. As more acres are burned, more retardant is to be delivered to wildfires. This can be translated into increase in the frequency of fire attack missions.. On average, 235'294 gallons of fire retardant was delivered to each acre of a fire in year 2006 [41]. Exploiting the given data, one can predict that the amount of fire retardant delivered to an acre of fire per year increases as drawn in Figure 30. As a result, there will be 2.72 acres increase in fire size which leads to 640'000 gallons rise in the delivery of retardants to an acre of fire annually.

It can be observed in Figure 31 that a 5'000-gallon capacity LAT will make 10'912 sorties in 2060 in contrast to 4'000 sorties in 2004.

Furthermore, the duration of fire season will grow each year. This growth could be as much as 10 to 30 percent in about 85 years [42]. This means that the current LAT contracts of 160 days could reach 208 days by 2100 and an average of 4 days is added to fire season every 7 years.

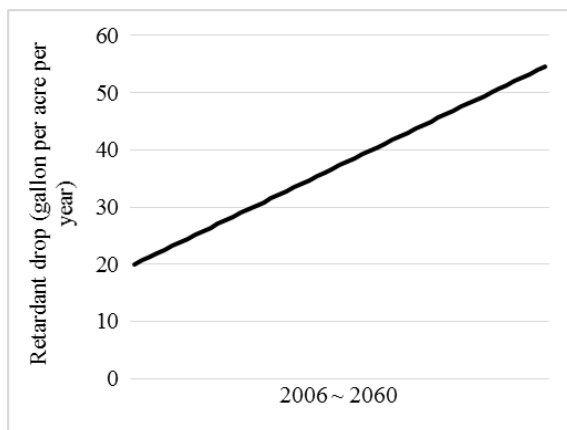


Figure 30: Annual Retardant Drop per Acre

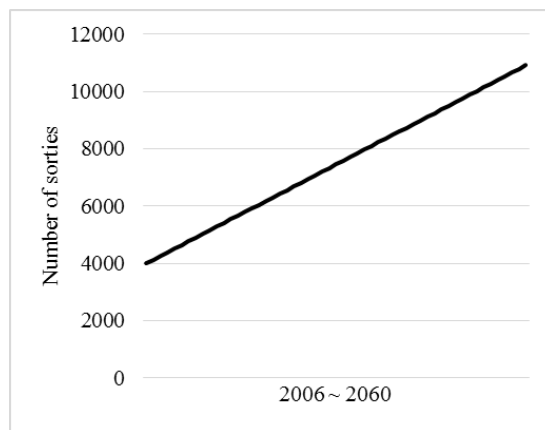


Figure 31 Prediction of number of sorties (based on a 5000 gallon airtanker)

5.3 Acquisition Plan

For the project to be feasible, a coherent acquisition plan is essential in which each of the interested parties is encouraged to partake. For the previous statement to become a reality, the expectations of players must be satisfied.

The reader must consider that the proposed plan is not a complex one, the error corresponding to the available cost estimation model is the reason that renders simulation of detailed models futile. In other words, the effort is to avoid getting into the trap of detailed complexity while simulating an acceptable dynamic complexity. Core players are introduced in the following (Figure 32):

- ➔ Operator (Private Contractor)
- ➔ Manufacturer
- ➔ Government (USFS)

In the acquisition plan, different scenarios in which three players interact are examined. The first player, the manufacturer, determines the unit cost of each LAT which is highly dependent on the predicted number of units to be produced. As the second player, USFS pays for the expensive aerial firefighting operations and in return, profits from preserving forest areas. As will be discussed later, the USFS will lose incentive to stay involved in the game if the cost of contracting exceeds their budget. The LAT operator of private sector is the third player in the proposed acquisition plan and must always be able to earn a profit.

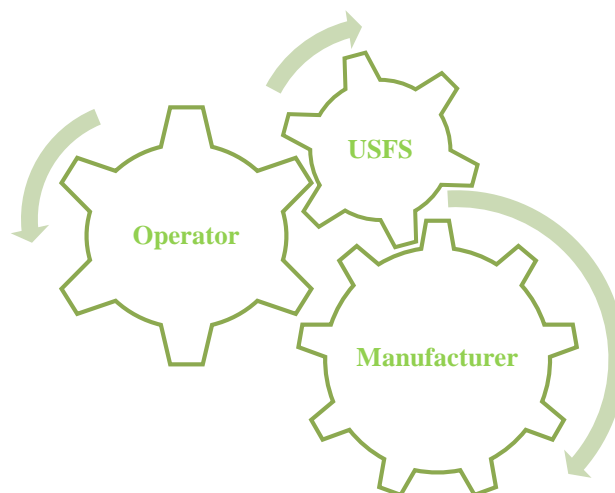


Figure 32: Aerial fire suppression stakeholders

5.3.1 Modeling

This section presents a summary of the scenarios examined in order to discover a coherent and practical acquisition plan. The bottom-line of profit in the acquisition plan design is that manufacturer and operator should be able to have a profitable business and also the costs for USFS to be within its projected budget for LAT operations.

5.3.1.1 Operator

In general, the operator is assumed to be a private contractor while sometimes USFS operates a LAT. the cost for the operator is modeled by finance, operation cost and insurance. Calculations are based on 160-day contracts [43]. As will be discussed in more detail, the operation hours and therefore the revenue of the LAT was concluded to be insufficient for the operator and it may need to be used during the rest of the year.

The LAT may be acquired by the operator through many ways (e.g. operating leases, leveraged leases, secured loans, aircraft backed bonds, etc.). Secured loan seems the most suitable option for the contractor to earn profit while operating the aircraft without the financial burden of buying it upfront. Different solutions can be found for the aforementioned financing type each proposing different risks and rewards, Finance Lease and Non-Recourse Investor Loan are two solutions to the problem [44], [45].

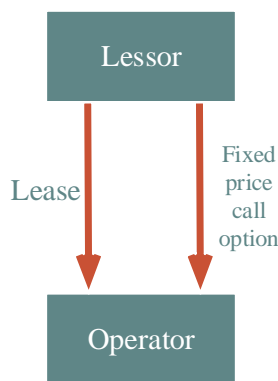


Figure 33: Finance Leasing

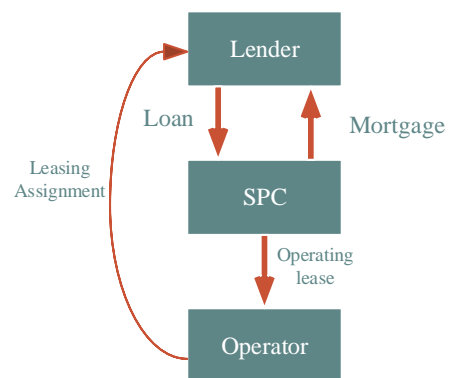


Figure 34: Non- Recourse Investor Loan

Table 13 summarizes parameters and their typical values regarding the loan. In all three methods the loan amount and duration is the same.

Table 13: Aircraft Loan Parameters

Parameter	Amount
Loan Value	85% of unit cost
Duration	60% of service life time
Interest rate	2%

Additionally, the insurance fees and the operation costs will be covered by the operator as well. The insurance cost is assumed to be 3% of the unit price. The operator revenue stream is modeled by daily availability and hourly flight rate charges for operations. The hourly flight rate was calculated by values of FHC (Flight Hour Cost), profit margin, firefighting annual sorties, and contract days.

5.3.1.2 Manufacturer

The manufacturer cost is calculated based on the firefighting performance presented in sections 2.1 to 2.3. The cost per unit declines as the number of units produced in total increases, mainly because the total fixed costs will be spread over a larger number of units. The number of requested aircraft will influence the unit cost proposed by the manufacturer, since the manufacturer assumes a sensible profit margin for this project.

5.3.1.3 Government

Aerial firefighting is supported by a budget share from USDA Forest Service, as supervised by the government. The impact of forest fires on agriculture, forestry, public health, tourism, etc... is significant, and as a governmental organization and the representative of people, USFS profits from less acres of forest burned. This in fact justifies the expensive use of air tankers. USFS devotes a percentage of their annual budget to LAT operations.

Furthermore, climate change and global warming continues to influence the likelihood of wildfires and therefore increases the suppression costs. Ref. [29] represents the ascending trend of cost of wildfire suppression from 1985 to 2013. It would be logical to assume that more LATs will be required for aerial suppression in the future. This organization should be capable of reimbursing the service fees agreed upon in contracts. The linear trend shown in [29] was used to estimate the suppression budget of USFS, 9% of this budget is devoted to LAT operations.

5.4 Results

The following section presents four scenarios. In the first scenario, general assumptions were made based on recommendations from the latest research and studies. Furthermore, modifications to certain parameters in the scenario was studied by changing one variable at a time and examining the profit of all three players.

5.4.1 Description of Scenario No. 1

Studies in the past have recommended an optimal number of 28 LATs for aerial firefighting. The cost of a new LAT, based on 28 units produced in total, will be approximately \$279M. Table 14 to Table 16 summarize the parameters of scenario 1, Daily availability and flight hour rates were obtained from similar aircraft data.

Table 14: contractor parameters in scenario no. 1

Operators			
Inputs	Contract Day	160	--
	FF Annual Sorties	216	--
	LAT Service Life Time	40	--
	Invest	42	Million US \$
	Loan	237	Million US \$
	Daily Availability Rate	29	Thousand US \$
	Flight Hour Rate	8.8	Thousand US \$
Outputs	Revenue [Per year]	7.7	Million US \$
	Cost (Loan, Insurance, Operation) [per year]	15.3	Million US \$
	Profit (Tax include) [per year]	-7.6	Million US \$

Table 15: manufacturer parameters in scenario no. 1

Manufacturer			
Inputs	Number Of Acquired AC	28	--
Output	Unit Cost	279	Million US \$

Table 16: USFS parameters in scenario no. 1

USFS			
Inputs	Year	2022	--
	Average Suppression budget [per year]	2375	Million US \$
	LAT Portion of Supp. Budget [per year]	216	Million US \$
	Cost of Contracting with 28 LAT	215	Million US \$
Output	more budget is needed		

This scenario is not acceptable, since the operator is losing money and also the incurred cost of USFS is more than its budget forecast. As a result of relatively low operation hours the DTE and acquisition costs comprise more than half of LCC in scenario no.1 as shown in Figure 35 which is not desirable.

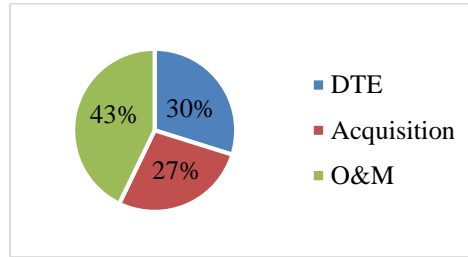


Figure 35: LCC Breakdown for scenario no.1

5.4.2 Description of Scenario No. 2

Disadvantage associated with the scenario no: 1 is the fact that Anahita fleet remains inactive during some significant part of the year, hence no fire is reported. Here, in scenario no: 2 we aim to keep the Anahita fleet operational for whole year. We fulfill this by keeping the other inputs unaltered, only the operator parameters. By doing such, we expect the net loss would be less that in scenario no: 1.

Table 17). As a result, in scenario no. 2 summarizes the parameters related to the operator in this state. For instance, despite the fact that other possible missions generate a higher profit margin, the profit was assumed to be equal to that of a firefighting contract in the additional 160 days. By doing such, we expect the net loss would be less that in scenario no: 1.

Table 17: contractor parameters in scenario no. 2

Operators			
Inputs	Contract Day	320	--
	FF Annual Sorties	432	--
	LAT Service Life Time	40	--
	Invest	42	Million US \$
	Loan	237	Million US \$
	Daily Availability Rate	29	Thousand US \$
	Flight Hour Rate	8.8	Thousand US \$
Outputs	Revenue [Per year]	15.5	Million US \$
	Cost (Loan, Insurance, Operation) [per year]	17.2	Million US \$
	Profit (Tax included) [per year]	-1.7	Million US \$

Figure 36 summarizes the results for scenario no.2 in which an improvement in O&M cost due to rise in the number of operation hours is seen. Having said that, LCC is still mainly consisted of DTE and acquisition costs which requires to be addressed. Low number of produced units is realized as the main cause.

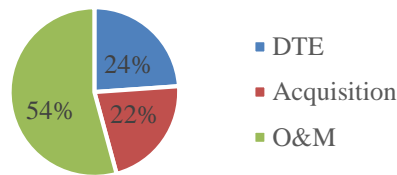


Figure 36: LCC Breakdown for scenario no.2

5.4.3 Description of Scenario No. 3

For both scenarios no: 1 and no: 2 the number of aircraft in Anahita fleet is amounted to a total of 28. However, the increase in recorded wildfires in the past decades, in one hand, and green movements, in the other hand is expected to create a political pressure built-up to force the governments worldwide to place orders for more LATs. Initial studies regarding wildfires in countries like Greece, Iran and Australia has led us to an estimate of 120 units of Anahita in addition to that of 28 demanded by the U.S. government. Table 18 and Table 19 summarize the parameters studied in scenario 3.

Table 18: contractor parameters in scenario no. 3

Operators			
Inputs	Contract Day	320	--
	FF Annual Sorties	432	--
	LAT Service Life Time	40	--
	Invest	19	Million US \$
	Loan	107	Million US \$
	Daily Availability Rate	29	Thousand US \$
	Flight Hour Rate	8.8	Thousand US \$
Outputs	Revenue [per year]	15.5	Million US \$
	Cost (Loan, Insurance, Operation) [per year]	9.9	Million US \$
	Profit (Tax included) [per year]	5.6	Million US \$

Table 19: manufacturer parameters in scenario no. 3

Manufacturer			
Inputs	Number Of Acquired AC	120	--
Output	Unit Cost	126	Million US \$

As a result of large development in number of units produced, the parameters related to unit cost i.e. DTE and acquisition are significantly reduced. The relatively large portion of O&M cost implies a more efficient usage of the LAT.

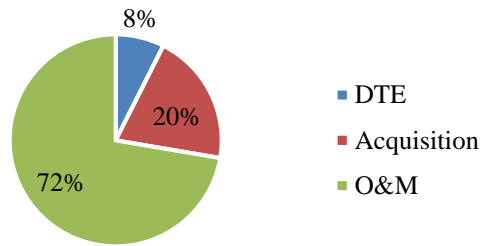


Figure 37: LCC Breakdown for scenario no.3

5.4.4 Description of Scenario No. 4

Additionally, to create a balance in the project operator’s profit margin was decreased so USFS can save more on expenditures. LCC breakdown of scenario no.4 is the same as its predecessor (See Figure 37).

Table 20: contractor parameters in scenario no. 4

Operators			
Inputs	Contract Day	320	--
	FF Annual Sorties	432	--
	LAT Service Life Time	40	--
	Invest	19	Million US \$
	Loan	107	Million US \$
	Daily Availability Rate	25	Thousand US \$
	Flight Hour Rate	7.8	Thousand US \$
Outputs	Revenue [per year]	14.7	Million US \$
	Cost (Loan, Insurance, Operation) [per year]	9.9	Million US \$
	Profit (Tax included) [per year]	4.8	Million US \$

Table 21: USFS parameters in scenario no. 4

USFS			
Inputs	Year	2022	--
	Average Suppression budget [per year]	2375	Million US \$
	LAT Portion of Supp. Budget [per year]	216	Million US \$
	Cost of Contracting with 28 LAT	206	Million US \$
Output	Less budget is needed		

5.5 Conclusion

Figure 38 provides a comparison among the four scenarios. As it is seen no: 4 has the lowest LCC among expected scenarios; which corresponds to a relatively more sustainable acquisition plan. Obviously, there are many other possible scenarios that could be examined with the similar approach.

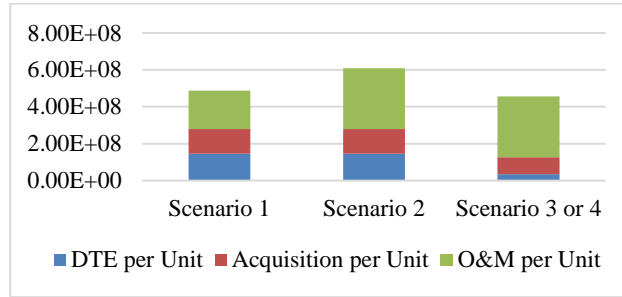


Figure 38: LCC per Unit of Different Scenarios

As indicated in 5.4.4 scenarios 3 and 4 differ in the amount of USFS financial pressure incurred to demonstrated in Figure 39 as daily availability and Flight Hour Rate (FHR) are reduced by approximately 20%.

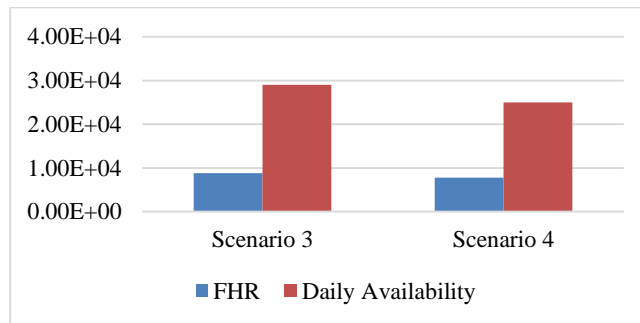


Figure 39: FHR and Daily Availability comparison of scenario 3 and 4

The comprehensive analysis of LCC per unit for four different scenarios has led to two key conclusions:

The operation of airtanker during an annual 160-day contract does not yield a rational LCC. Operating an LAT solely for fire attack in the US will not lead to a sustainable cycle of money and services. Hence, extra missions should be added to the capability of the LAT so it can perform missions during non-fire season, the LAT must be able to accept additional contracts to operate as a firefighter in southern hemisphere regions, especially Australia, or perform multiple roles e.g. disaster relief, liquid spraying, cargo delivery, etc. as secondary missions.

It is required to increase the number of LATs to be built, Since 28 LATs, as recommended in [46] limited to use in USA lead to a high unit cost and clearly it is not economical. According to the fact that wildfires are increasing all over the planet, everyone is responsible to save the earth. The international agreements on forest fire maintained by Food and Agriculture Organization of the United Nations (FAO) were proposed [47], for example:

“To facilitate mutual assistance in wildland firefighting between Australia, New Zealand and the United States of America (Article I)”

Implies that the LAT fleet should not be restricted to national forests only, but to serve other nations as well. The acquisition plan will become more sustainable by the growth in the number of produced unit.

This proposition will become a feasible solution by a justifiable acquisition plan in which foreign operators are also supported by leasing, this could be accomplished by means of Export Credit Loan of the Export-Import Bank of the United States, this proves feasibility of the plan and guarantees minimal risk of acquisition for all players, even manufacturer [48].

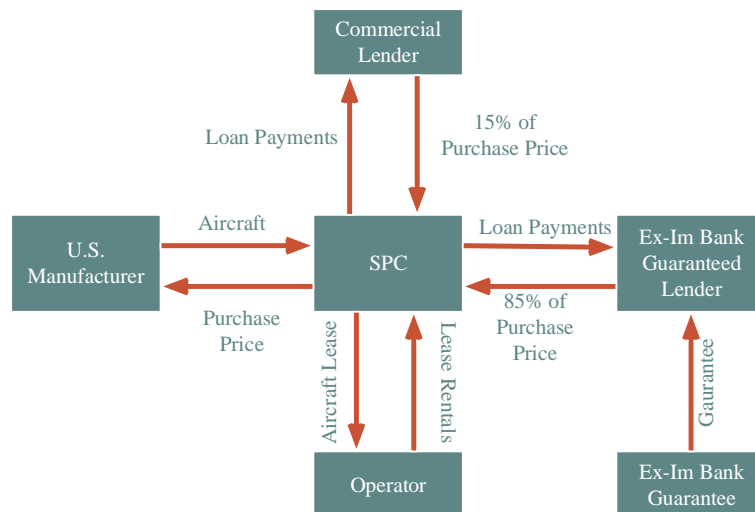


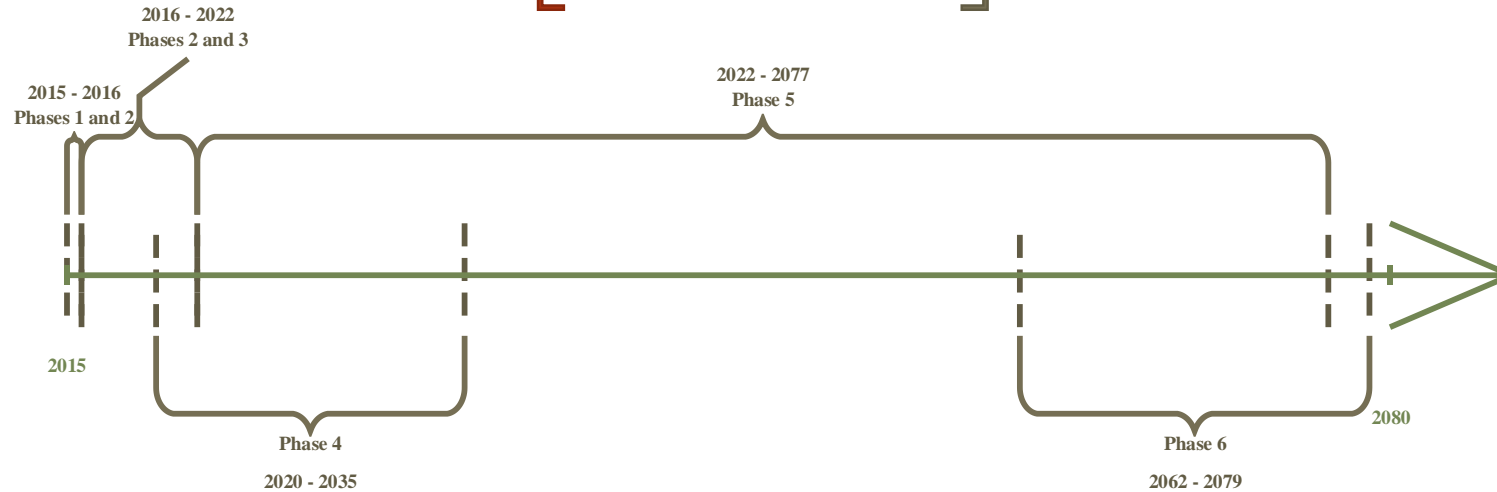
Figure 40: Export Credit Loan (Ex-Im Bank)

The lifecycle of Anahita is drawn in Figure 41.

6 PARAMETRIC STUDY

In this section mission and drag polar pre assumed parameters are to be finalized via using carpet plots to balance total incurred cost and time.

Anahita's Life Cycle



Legends

Phase 1: Planning and Conceptual Design
 Phase 2: Preliminary Design and System Integration
 Phase 3: Detail Design and Development
 Phase 4: Manufacturing and Acquisition
 Phase 5: Operation and Support
 Phase 6: Disposal

Durations

Phases 1, 2 and 3 ~ 6.5 yrs.
 Phase 4 ~ 15 yrs.
 Phase 5 ~ 55 yrs.
 Phase 6 ~ 17 yrs.

Assumptions

1- LAT Service Life Time (SLT) = 40 yrs.
 2- LAT Disposal Duration = 2 yrs.

Figure 41: Anahita's Lifecycle Plan

6.1 Mission Parameters Trade-off Study

According to the cost of fire estimation model developed in section 4.4.2 and Anahita’s operation cost model, it is possible to determine the time and cost of operation while varying cruise altitude and speed.

One of the figures of merit is number of sorties between refueling operation. The Figure 42 shows number of refueling operations to carry out 4 sorties.

In the Figure 42 total incurred cost due to fire and suppression operations are shown in the different conditions. SN refers to number of sorties without refueling, and VCO corresponds to velocity of cruise-out. The figure above shows trend of changes in the cost and time while performance parameters are deviating. As it is obvious in the minimum point SN=2 and VCO=390. In the two top plots changes in time and cost due to varying cruise-in speed and altitude of both cruise-in and cruise-out phases are shown. These trends are constant in all the plots. Since carpet plot is discrete, to determine the optimum point there is need for optimization algorithms.

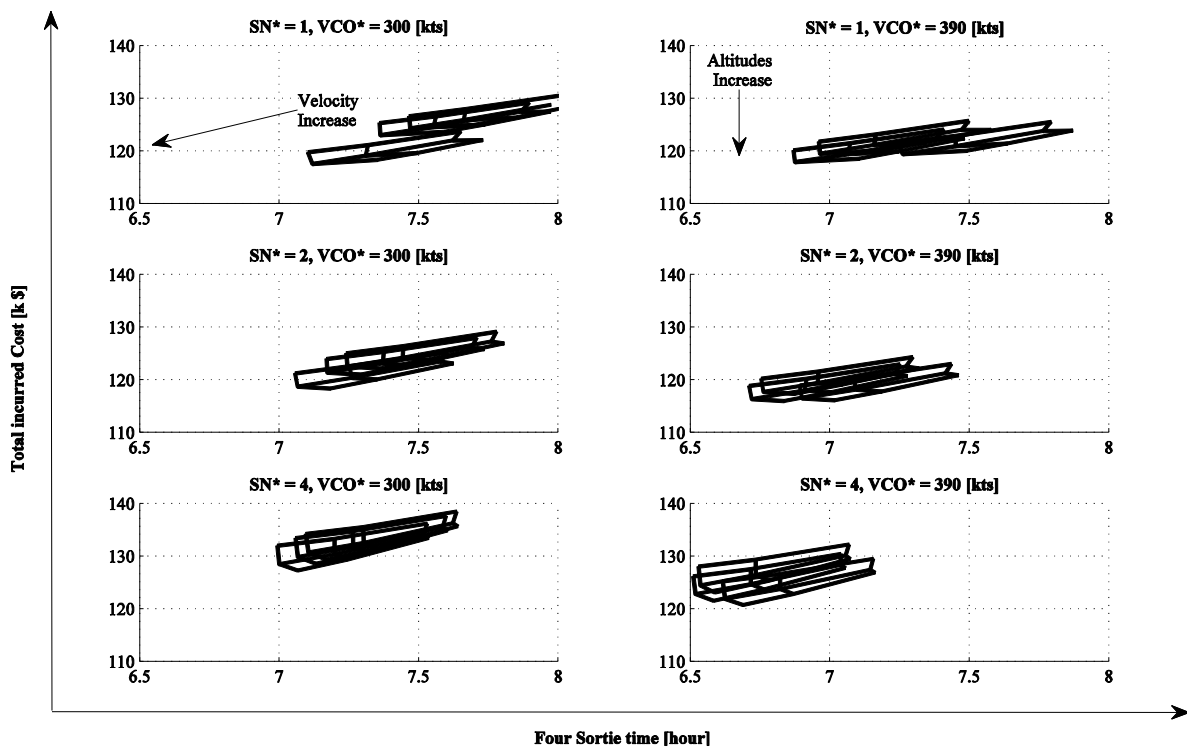


Figure 42: Mission Parameters Carpet Plots

6.2 Performance Parametric Study

According to known initial values of C_{D0} and AR (section 4.1.1) a carpet plot of flight hour cost and time to establish a fire line is presented in the Figure 43.

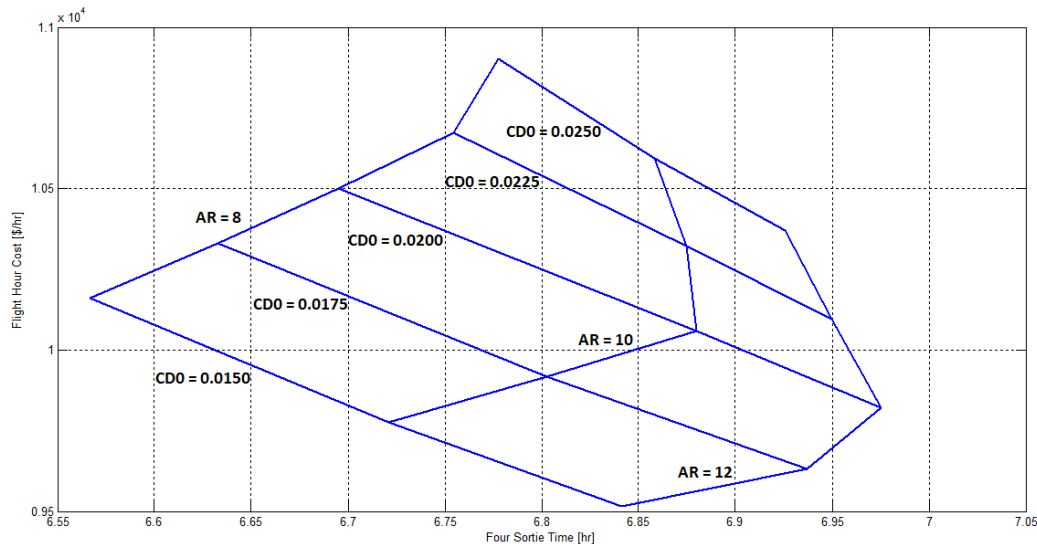


Figure 43: FHC vs 4 Sortie Time Sensitivity to Cd0 and AR Carpet Plot

An increase in AR will lead to a decrease in operational cost. In AR=12 with the increasing of C_{D0} (more than 0.0175) the operational cost will increase drastically, which is unusual. The moderate slope of AR=10 with increasing of C_{D0} , shows a suitable area. With this basis the point of AR=10 and $C_{D0}=0.0175$ will be chosen, as was chosen before. It should be considered that if the reduction of C_{D0} can be obtained, the efficiency will be increasing by decreasing cost and time to establish a fire line both. More detailed evaluation of C_{D0} feasibility will be carried out on next design levels.

6.3 Results of Initial Sizing and Mission Refinement

For determining the design point there should be a matching diagram. Matching diagram is drawn with help of all requirements and performance characteristics of Anahita. Figure 44: Matching Diagram of Anahita illustrates matching diagram for Anahita and Table 22 defines the design point.

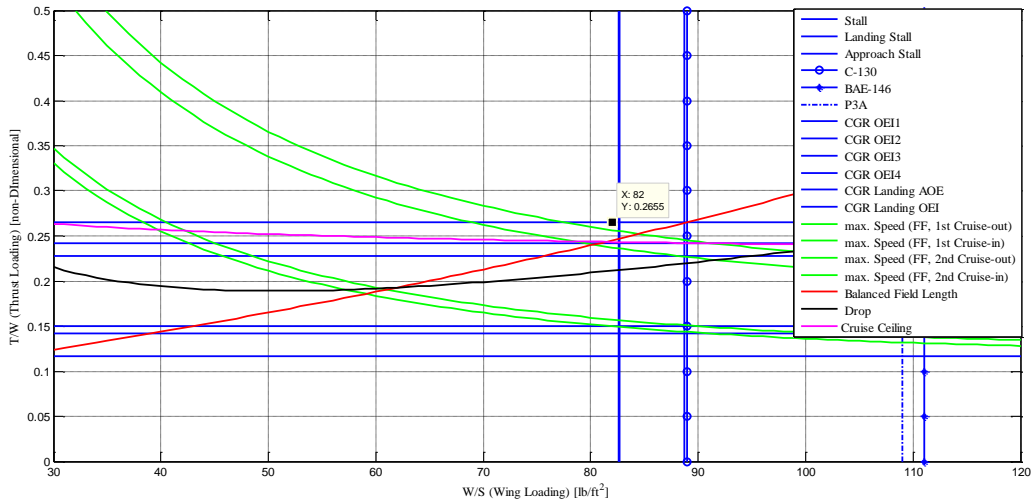


Figure 44: Matching Diagram of Anahita

Table 22: Design Point Characteristics

Overall		Firefighting		repositioning	
MTOW	131000 lb	Required Fuel Weight	18000 lb	T.O. Weight	81200 lb
$W_{O.E}$	68000 lb	1 st Sortie Cruise-out Altitude	27000 ft	Required Fuel Weight	13600 lb
$W_{max.fuel}$	18000 lb	2 nd Sortie Cruise-out Altitude	28300 ft	Cruise Altitude	40000 ft
$W_{max.payload}$	45000 lb	1 st Sortie Cruise-out Altitude	38000 ft	Cruise Speed	390 knots
$\left(\frac{W}{S}\right)_{MTOW}$	$82 \frac{lb}{ft^2}$	2 nd Sortie Cruise-out Altitude	39600 ft		
$\left(\frac{T}{W}\right)_{max.Sea Level}$	0.26	Cruise (out/in) Speed	390 knots		

Since Anahita is multi role, the payload-range diagram is critical for analyzing the other missions.(Figure 45)

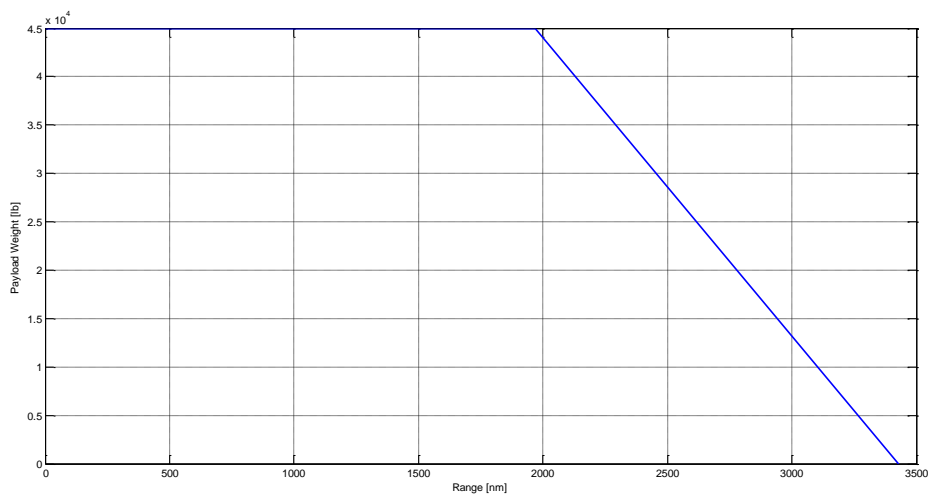


Figure 45: Payload vs. Range Diagram for Anahita

7 Anahita COMPONENT SIZING

7.1 Drop System Design

Drop system is vital part of firefighting mission. From the requirement hierarchy design requirements of drop system are: **5000 US gallon retardant/water capacity, slushing resistant, capable of particular in-flow and out-flow retardant rate, capable of 3 separate drops, easy to inspect and detachability.**

7.1.1 System Drop Type Selection

There are several drop system types, three of them that qualified to be options for decision making for the LAT are shown in Table 23 with their pros and cons:

Table 23: Pros and cons of each drop system

Type	Pros	Cons
3 spherical Containers	- No slushing problem	- Problem in manufacturing - Higher cost - 3 containers → more cost - Cg travel issue with 3 containers
One trapezoidal container	- less manufacturing cost than spherical	- has slushing problem - less precision than spherical
One cylindrical container	- less manufacturing cost than spherical - more slushing resistance than trapezoidal	

Using the AHP method, the final decision has led us to choose one cylindrical container for drop system.

7.1.2 Tank Characteristics

In order to find the best geometrical features of the container, two constraints were dominant:

- ➔ Volume needed for retardant, which must be 5000 gallons.
- ➔ A good finesse ratio for the container in order to have a proper finesse ratio for the aircraft.

Checking the suggested values in reference [49] for similar airplanes, the final geometry of the container is shown in Table 24.

Table 24: Geometry of the container

Length (ft.)	Diameter (ft.)	Finesse ratio
8.5	2.5	3.4

Three entries are designed at the bottom of the container for loading and reloading. With this configuration the container can be loaded with engines on. The middle entry is also used for drop. The reloading process takes 5 minutes.

The container must be pressurized so the drop operation will be more precise and there will be no splashing.

Two circular rings with small holes are designed in order to avoid slushing in the container. The distance between each hole is designed based on the suggestions offered by [50]. Two hollow circular rings are also put for further resistance to slushing.

The height of the container with all its systems is as high as a normal human body so that eye inspection could be done after each flight. Also on each side about 1.5 feet is dedicated to let the inspector to walk beside the container and do the inspection.

The thickness of the skin of the container is enough to tolerate the pressure that is exerted for drop precision.

At the bottom of the container, there are three stands in order to hold the container.

The container is built on a surface that allows it to be carried easily and it will be fixed to the bottom of the fuselage by bolts and nuts. So if any problem occurred during the service, the container could be disconnected and be replaced with a new one in a few minutes.

A 3 view of the drop system can be seen in Figure 46.

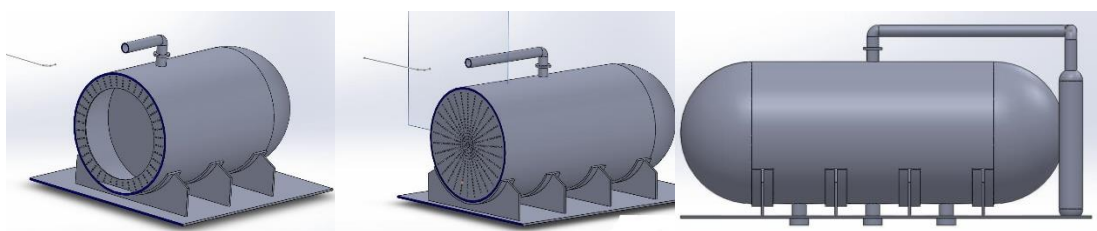


Figure 46: 3-view of drop system

7.2 Fuselage

According to design objectives and requirements derived for the design, lowering the development cost is substantial, if an existing fuselage can be chosen with respect to drop system, the need for building new infrastructure diminishes.

7.2.1 Procedures for choosing an existing fuselage

This section presents the steps completed by the team through the process of finding the desired and possibly already existing fuselage.

7.2.1.1 Limitations

The (parameters) limitations of fuselage cross section and length are summarized in Figure 47.

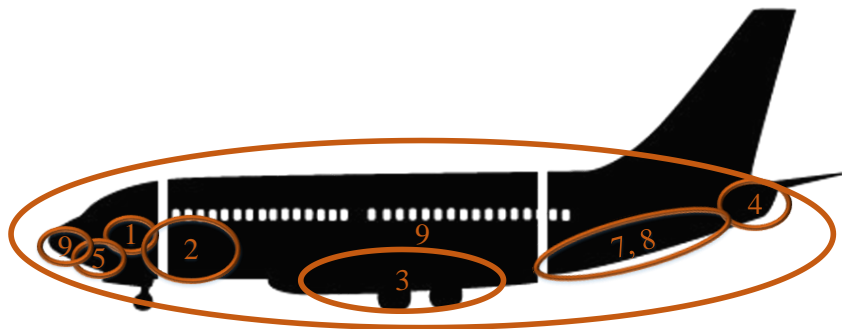


Figure 47: Limitations and Their Impact Zone

- | | |
|---|--------------------------------|
| 1- Number and weight of the cockpit crew members | 2- Base Drag |
| 3- Number and weight of special duty crew members | 4- Cargo door |
| 5- Weight and volume of drop system | 6- Upsweep angel |
| 7- APU | 8- Drag divergence Mach number |
| 9- Radar Equipment | |

7.2.1.2 Candidates for existing fuselage

The dimensions of the drop system after its initial design was used to determine the cross section of the fuselage, extra room was added for inspection and maintenance, this value of desirable fuselage cross section matches two existing sections: Boeing 707, 727, 737, 757

The diameter of this cross section is 12.33ft and it is one of the most widely used cross sections in the history of airplane design it has been used in 4 Boeing airplanes (707,727,737,757). This 121 by 104-inch cross section has an advantage over the cross section of B737 as it may allow for a cargo door in the aft fuselage which, for the purpose of this design, is more suitable than the side cargo door of B737. After consulting with the drop system design team, and weighting the pros and cons of the two candidates, the cross section of C-130 was selected for the fuselage of Anahita.

Table 25: Fuselage cross sections

Aircraft	Cross Section	Max. Height (D _w)	Max. Width (D _b)
Boeing 737	D = 12.33 ft.	-	-
C-130	121 by 104 inch ²	14.7 ft.	13.9 ft.

7.2.2 Fuselage Length

In this section the fuselage length will be determined.

There is no limitation on the fuselage length except **base drag, cargo door** and **drag divergence Mach number** (the drop systems length is not comparable to its diameter and so it does not affect the fuselage’s length):

Using Fig 3.1 of Ref. [51] it is known that the best fineness ratio for base drag in the fuselage is between 4-8.

For the aft body the main limitation is the cargo door which its dimensions are in Table 26.

7.2.2.1 Aft body

The main limitation here is the cargo door and it will affect the other parts of the aft body.

The total length of the aft body is 40 ft. (23 ft. cargo door, 17 ft. rest of the aft body)

Table 26: Cargo door dimensions

Width (in)	Height (in)	Length (in)
120	110	276

For the nose, drag divergence Mach number and cockpit are the two major limitations. Since Anahita is expected to cruise at speeds above Mach 0.7, the nose should have a M_{DD} of 0.76 [51], this results in a nose fineness ratio of 1.077 and a nose length of 14 ft.

There are two limitations that affect the main body of the fuselage, Base drag and Cargo capacity. Since the design of Anahita is directly related to its primary mission, the former constraint is of higher importance.

The selected cross section for Anahita is somewhat rectangular with large fillets on the ****sides***, the diameter of this cross section is therefore calculated approximately as 13 ft.

The overall Fineness ratio of Anahita is 7.69. As a result, the overall length of the aircraft and the length of the main body are calculated as 100 ft. and 46 ft., respectively.

Table 27: Fuselage Length Summary

Aft body (ft.)	Main body (ft.)	Nose (ft.)	Total Fuselage Length-l _f (ft.)
40	46	14	100

7.2.3 Cockpit

The cockpit of this plane should be able to enclose three crew personnel, Pilot, Co-pilot, observer. The cockpit of the C-130 is for a 4-man team, which consists of pilot, co-pilot, navigator and flight engineer.

For the cockpit design the considerations mentioned in Ref. [51] must be taken care of.

The C-130 cockpit already passes all of these constraints, subsequently Anahita utilizes the same cockpit with the following changes proposed:

1. The flight engineer's seat will be removed
2. The navigator's instruments will be replaced with the observer's instruments
3. The Virtual Reality system will be online, as will be explained in detail in section 3.1.8.

7.3 Wing

The general procedure of Class I Method of sizing the wing of Anahita is summarized in Figure 48. The procedure is quite the same as introduced in Ref. [49], however some marginal changes, e.g., deciding on taper ratio before sizing high lift devices is made.

The main challenge in designing the wing was the relatively low stall speed of Anahita. As a consequence, it was not possible to employ a swept wing and this lead to some problems with critical Mach number of the wing in high cruise speeds. Moreover, fatigue considerations and stall behavior of the wing were important.

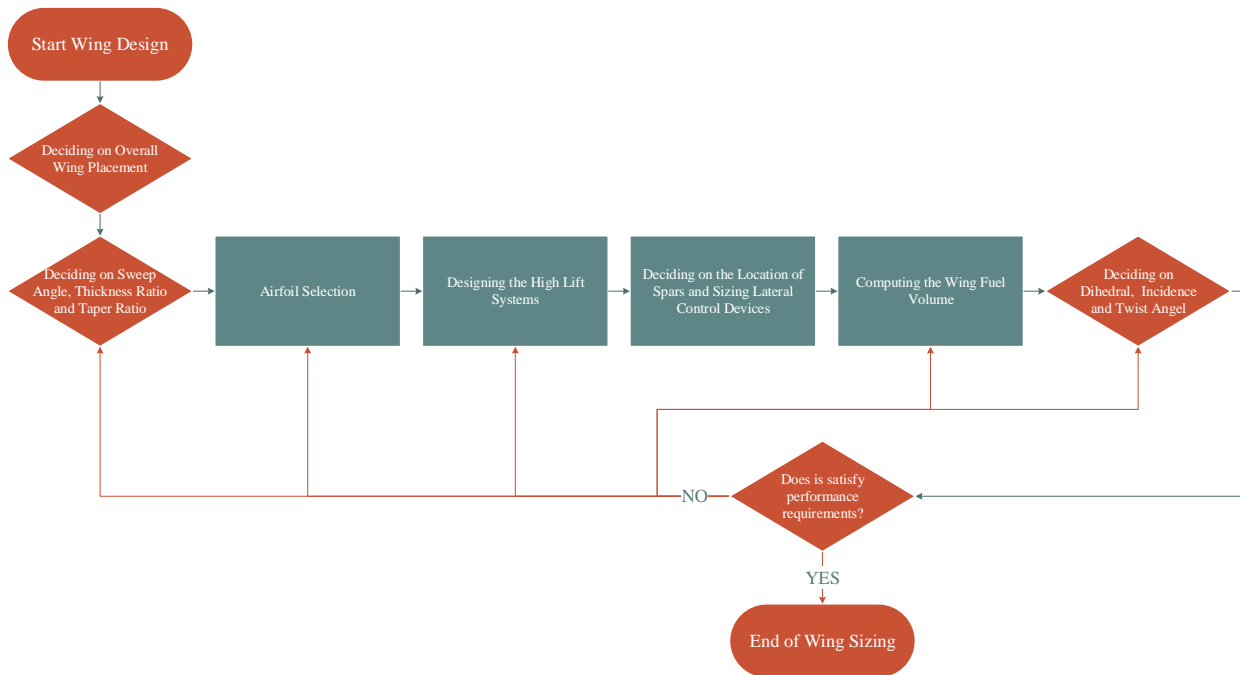


Figure 48: Procedure of Class I Tail Sizing

7.3.1 Overall Wing/Fuselage Arrangement

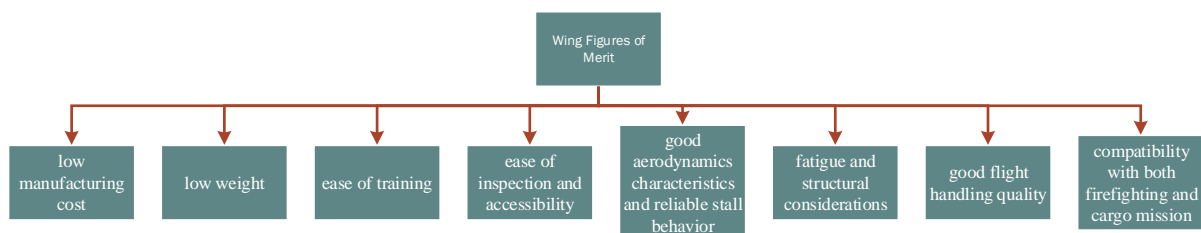


Figure 49: Wing Figures of Merit

Considering merits in Figure 49, the decision between the three arrangements, i.e., high-wing, mid-wing and low-wing is made by weighting them with regard to their level of importance.

As an aerodynamics point of view, high-wing has more frontal area and as a result more parasite drag. Besides, due to higher lift coefficient, it suffers from high induced drag. The lateral stability is good, however it makes the lateral control relatively weaker (Ref. [21]). Farther, the choice of high-wing arrangement would limit us to the landing gears which were connected and retracted in the fuselage since weight would have increased drastically.

Nevertheless, the high-wing arrangement produces more lift and this means lower stall speed which was of considerable importance for Anahita. In addition, the inspection of high-wings especially those with anhedral

angle is much simpler and the weight is lower. Furthermore, because of the type of mission, the higher the wing is placed, the possibility of debris suction into the engine is lowered. Another consideration was that because of the purpose of Anahita, it required much more ground operations. Consequently, the high-wing arrangement could prevent potential ground vehicles accidents with the wing.

To summarize, the high-wing arrangement ranked higher and was chosen for the wing/fuselage arrangement.

7.3.2 Deciding On Sweep Angle, Thickness Ratio and Taper Ratio

Initially, the stall speed of the aircraft in the drop phase was the greatest obstacle in front of the wing design team. The maneuver load factor required the wing to produce higher lift and this is in contradiction with using a swept wing. Further, ref. [52] explains that the majority of missions are taken place in a 100 nm radius which is half of the range of the design point. The reduction in the range makes it practically hard to achieve the high speed cruise flight conditions of the 200 nm missions. The consequence is that Anahita should have acceptable cruise efficiency in lower speeds too. These facts persuaded ShadX wing design team to employ no quarter-chord sweep angle for the wing. At this level a thickness of 17% for the root and 13% for the tip of the wing was chosen.

Nicolai (Ref. [22]) suggests that a wing with a taper ratio of 0.35 will generate a nearly elliptical lift distribution. Since 0.35 is fair enough for the weight equations too, it is selected as the taper ratio of Anahita’s wing.

Table 28: Sweep Angle, Thickness Ratio and Taper Ratio of the Wing

$\Lambda_{c/4}$ (degree)	$(t/c)_{w_r}$	$(t/c)_{w_t}$	λ_w
0	0.17	0.13	0.35

The performance requirements of Anahita are presented in Table 29.

Table 29: Performance Requirements

$\left(\frac{W}{S}\right)_{TO}$ $\left(\frac{\text{lb}}{\text{ft}^2}\right)$	W_{TO} (lb)	AR_w	$C_{L_{cruise}}$
82	131000	10	0.4 ÷ 0.6

These requirements lead to the geometric parameters of Table 30 for the wing.

Table 30: Geometric Parameters of the Wing

S (ft ²)	b_w (ft)	\bar{c}_w (ft)	c_{t_w} (ft)	c_{t_w} (ft)
1597.6	126.4	12.6	17.7	6.2

7.3.3 Airfoil Selection

The main challenge here was to choose an airfoil with high lift coefficient in high Reynolds numbers, a good interval of constant drag in the vicinity of cruising lift coefficient and an acceptable critical behavior.

NASA LANGLEY MS Series airfoils are one of the best possible choices for the airfoil of Anahita. Figure 50 illustrates the linear C_l curve of two airfoils of this family, i.e., MS (1)-0317 and MS (1)-0313. They provide high lift coefficients while maintaining the low drag coefficient in cruising angle of attack. Moreover, the constant drag coefficient of airfoils in the neighborhood of cruising lift coefficient, i.e., $0.4 \div 0.6$, enables Anahita to cruise sufficiently. These two airfoils were selected for Anahita’s root and tip, respectively.

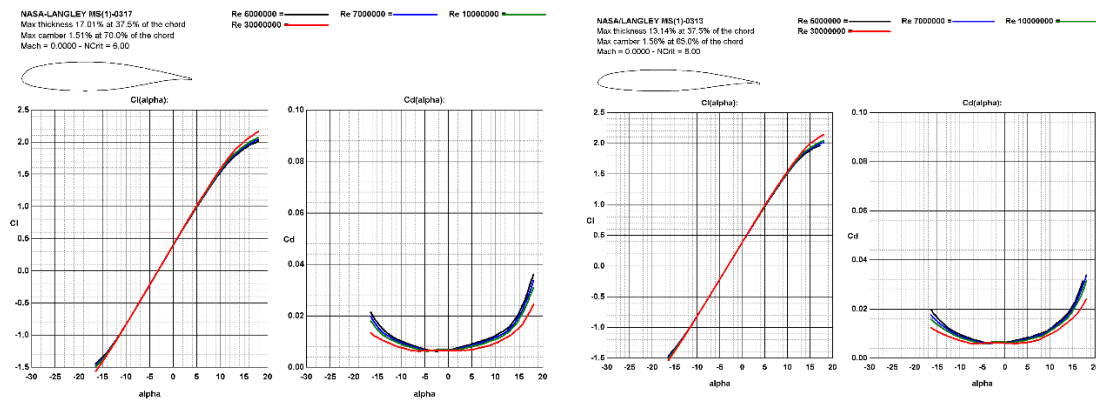


Figure 50: Lift and Drag Coefficients vs. AoA for MS (1)-0317 & MS (1)-0313

According to the mission profile, it can be observed that the highest Mach number is 0.698. It should be verified that the selected airfoils can bear this condition. The critical Mach number is considered the Mach number in which the rate of change in drag coefficient with Mach number exceeds 0.1. Figure 17 of Reference [53] presents the C_d vs. Mach number for the selected airfoils of Anahita in $Re = 1.6 \times 10^7$. Digitizing these curves and calculating the rate of change, the critical Mach number of the selected airfoils are roughly higher than 0.7 which is a good accuracy for this class of sizing.

7.3.4 Designing the High Lift Systems

Table 31 shows the equivalent Re numbers and wing section maximum lift for the root and the tip of the wing for different missions. Note that it is assumed that the stall angle is 17° .

Table 31: Re Number and Maximum Lift Coefficient

Mission	Re		$C_{L_{max}} (\alpha = 17^\circ)$		$1.1 \times C_{L_{max}}$	$k_\lambda \left(\frac{C_{L_{max_r}} + C_{L_{max_t}}}{2} \right)$	% Error
	Root	Tip	Root	Tip			
Cruise In	2.2×10^7	7.7×10^6	2.10	1.99	2.04	1.96	3.9
Cruise in – Max Speed	2.4×10^7	8.4×10^6	2.10	2.00	2.04	1.96	3.9
Cruise Out	3.2×10^7	1.1×10^7	2.12	2.02	2.04	1.98	2.9
Cruise out – Max Speed	3.6×10^7	1.2×10^7	2.12	2.03	2.04	1.98	2.9
Drop	1.9×10^7	6.8×10^6	2.11	1.98	-	-	-
Takeoff	2.7×10^7	9.3×10^6	2.09	2.01	-	-	-
Approach	1.3×10^7	4.6×10^6	2.06	1.95	-	-	-
Landing	1.6×10^7	5.7×10^6	2.08	1.97	-	-	-

Where in Table 31 it is assumed that Anahita is long-coupled aircraft and k_λ is equal to 0.956 for $\lambda = 0.35$. This table demonstrates that the percentage of error is less than 5 for all of the clean conditions, hence the clean wing is satisfactory for this class of design.

Furthermore, the incremental values of maximum lift coefficients which need to be produced by high lift devices are presented in Table 32.

Table 32: Incremental Values of Maximum Lift Coefficients

Mission	$C_{L_{max}}$	$\Delta C_{L_{max}}$	$\Delta C_{L_{max}}$ with Krueger Flaps
Drop	3.1	1.31	1.02
Takeoff	3.3	1.52	1.21
Approach	3.3	1.52	1.21
Landing	3.7	1.94	1.59

Since these incremental values are relatively high, Krueger flaps in addition to Single Slotted Fowler flaps are employed for the wing. The effect of Krueger flaps is taken in by Equation **Error! Reference source not found.** where c'' the chord length of the wing section is when the Krueger flaps are deployed. For this class of sizing, it is assumed that $c''/c = 1.1$.

$$\Delta C_{L_{max}} = 1.05 \left(\frac{C_{L_{max}}}{(c''/c)} - C_{L_{max_{clean}}} \right)$$

Finally, the flaps are sized using the relations suggested in Ref. [49] for single slotted Fowler Flaps. For this purpose, values of C_{l_α} are presented Table 33. Since the wing is mounted into the fuselage, η_i (Figure 7.2 of Ref.

[49]) is at least $D_w/b_w = 0.12$. Assuming $c_f/c = 0.3$ (Figure 7.8 of Ref. [49]), the results are summarized in Table 34.

Table 33: Calculation of C_{l_α}

Mission	C_{l_α}		$\frac{k_\lambda}{2}(C_{l_{ar}} + C_{l_{at}})$	Mission	C_{l_α}		$\frac{k_\lambda}{2}(C_{l_{ar}} + C_{l_{at}})$
	Root	Tip			Root	Tip	
Drop	7.20	6.83	6.70	Approach	6.66	6.66	6.37
Takeoff	7.04	6.76	6.60	Landing	6.25	6.69	6.19

Table 34: Results of High Lift Devices Sizing

Mission	δ_f	η_i	η_o	Mission	δ_f	η_i	η_o
Drop	25	0.12	0.56	Approach	30	0.12	0.61
Takeoff	30	0.12	0.59	Landing	40	0.12	0.72

7.3.5 Deciding on the Location of Spars and Sizing the Lateral Control Devices

From the data base of aircrafts, the aileron-to-wing area ratio is about 0.044. This means:

$$S_a = 0.044 \times S = 70.3 \text{ (ft}^2\text{)}$$

Ref. [20] suggests the front spar to be located at 15 to 30 percent of the chord and the rear spar 65 to 75 percent of the chord. Deciding the rear spar to be located at 0.69 chord, the front spar should be placed in a manner that the shear center of the wing box be located near enough to the aerodynamic center of the wing in order to prevent torsion of the wing. This decision means that ailerons can be started at 0.70 chord.

Table 34, forces that ailerons should be started at least at 0.73 semi-span. Finally, these data in addition to geometric equations lead to Table 35.

Table 35: Geometric Parameters of the Aileron

η_{i_a}	c_{i_a} (ft.)	η_{o_a}	c_{o_a} (ft.)
0.73	2.8	0.95	2.0

Figure 51 illustrates a dimensioned drawing of the wing planform.

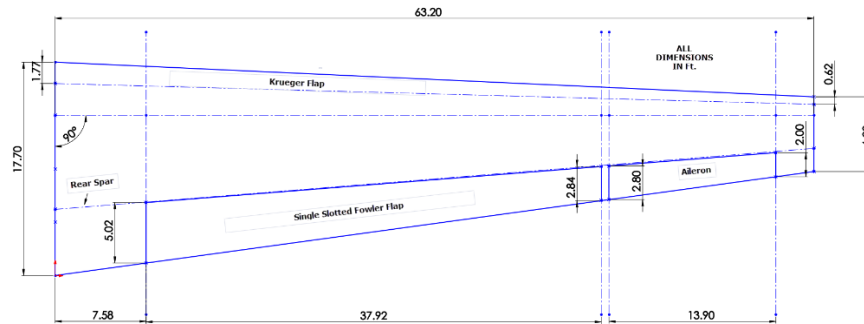


Figure 51: Dimensioned Drawing of the Wing

7.3.6 Computing the Wing Fuel Volume

Ref. [49] suggests from Torenbeek an equation for estimating wing fuel volume in preliminary design. This equation yields into $V_{WF} = 1587.1 \text{ ft}^3$. The required fuel weight is 15000 lb which is equal to 334.1 ft^3 of fuel volume. This means the wing volume is enough.

7.3.7 Dihedral Angle, Incidence Angle and Twist Angle

The anhedral angle of the high-wing may make it lighter and easier to inspect. Consequently, an anhedral angle of 5 degrees is considered for the wing at this level of design (Table 36).

Figure 50 shows that for a 0.4 cruising lift coefficient, a zero angle of attach is needed. However, since prevention of tip stall requires a wash-out twist angle (Ref. [49]), the incidence angle of the wing is decided to be -2 degrees (Table 36).

And finally, for a better stall behavior, a wash-out twist angle of -2 degrees is preferred here (Table 36).

Table 36 Dihedral, Twist and Incidence Angles

Γ_w (degree)	i_w (degree)	ϵ_{i_w} (degree)
-5	2	-2

7.3.8 Structural and Fatigue Considerations

First of all, the fatigue calculations could be neglected, if the factor of safety is considered equal to $1.5 \times 1.5 = 2.25$. Since a 2.25 factor of safety leads to an overweight design and also according to FAR-25 regulation, the fatigue design must be considered on the basis of damage tolerant criterion, an initial crack must be assumed in the structure, and this crack must not reach to its critical length during the entire life of the airplane.

Visual inspections must be performed after each flight-cycle in order to discover probable impediments. After 8 to 10 years, a fundamental inspection must be done in order to measure any initiated crack’s length and predict its critical length in order to find the residual life of the airplane. The eddy current method would be the most efficient method of inspection and is suggested as the inspection method.

The most sensitive and damage susceptible regions in the plane which must be supervised meticulously are the wing and fuselage intersection, the connection of the engine to the wing, the root of the wing, the root of the horizontal and vertical tail and the vicinity of rivet zones.

At the end, considering the temperature gradient each part of the aircraft is exposed to, Table 37 suggest the materials to be used for the parts.

Table 37: Material of Different Parts

Part	Material	Part	Material
Upper Stringers In Wing Box	Al 7075 T6	Upper Skin Of The Wing	Al 7075 T6
Lower Stringers In Wing Box	Al 2024	Skin Of The Fuselage	Al 2024 T3
Lower Skin Of The Wing	Al 2024	Stringers In Fuselage	Al 7075 T6

7.4 Tail Sizing

The general procedure of Class I Method of sizing the tail of Anahita is summarized in Figure 52: Procedure of Class I Tail Sizing as introduced in Reference [49].

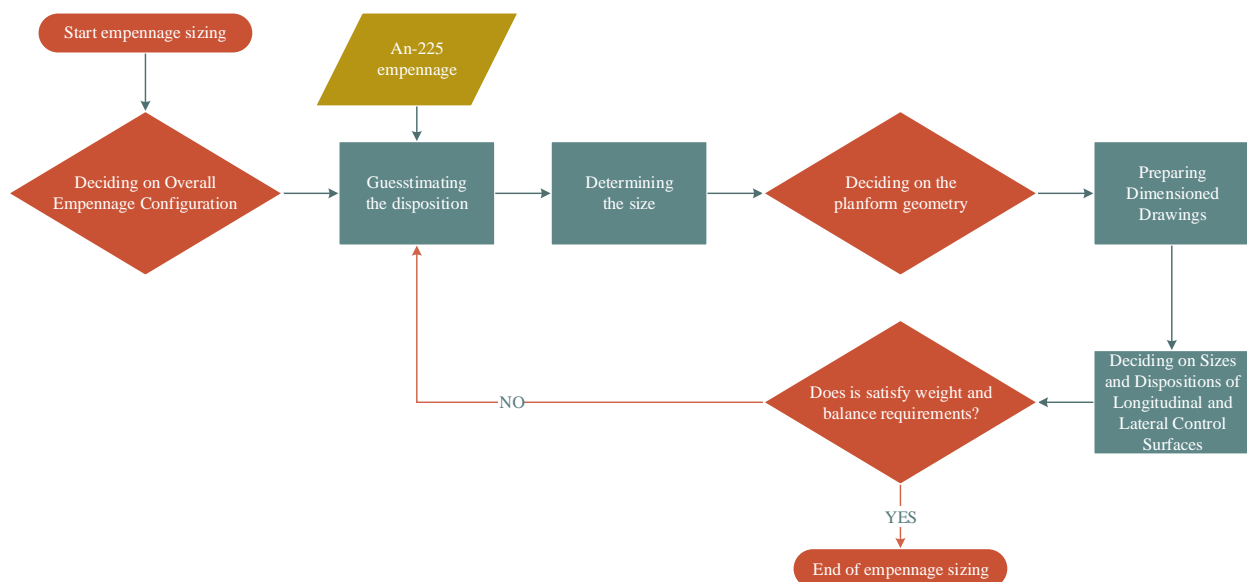


Figure 52: Procedure of Class I Tail Sizing

7.4.1 Overall Empennage Configuration

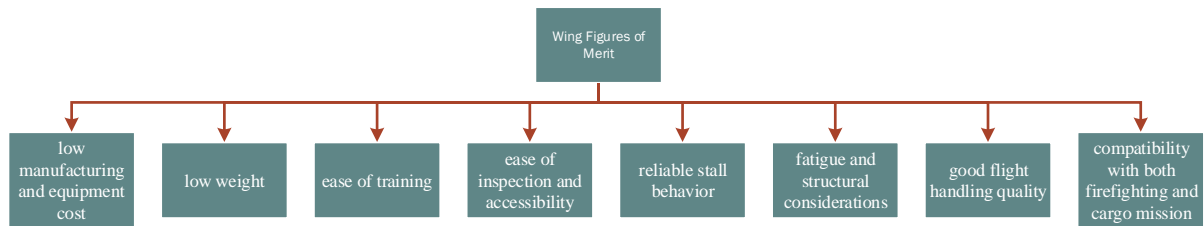


Figure 53: Tail Figures of Merit

Considering merits in Figure 53, three configurations were chosen; Conventional, T-tail and H-tail. The decision between these three configurations is made by weighting the merits with regard to their level of importance.

The H-tail configuration is more complex and needs stronger structural joints and as a result, higher weight is associated with it. Moreover, since vertical tails are connected at the ends of the horizontal tail, it makes it extremely difficult to employ variable incident horizontal tail. Farther, the simulator development may be arduous since there are not too many aircrafts benefiting from H-tails so far and the result is more complexity in training.

However, for H-tail configurations, because of its shorter vertical tails, the visual inspections are made easier. Since the damage tolerant philosophy in fatigue considerations is highly dependent on these inspections, it results to a better satisfaction of fatigue requirements. Besides, our angle of attack is mainly around 0 and this means that the engine wakes do not affect the tail structure too much and as a result, fatigue concerns are not considerable again. Vertical tails act as wing fences for horizontal tail. This makes the horizontal tail more efficient and consequently, shorter. Finally, the H-tail configuration has better stall behavior than conventional and t-tail configurations, since because of the vertical tails, tip stall of horizontal tail is much more controlled.

To summarize, H-tail scored higher and was chosen for the overall configuration of the empennage based on the discussion above.

7.4.2 Guesstimating the Disposition of Empennage

There are not too many aircrafts that benefit from the H-tail configuration as their empennage. Due to this lack of sufficient database, the sizing was done only with regard to An-225 aircraft. This aircraft uses high-wing and turbofan as power plant and can be a good choice as a target aircraft for sizing the empennage. The moment arms,

tail volume coefficients and control surfaces' fractions are calculated and presented in Table 38, where x_h and x_v are defined in Figure 8.1 of Ref. [49]. These values lead to $x_h = 46$ ft. and $x_v = 57$ ft.

Table 38: Moment Arms, Tail Volume Coefficients and Control Surfaces' Fractions

$\frac{x_h}{l_f}$	$\frac{x_v}{l_f}$	\bar{V}_h	$\frac{S_e}{S_h}$	\bar{V}_v	$\frac{S_r}{S_v}$
0.46	0.57	0.89	0.30	0.07	0.23

7.4.3 Size of the Empennage

For determining the size of empennage, the so-called \bar{V} -method is used. The coefficients are as defined in Ref. [49]. This method results in data provide by Table 39.

Table 39: Calculated Tail Areas

S_h (ft ²)	S_e (ft ²)	S_v (ft ²)	S_r (ft ²)
389.5	116.8	248.0	57

7.4.4 Planform Geometry of the Empennage

7.4.4.1 Horizontal Tail

The planform geometry for horizontal tail is chosen as a simple swept, tapered wing with dihedral. The characteristics of the horizontal tail geometry are summarized in Table 40.

Table 40: Characteristics of the Horizontal Tail Planform Geometry

AR_h	$\Lambda_{c/4h}$ (deg)	λ_h	Γ_h (deg)	i_h (deg)	Airfoil
4	40	0.6	10	-3.5	NACA 0014

The selected sweep angle is because of critical Mach number considerations for the tail. The sweep angle should satisfy the increment of $\Delta M_{cr} = 0.05$ for tail [49].

The reason behind the negative incident angle of the horizontal tail is the type of stability chosen for Anahita. Since it has to operate in fire zones and must tolerate the gusts existing in those areas, and due to its relatively low stall speed, stall considerations are extremely important. Consequently, It was decided to use the static stability presented in Figure 54. In this type of stability, when the angle of attack increases, the negative lift of horizontal tail goes to zero which means a nose pitching down moment.

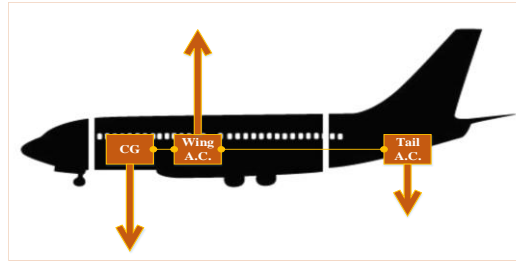


Figure 54: Static Stability Mode

Using the definitions, the geometric parameters of horizontal tail is calculated and represented in Table 41.

Table 41: Horizontal Tail Geometric Parameters

b_h (ft)	\bar{c}_h (ft)	c_{r_h} (ft)	c_{t_h} (ft)
39.5	9.9	12.1	7.3

NACA 0014 is chosen for the airfoil of the horizontal tail. This airfoil is chosen because of its linear behavior in high Reynolds regimes and the symmetry it provides. Figure 55 demonstrates these characteristics of NACA 0014 in Anahita’s Reynolds intervals. Besides, its 14% thickness allows using stronger spars for connecting the vertical tail to the horizontal tail. Table 42 illustrates the critical Mach number of the root and tip of the horizontal tail for different missions at -3.5 degree angle of attack. This data is extracted from Figure 6.1b of Reference [49]. Table 42 demonstrates that the critical Mach number increment of the horizontal tail is more than 0.05 since the cruise critical Mach number is 0.70.

Table 42: Critical Mach Number for Horizontal Tail in Different Missions and Legs – $\alpha = -3.5$ deg.

	Root Reynolds	Root C_l	Root M_{cr}	Tip Reynolds	Tip C_l	Tip M_{cr}
Max. Cruise In	1.65×10^7	-0.4014	0.75	9.93×10^6	-0.39895	0.75
Max. Cruise Out	2.43×10^7	-0.4038	0.75	1.46×10^7	-0.40085	0.75
Drop	1.32×10^7	-0.40035	0.75	7.95×10^6	-0.39775	0.75
T.O. / Landing	1.51×10^7	-0.401	0.75	9.11×10^6	-0.39835	0.75

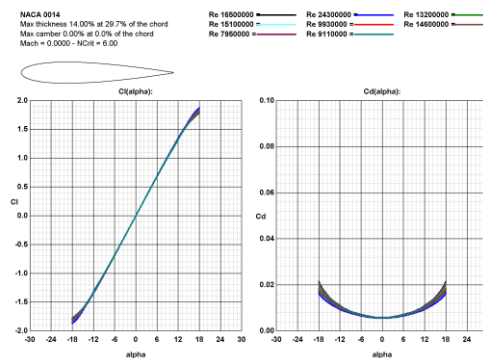


Figure 55: Lift and Drag Curves for NACA 0014

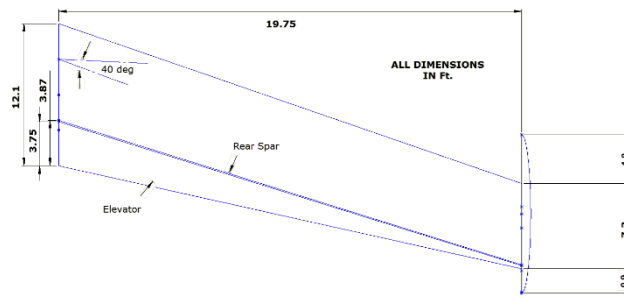


Figure 56: Dimensioned Drawing of the Horizontal Tail

7.4.4.2 Vertical Tail

The planform demonstrated in Figure 57 with corresponding ratios (Table 43), which are borrowed from An-225, is used for each of vertical tails. This planform results in geometric data represented in Table 44 for Anahita.

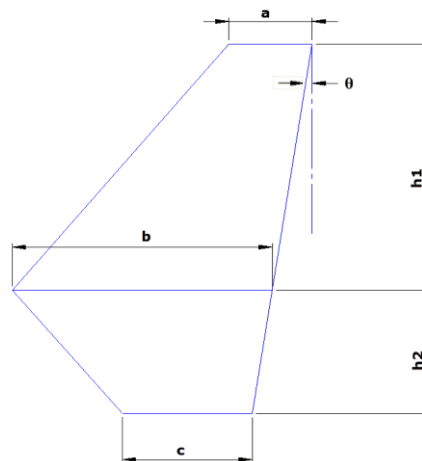


Figure 57: Planform of the Vertical Tail

Table 43: Planform Ratios for Vertical Tail

$\frac{a}{b}$	$\frac{b}{c}$	$\frac{h_1}{h_2}$	$\frac{D_h}{h_2}$	θ (deg)
0.32	2	2	2.3	9.18

Table 44: Planform Parameters for Vertical Tail

a (ft.)	b (ft.)	c (ft.)	h_1 (ft.)	h_2 (ft.)	θ (deg.)	Airfoil
3.2	10.0	5.0	12.1	6.0	9.18	NACA 0015

7.5 Sizes and Dispositions of Longitudinal and Lateral Control Surfaces

7.5.1 Elevators

In Table 39, it is shown that $S_e = 116.8 \text{ ft}^2$. The horizontal tail’s wing box should be designed such that it can bear the moment of vertical tail. Besides, the shear center of the wing box must match with the aerodynamic

center of the airfoil. For this level of design, it was chosen the rear spar of the horizontal tail to be located at 68% chord. This meant that the elevator chord shouldn't have exceeded 30÷31% of the total chord.

Supposing elevator chord starts at 71% chord, the available S_e can be calculated as follow:

$$S_e = 2 \times \left[\frac{b_h}{2} \times \left(\frac{c_{r_h} + c_{t_h}}{2} \right) \times (1 - 0.71) \right] = 118.8 \text{ ft}^2$$

Which is greater than 116.8 ft^2 . Please consider that the calculation of tail volume coefficients was done using unconnected areas. i.e., it included the area inside the fuselage. A dimensioned drawing of the horizontal tail is presented in Figure 56.

7.5.2 Rudders

In Table 39, it is shown that $S_r = 57.0 \text{ ft}^2$.

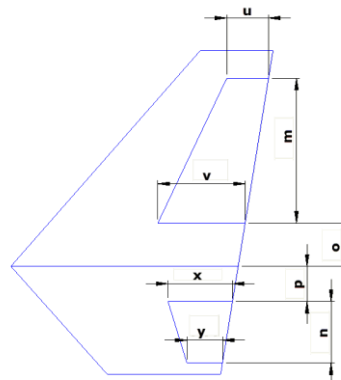


Figure 58: Rudder Planform Parameters

Figure 58 illustrates the basic parameters for sizing the rudder. The main challenge here was the prevention of elevators and rudders to jam each other. Assuming ± 40 degree for elevator deflection, the vertical displacement of elevator can be calculated as:

$$d_{e_v} = 0.31 \times c_{t_h} \times \sin(40) = 1.5 \text{ ft.}$$

Which means the rudders should start at least at $h_{1,2} - 1.5 \text{ ft.}$. For safety reasons, this threshold is considered to be 1.8 ft. The vertical spar will be located at 64% chord. It means that the rudder can start at approximately 65% chord. Using some geometric relations for trapezoid, the following can be achieved:

$$S_r = 56.9 \text{ ft}^2$$

Which is quite satisfactory for this class of sizing. Table 45 presents the summary of rudder dimensions with respect to Figure 58.

Table 45: Summary of Rudder Dimensions

u (ft.)	v (ft.)	x (ft.)	y (ft.)	m (ft.)	n (ft.)	o (ft.)	p (ft.)
1.3	3.1	2.1	3.0	9.2	3.1	1.8	1.8

7.6 Propulsion System Selection and Placement

7.6.1 Engine Type Selection

In this section the selection of the type of engine is desired (between turbofan and turboprop). To do so, a list of pros and cons has been used.

7.6.1.1 Figures of merit

Unit Cost	Specific Thrust
Thrust Specific Fuel Consumption	Ceiling
Propulsive Efficiency	Throttle Response
Maintainability	Stability (Torque)
Max speed	Fatigue (Vibration, ...)

7.6.1.2 Pros and cons

Pros and Cons for the position of the engine relative to the wing is presented in Table 46 using Refs. [54], [55], [23], and [56].

Table 46: Turboprop Vs. Turbofan Pros and Cons

	Turbofan	Turboprop
Pros	<ul style="list-style-type: none"> - has more propulsive efficiency in higher altitudes than turboprop. - can support high subsonic and even supersonic speeds. - has more Thrust/Weight ratio (Specific Thrust) than turboprop. - can go to higher altitudes than turboprop 	<ul style="list-style-type: none"> - better propulsive efficiency in lower altitudes - better SFC than turbofan - cheaper than turbofan
Cons	<ul style="list-style-type: none"> - more expensive than turboprop - more SFC than turboprop - more time needed for throttle response than turboprop 	<ul style="list-style-type: none"> - needs propellers - less maintainable than turbofan due to external propeller - cannot exceed the 360-380 knots max speed - cannot exceed 27000 ft. altitude - Propeller torque will endanger stability - more vibration and a longer shaft with a propeller attached on it will increase Fatigue than turbofan

7.6.1.3 Conclusion

And with the following pros and cons for both of the engine types it is qualitatively concluded that turbofan is better suited for our mission.

7.6.2 Engine Placement

In this section the selection of where to put the engine is desired (between Under the wing and Padded beside the fuselage) to do so a table of pros and cons and expert choice has been used.

There were more possible options for engine placement like (on the wing, in the wing, ...) but after some studying it was obvious that these placement options are not suitable for this purpose so they were eliminated before the final decision between the 2 remaining options (Under the wing, Padded beside the rear fuselage)

7.6.2.1 Figures of merit

- Fatigue (Exhaust gas, Temperature)
- C_g Travel
- Aerodynamic efficiency
- Maintainability (accessibility)
- Complexity (makes which are more complex)
- Stall
- Safety
- Rate of Climb
- Geometry Change (what changes will be imposed by them?)
- Stability
- Weight (overall aircraft)
- Flight Handling Quality

7.6.2.2 Pros and Cons

Pros and Cons for the position of the engine relative to the wing is presented in Table 47 using Refs. [54], [55], [23], and [56].

Table 47: Position of the Engine Relative to the Wing Pros and Cons

	Under the wing (UTD)	Podded beside the rear fuselage (PBTRF)
Pros	<ul style="list-style-type: none"> - Improves the overall aerodynamic efficiency of the wing - more accessible therefore maintainable than PBTRF - Good behavior in high AoA's (good for stall) - is prone to pitch up 	<ul style="list-style-type: none"> - will put the exhaust gas directly on horizontal tail (FHQ) - Positive role in Aircraft Longitudinal Stability - leads to more bending moment which will result in lightening the weight of the whole aircraft
Cons	<ul style="list-style-type: none"> - makes the wing more complex 	<ul style="list-style-type: none"> - increase the temperature in the rear fuselage by up to 5 degrees

- needs a larger Vertical tail and Rudder than PBTRF - Danger in fire emergency situations in engine	- makes the Fuselage more complex - bad for deep stall - will impose a T-tail - will put the exhaust gas directly on horizontal tail (fatigue)
---	---

7.6.2.3 Conclusion

And with the following pros and cons for both of the engine types it is qualitatively concluded that Under the wing option is better suited for our mission.

7.6.3 Engine Selection

The thrust to weight ratio obtained in was used to select the turbofan engine that meets the requirements that has been set earlier in the performance sizing.

Table 48: Engine Required Thrust

W [lb]	T total [lb]	T tech [lb]
131000	34600	17300

Now the engine databases are used to find an appropriate engine for this mission.

7.6.3.1 Pratt and Whitney 1000G Engine family

This is the most suitable engine for both of the above missions because the engine:

- ❖ Is 15-16% more fuel efficient than previous versions like IAE V2500 → can save up to \$1200000 per aircraft per year. (Catalogue)
- ❖ Will cut the carbon emissions by 3600 tons per aircraft per year. (Catalogue)
- ❖ Produces 50% less NO_x. (Catalogue)
- ❖ Produces 75% less noise (increased operations within curfews). (Catalogue)
- ❖ Will eventually save more than 20% in total operation cost. (Catalogue)
- ❖ Is truly scalable depending on the required thrust 15000 lb. to 40000 lb. thrust.

7.6.3.2 PW 1200G Series

These series range from 15000-17000 lb. of thrust and are suitable for 1 & 2 sortie mission.

7.6.4 Selected Engine Performance Characteristics

Two engines that where selected are characterized in Table 49.

Table 49: Selected engine performance characteristics

Engine	PW1200G
Thrust (lb.)	15-17 k
Fuel Burn (vs. current engines)	-12-15%
Noise (vs. stage 4)	-15 dB
Emissions-NO _x (Margin to CAEP 6)	-50%
Fan Diameter (inches)	56
Stage Count	1-G-2-8-2-3
Entry into service	2017

Derived Characteristics:

1. The weight of 81 inches’ diameter engine (PW1100G) is 6300 lb.
2. Bypass ratio 9:1
3. Current Engine SFC’s are about 0.35 (V2500) the older version of this engine (similar applications) so it can be derived that this engines SFC ranges between 0.3 to 0.31

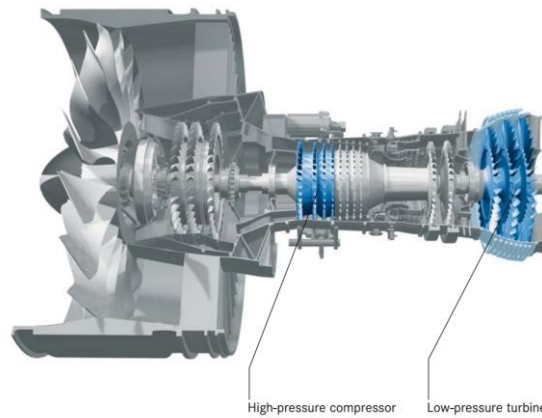


Figure 59 Engine’s Cutaway (Source: MTU Aero Engines)

According to section 4.2.4 in addition to classic brakes, there is a need for thrust reversal, and for that a cold-stream thrust reversal have been used in this engine, it can redirect the thrust by up to 40%.

7.7 WEIGHT AND BALANCE

The landing gear for Anahita was designed through an iterative process of defining the center of gravity by weight and location of all the components, starting with a tentative value for location of the landing gear and correcting it in every iteration, eventually arriving at a location which satisfies the some particular requirements.

7.7.1 Components and Systems Weight Calculations

A database was used in estimation of the component weights; this method provides more accurate results when used with a correction factor compared to other methods of estimation of component weights such as empirical correlations as suggested by some design textbooks

The database used for this section is derived from ref. [56].

7.7.2 Component Weight

The H-tail configuration of the Anahita entails a correction to the conventional component weight database, a correction factor of 2 was identified as a reliable adjustment since the H-tail is heavier than other conventional tail configurations. The weight of the drop system was assumed to be 15000 lb. Table 50 summarizes the weight of components for Anahita. This results in an empty weight of 68920 lb.

Table 50: Weight Components

Airplane	MTOW [lb.]	Wing Group	Tail Group	Fuselage Group	Landing Gear	Surface Controls	Nacelle Group	Drop System
LAT(Percent)	134000	11.11667	5.043333	11.275	4.111667	2.12	1.316667	11.194
LAT(Value)	134000	14896.3	6758.1	15108.5	5509.63	2840.8	1764.3	15000

According to section 4.1. the empty weight is supposed to be 70000 lb. Obviously the empty weight calculated in this section is via an approximation method, and consider that both methods for defining empty weight is based on database. Since it is preliminary phase and these two values are near, so from the feasibility point of view it is acceptable.

7.7.3 C.G & Landing Gear Location

The disposition of center of gravity was calculated by an iteration process described earlier. Figure 60 and Table 51 indicates the final location of C.G and the components.

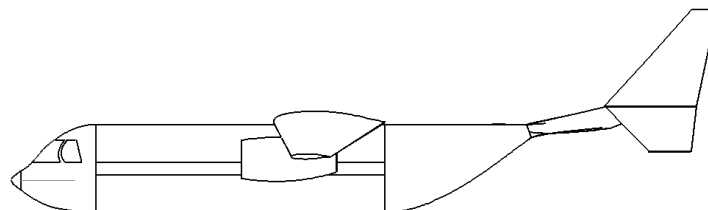


Figure 60 Side view of Anahita

Table 51: Final Location of C.G. & Components

Weight	Wing Gr	Tail Gr	Fuselage	L.G.	Surface control	Nacelle Gr + Engine	Drop System	Center Gravity
Weight [lb.]	14855.39	6758.067	15214.58	5480.97	2838.57	8772.52	15000	68920.1
X [ft.]	50	95	45	52	62	48	23	47.8
Z [ft.]	19.9	19	12.9	3	19	16.5	12.9	14.9

Some criteria, such as tip-over, limit landing gear location. Table 52 shows these criteria and the associated limits.

Table 52: Tip over and clearance criteria

Criteria	Longitudinal Tip Over	Lateral Tip Over	Longitudinal Ground Clearance
Limitation	15 Degree	55 Degree	15 Degree
Actual	15.58 Degree	70.1 Degree	24.58 Degree

8 CONCLUSION AND RECCOMENDATION

The risk of operation in the current piloted systems were shown to be remarkably high in Table 4. Automation support was proposed as a mitigation to reduce the impact of pilot errors on the fate of operations. and proved to bring more safety by reacting in a timely manner, and bring effectiveness by focusing maintenance during ground operations. It was then concluded that next builds of Anahita has the capabilities of being remotely operated as it employs the technologies and sensing required to provide sufficient view and control of the operations. In this mode, the operating cost lowers by at least 15% and additionally, there is no threat opposed to pilots. The only constraint to the RPA program is still the reliability of autonomous systems for heavy aircraft which has not yet been proven.

Anahita carries out the primary mission of Fire Attack in the most cost-effective and time-efficient manner for a 200nm range of operation, as an additional capability, the iterative method used in section ### could be embedded in Anahita's flight system in order to compute the optimal values of in and out cruise speeds and altitudes in any operation range.

It was realized that the 160-day contracts do not result in economical solutions to the LCC of Anahita, therefore, additional capability of performing alternate missions was considered. The 160 contracts per year were predicted to reach 208 by 2100, this indicates that the firefighting operation hours will increase in the future.

Increase in the fleet was recommended in order to lower the unit cost, this was justified based on the increasing number of fires and 37 international agreements on forest fires between US and other countries, it was then indicated money for every player is guaranteed by Export Credit Loan, so foreign contractors could also be involved.

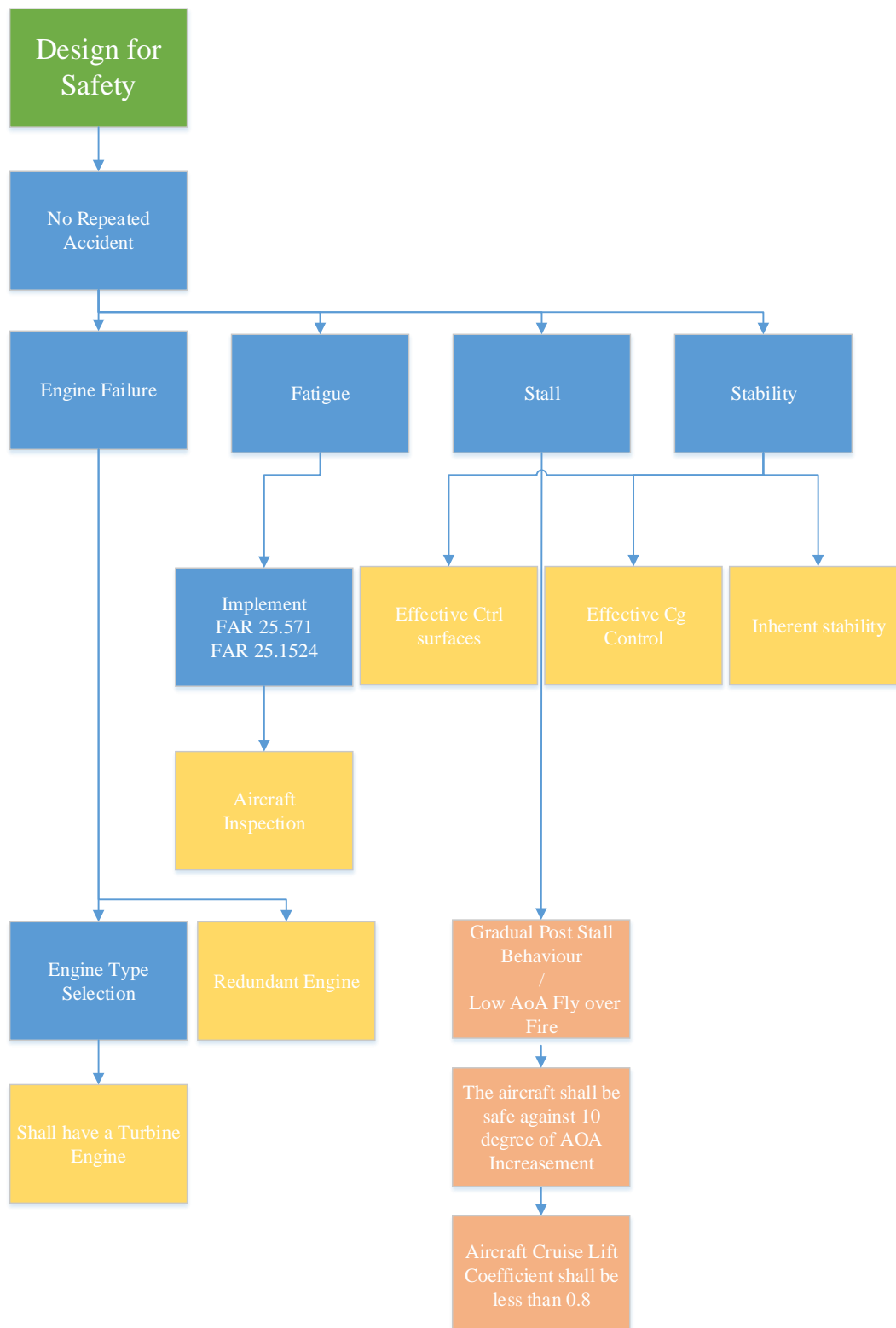
Requirement	Section	Compliance
Value		
Off the shelf engine technology	Section 7.6.3	Yes
Entry into service of 2022	Section 3.5	Yes
Airtanker may need to have less than 9500\$ daily availability cost	Section 5.4	Changed
Airtanker shall have an operational life time of no less than 20 years	Section 5.4	Yes
Airtanker may need to have less than 6000\$ flight hour cost	Section 5.4	Changed
Reliability		
Airtanker shall have a ferry range of 2500 nm	Section 6.3	Yes
Airtanker shall provide cruise L/D of more than 7	Section 4.3	Yes
The wing shall provide cruise lift coefficient of at least 0.15	Section 7.3.4	Yes
Airtanker shall have a BFL of 5000 ft.	Section 4.2.4	Yes
Airtanker shall have a T.O. max lift coefficient of at least 3	Section 7.3.4	Yes
Airtanker shall have a reload time of less than 10 minutes (with engines on)	Section 7.1	Yes
The retardant tank shall have a loading rate of at least 500 gal./min.	Section 7.1	Yes
Airtanker shall have a dash speed of more than 300 knots on return trip	Section 6.3	Yes
Airtanker shall have a cruise-in altitude of higher than 15000 ft.	Section 6.3	Yes
Airtanker shall have a critical Mach number values of at least 0.55	Section 7.3, 7.4	Yes
Airtanker shall commence a full turn between each equal drop	Section 3.4	Yes
Airtanker shall provide 3 retardant drop per sortie	Section 7.1	Yes
Airtanker shall follow the smoke line	Section 3.1.8	Yes
Airtanker shall provide a forward observation function	Section 3.1.8	Yes
Airtanker shall build a fire line with 4 sorties	Section 6.3	Yes
Airtanker shall have a retardant capacity of 5000 gal. volume	Section 7.1	Yes
Airtanker shall have an operational range of 200 nm	Section 4.1	Yes
Airtanker shall have a drop altitude of below 300 ft. AGL	Section 4.2.5	Yes
Airtanker shall be propertyed by TCAS	Section 3.1.8	Yes
Airtanker shall have a drop speed of below 150 knots	Section 4.2.5	Yes
Airtanker shall have a stall speed of 90 knots	Section 4.2.1	Yes
Airtanker is not allowed to experience load factors of more than 2.3 during drop	Section 4.2.5	Yes
Airtanker shall be capable of providing max lift coefficient of at least 2.2 during drop	Section 7.3.4	Yes
Wing may not have sweep angel	Section 7.3.2	Yes
Safety		
Airtanker shall have Gradual post stall behavior/ low AoA fly over fire	Section 7.3.3	Yes
Airtanker shall be safe against 10 degree of AoA increase	Section 7.3.3	Yes
Airtanker cruise lift coefficient shall be less than 0.8	Section 6.3	Yes

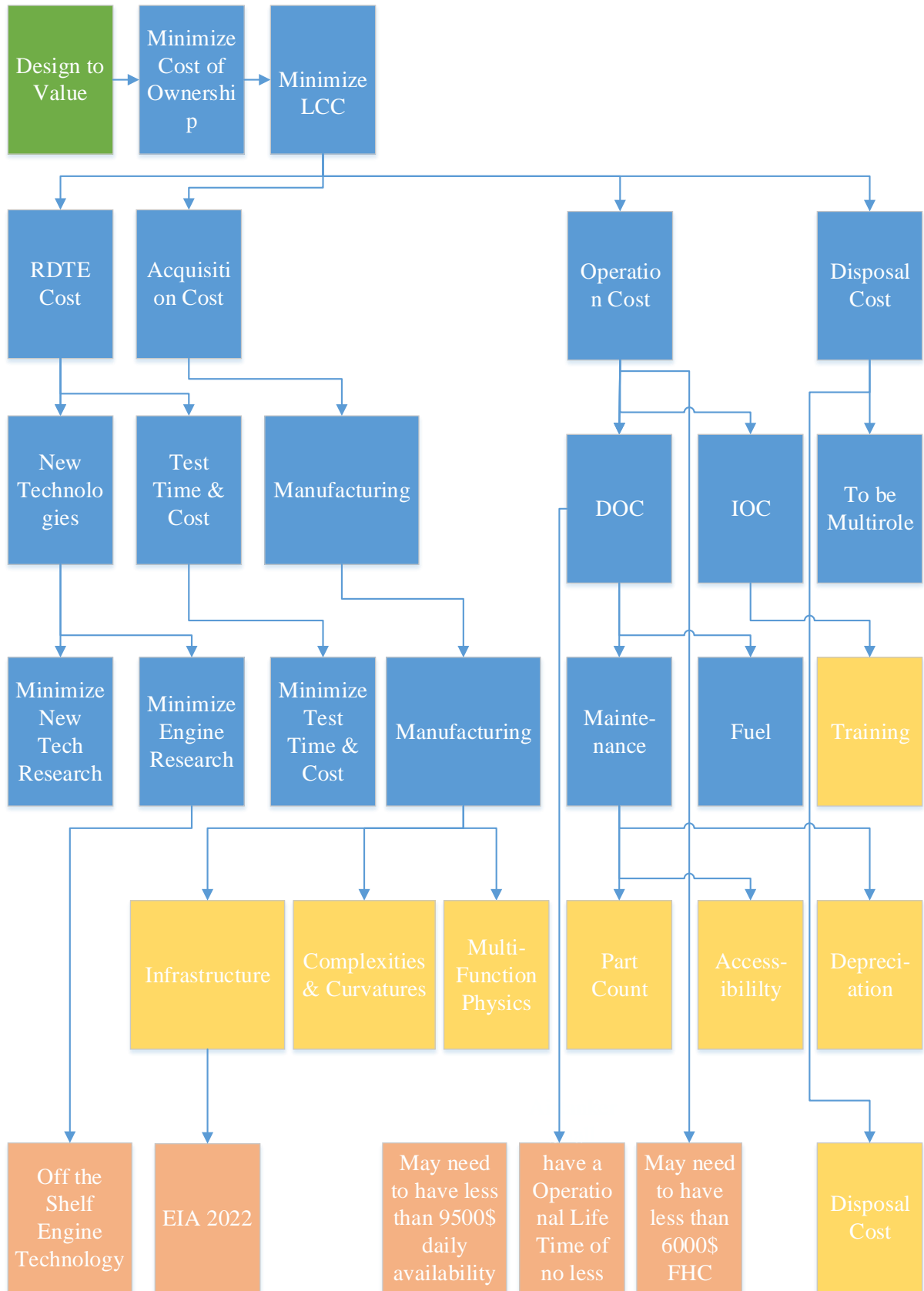
9 References

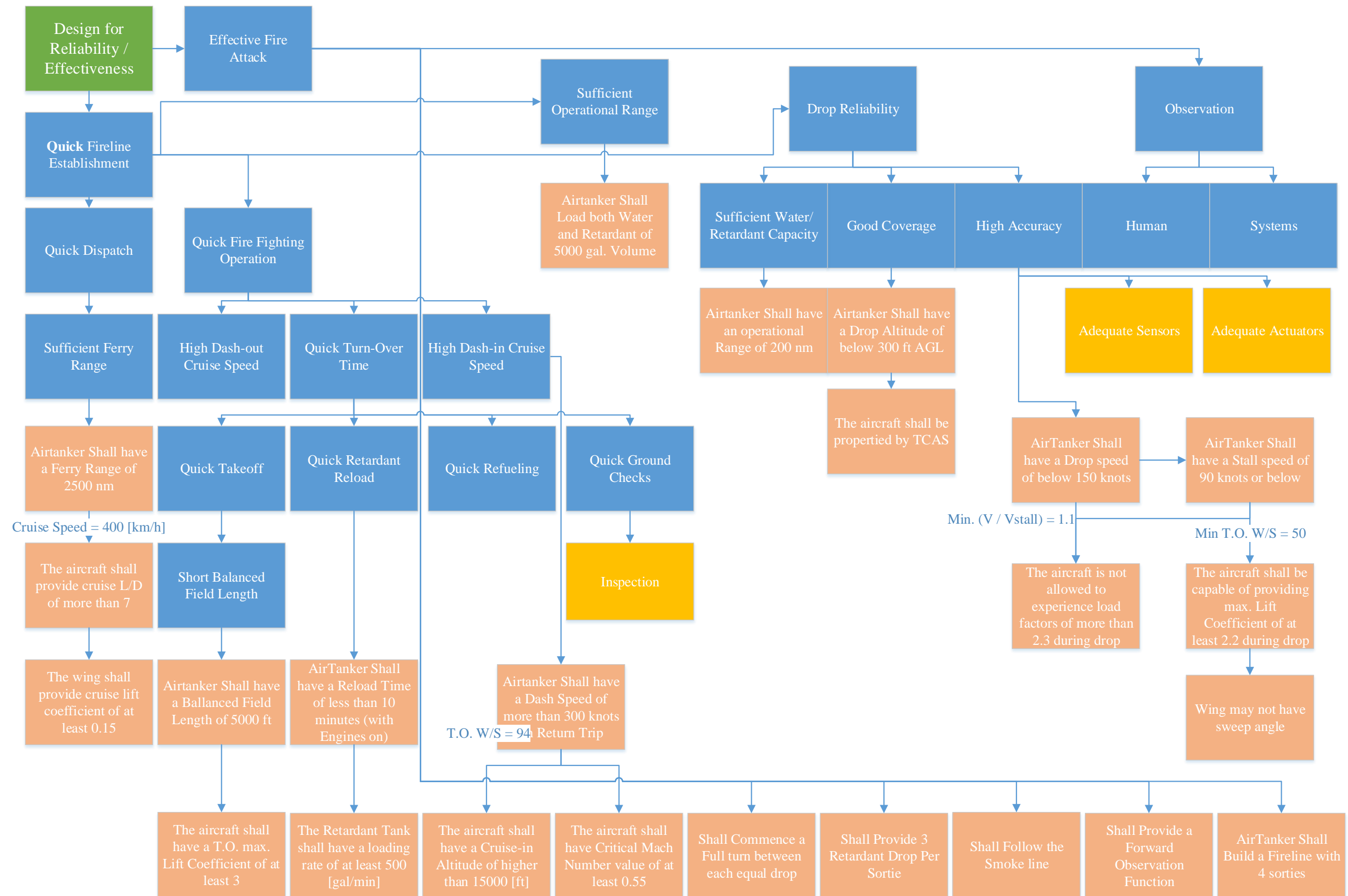
- [1] J. Elkington, *Cannibals with Forks*, Oxford: Capstone, 1997.
- [2] C. s. Wasson, *Systems Design and Development Concept Principles and Practice*, New jersey: wiley interscience, 2006.
- [3] T. L. Saaty, "Decision making with analytical hierarchy process," *Int. J. Services Sciences*, vol. 1, no. 1, pp. 83-98, 2008.
- [4] M. A. Kay, "Cost As An Independent Variable (CAIV) Principles and Implementation," in *AIAA Space Technology Conference*, Albuquerque, 1999.
- [5] J. G. Land, "Differences in Philosophy - Design to Cost vs. Cost As an Independent Variable," pp. 24-28.
- [6] F. P. S. LLC, "Safety Impact Analysis for Large Airtanker Operations," USDA Forest Service, San Dimas, 2012.
- [7] S. W. A. Dekker, "MABA-MABA or Abracadabra? Progress on human-automation coordination," pp. 5-6, 2002.
- [8] NASA, "Civil UAV Capability Assessment," NASA, 2004.
- [9] L. Save, "Designing Human-Automation Interaction: a new level of Automation Taxonomy," pp. 48-50, 2012.
- [10] Fire Program Solutions LLC, "Safety Impact Analysis for Airtanker Base Operations," Fire Program Solutions LLC, Sandy, Oregon, 2012.
- [11] ICAO, "Manual on Remotely Piloted Aircraft Systems (RPAS)," ICAO, Montreal, 2015.
- [12] R. Austin, "Mass domains of manned and unmanned aircraft," in *Unmanned Aircraft Systems*, Wiley, 2010, p. 92.
- [13] n. & grumman, "F35," northrop & grumman, 4 4 2016. [Online]. Available: <https://www.f35.com/about/capabilities/missionsystems>. [Accessed 4 4 2016].
- [14] P. S. Morrell, *Moving Boxes by air (The Economics of International air cargo)*, Farnham, Burlington: Ashgate, 2011.
- [15] P. K. I. a. M. Andrea Popescu, "The Air Cargo Industry," in *International Transportation: Moving Freight in a Global Economy*, Eno Transportation Foundation, 2010, p. 30.
- [16] D. M. Buede, *The Engineering Design of Systems*, New Jersey: John Wiley & Sons, 2009.
- [17] M. B. O. J. M. L. Corey R. Butler, "Aviation-Related Wildland Firefighter Fatalities, United States, 2000-2013," *Morbidity and Mortality Weekly Report*, p. 4, 15 July 2015.
- [18] d. Stinton, *The anatomy of the airplane*, Amer Inst of Aeronautics, 1998.
- [19] J. Roskam, *Airplane Design Part 1*, kansas: darcorp, 1985.
- [20] J. Roskam, *Airplane Design Part III: Layout Design of Cockpit, Fuselage, Wing and Empennage: Cutaways and Inboard Profiles*, Kansas: Roskam Aviation and Engineering Corporation, 1986.
- [21] M. H. Sadraey, *Aircraft Design a Systems Engineering Approach*, New Hampshire, USA: John Wiley & Sons, Ltd., Publication, 2013.
- [22] L. M. Nicolai and G. E. Carichner, *Fundamentals of Aircraft and Airship Design, Volume I - Aircraft Design*, American Institute of Aeronautics and Astronautics, Inc., 2010.
- [23] M. H. Sadrayi, *Aircraft Design A System engineering Approach*, Kansas: Wiley, 2013.
- [24] J. Roskam and E. Lan, *Airplane Aerodynamic and Performance*, DAR cooperation, 1997.
- [25] J. D. Anderson Jr., "Aircraft Performance and Design," McGraw Hill.
- [26] "Special Mission Airworthiness Assurance Guide," Usfs, Fire And Aviation Management, 2010.
- [27] AIAA, "RFP (2015-2016 Graduate Team Aircraft)," AIAA, 2015.
- [28] A. Stepanov and J. MacGregor Smith, "Modeling wildfire propagation with Delaunay triangulation and shortest path algorithms," *European Journal of Operational Research*, pp. 755-788, 2012.

- [29] P. Howard, "FLAMMABLE PLANET: Wildfires and the Social Cost of Carbon," September 2014. [Online]. Available: http://costofcarbon.org/files/Flammable_Planet__Wildfires_and_Social_Cost_of_Carbon.pdf.
- [30] "Interagency Airtanker Base Operation Guide," National Wildfire Coordinating Group, 2011.
- [31] J. Roskam, Airplane design part 8, 1990.
- [32] "Inflation Calculator: Bureau of Labor Statistics," [Online]. Available: http://www.bls.gov/data/inflation_calculator.htm. [Accessed 5 May 2016].
- [33] "Fuel Prices | Aiglle Flight Support," [Online]. Available: <http://aiglle.co.uk/fuel-prices/>. [Accessed 28 April 2016].
- [34] "USAjobs," [Online]. Available: <https://www.usajobs.gov/GetJob/ViewDetails/431156700/>.
- [35] R. Austin, Unmanned Aircraft Systems, New Jersey: John Wiley & Sons, Inc., 2010.
- [36] L. T. J. J. Ivan Koblen, "Selected Aspects of Aviation Equipment Disposal Issue," *Management and Socio-Humanities*, p. 7.
- [37] SBAC, "End of Aircraft life cycle initiatives," *SBAC Aviation and Environmental Briefing Papers*, p. 7.
- [38] D. A.-K. C. M. Samira Keivanpour, "Toward a Strategic Approach to End-of-life Aircraft Recycling Projects," *Journal of Management and Sustainability*, vol. 3, no. 3, p. 19, 2013.
- [39] AFRA, "afraassociation.org," Aircraft fleet Recycling Association, 5 5 2016. [Online]. Available: <http://www.afraassociation.org/aircraftrecyclingdirectory.cfm>. [Accessed 5 5 2016].
- [40] "Large Airtanker Modernization Strategy," USDA Forest Service, 2012.
- [41] U. F. Service, *Large Airtanker Modernization Strategy*, USDA Forest Service, 2012.
- [42] D. McKenzie, F. Heinsch and W. Heilman, "Wildland Fire and Climate Change," January 2011. [Online]. Available: <http://www.fs.usda.gov/ccrc/topics/wildland-fire>. [Accessed 23 April 2016].
- [43] WildfireToday, 2015. [Online]. Available: <http://wildfiretoday.com/documents/NextGen2Awards.pdf>.
- [44] PK Air Finance, *Portfolios, Modeling Aircraft Loan & Lease*, Luxemburg: PK Air Finance, 2013.
- [45] AirFinance, "What is Airfinance?," AirFinance, 2016. [Online]. Available: <http://www.airfinancejournal.com/resources/what-is-aviation-finance.html>. [Accessed 15 4 2016].
- [46] "Wildland Fire Management Aerial Application Study," National Interagency Fire Center, Boise, 2005.
- [47] FAO/ITTO, "Legal Frameworks for Forest Fire Management: International Agreements and National Legislation," FAO, Rome, 2005.
- [48] Ex-Im Bank, "Finance Lease Structure," Export-Import Bank of the United States, [Online]. Available: <http://www.exim.gov/what-we-do/loan-guarantee/transportation/finance-lease-structure>. [Accessed 15 May 2016].
- [49] J. Roskam, "Airplane Design Part II: Preliminary Configuration Design and Integration of the Propulsion System," Roskam Aviation and Engineering Corporation, Ottawa, Kansas, 1985.
- [50] R. G. Budynas, Shigley's Mechanical Engineering Design, New York: Mc Graw Hill, 2011.
- [51] J. Roskam, Airplane design part 3, Kansas: Darcorp, 1985.
- [52] Special Mission Airworthiness Assurance Guide for Aerial Firefighting and Natural Resource Aircraft, U.S. Forest Service Fire and Aviation Management, 2011.
- [53] R. J. McGhee, W. D. Beasley and R. T. Whitcomb, NASA Low- and Medium-Speed Airfoil Development, Hampton, Virginia: National Aeronautics and Space Administration, 1979.
- [54] L. M. Nicolai, Volume I Aircraft Design, Blacksburg: AIAA, 2012.
- [55] J. Roskam, Airplane Design Part 6, Kansas: Darcorp, 1985.
- [56] E. Torenbeek, Synthesis of Subsonic Airplane Design, Delft: Delft university press, 1982.

10 APPENDIX A: Objective Hierarchy







11 APPENDIX B: Equations

$$L = nW = \frac{1}{2} \rho V^2 S C_L \Rightarrow C_L = \frac{nW}{\frac{1}{2} \rho V^2 S} = \frac{n}{\frac{1}{2} \rho V^2} \cdot \left(\frac{W}{S}\right)_{drop}$$

$$T = D = \frac{1}{2} \rho V^2 S (C_{D_0} + K C_L^2)$$

$$\frac{T}{W} = \frac{D}{W} = \frac{\frac{1}{2} \rho V^2 S C_D}{\frac{1}{2} \rho V^2 S \frac{C_L}{n}} = \frac{n (C_{D_0} + K C_L^2)}{C_L}$$

$$= \frac{n}{\frac{1}{2} \rho V^2 \cdot \left(\frac{W}{S}\right)_{drop}} \cdot \left(C_{D_0} + K \frac{n^2}{\left(\frac{1}{2} \rho V^2\right)^2} \cdot \left(\frac{W}{S}\right)_{drop}^2 \right)$$

$$= \frac{\frac{1}{2} \rho V^2}{\left(\frac{W}{S}\right)_{drop}} \cdot \left(C_{D_0} + K \frac{n^2}{\left(\frac{1}{2} \rho V^2\right)^2} \cdot \left(\frac{W}{S}\right)_{drop}^2 \right)$$